AN ABSTRACT OF THE DISSERTATION OF

Jacob L Strunk for the degree of Doctor of Philosophy in Forest Resources presented on June 14, 2012
Title: Estimation and Modeling of Selected Forest Metrics with Lidar and Landsat

Abstract approved:

_____

Temesgen Hailemariam

Lidar is able to provide height and cover information which can be used to estimate selected forest attributes precisely. However, for users to evaluate whether the additional cost and complication associated with using Lidar merits adoption requires that the protocol to use lidar be thoroughly described and that a basis for selection of design parameters such as number of field plots and lidar pulse density be described. In our first analysis, we examine these issues by looking at the effects of pulse density and sample size on estimation when wall-to-wall lidar is used with a regression estimator. The effects were explored using resampling simulations. We examine both the effects on precision, and on the validity of inference. Pulse density had almost no effect on precision for the range examined, from 3 to .0625 pulses / m^2. The effect of sample size on estimator precision was roughly in accordance with the behavior indicated by the variance estimator, except that for small samples the variance estimator had positive bias (the variance estimates were too small), compromising the validity of inference. In future analyses we plan to provide further context for wall-to-wall lidar-assisted estimation. While there is a lot of literature on modeling, there is limited information on how lidar-assisted approaches compare to existing methods,

and what variables can or cannot be acquired, or may be acquired with reduced confidence. We expand our investigation of estimation in our second analysis by examining lidar obtained in a sampling mode in combination with Landsat. In this case we make inference about the feasibility of a lidar-assisted estimation strategy by contrasting its variance estimate with variance estimates from a variety of other sampling designs and estimators. Of key interest was how the precision of a two-stage estimator with lidar strips compared with a plot-only estimator from a simple random sampling design. We found that because the long and narrow lidar strips incorporate much of the landscape variability, if the number of lidar strips was increased from 7 to 15 strips, the precision of estimators with lidar can exceed that of estimators applied to plot-only SRS data for a much larger number of plots. Increasing the number of lidar strips is considered to be highly viable since the costs of field plots can be quite expensive in Alaska, often exceeding the cost of a lidar strip. A Landsat-assisted approach used for either an SRS or a two-stage sample was also found to perform well relative to estimators for plot-only SRS data. This proved beneficial when we combined lidar and Landsat-assisted regression estimators for two-stage designs using a composite estimator. The composite estimator yielded much better results than either estimator used alone. We did not assess the effects of changing the number of lidar strips in combination with using a composite estimator, but this is an important analysis we plan to perform in a future study.

In our final analysis we leverage the synergy between lidar and Landsat to improve the explanatory power of auxiliary Landsat using a multilevel modeling strategy. We also

incorporate a more sophisticated approach to processing Landsat which reflects temporal trends in individual pixels values. Our approach used lidar as an intermediary step to better match the spatial resolution of Landsat and increase the proportion of area overlapped between measurement units for the different sources of data. We developed two separate approaches for two different resolutions of data (30 m and 90 m) using multiple modeling alternatives including OLS and k nearest neighbors (KNN), and found that both resolution and the modeling approach affected estimates of residual variability, although there was no combination of model types which was a clear winner for all responses. The modeling strategies generally fared better for the 90 m approaches, and future analyses will examine a broader range of resolutions. Fortunately the approaches used are fairly flexible and there is nothing prohibiting a 1000 m implementation. In the future we also plan to look at using a more sophisticated Landsat time-series approach. The current approach essentially dampened the noise in the temporal trend for a pixel, but did not make use of information in the trend such as slope or indications of disturbance – which may provide additional explanatory power. In a future study we will also incorporate a multilevel modeling into estimation or mapping strategies and evaluate the contribution of the multilevel modeling strategy relative to alternate approaches.

Estimation and Modeling of Selected Forest Metrics with Lidar and Landsat

by

Jacob L Strunk

A DISSERTATION

submitted to

Oregon State University

in partial fulfillment of
the requirements for the
degree of

Doctor of Philosophy

Presented June 14, 2012

Commencement June 2013

Doctor of Philosophy dissertation of Jacob L. Strunk presented on June 14, 2012.

APPROVED:

_____

Major Professor, representing Forest Resources

_____

Head of the Department of Forest Engineering Resources and Management

_____

Dean of the Graduate School

I understand that my dissertation will become a part of the permanent collection of Oregon State University libraries. My signature below authorizes release of my dissertation to any reader upon request.

_____

Jacob L Strunk, Author

ACKNOWLEDGEMENTS

I must first express my appreciation to my wife Kaori I. Strunk for her love and support. It has been a busy and difficult period with many sleepless nights, but I have been always happy and content because I have had you by my side. Let us travel, pick fruit, dig clams, garden, and otherwise continue to have fun together for a very long time.

The process to completion has been difficult and complex, but not as difficult or complex as it might have been. I would like to thank Dr. Temesgen Hailemariam for offering me freely of his guidance and wisdom throughout my PhD. I couldn't ask for a better mentor, content to let me hare off in the wrong direction if I was so inclined, until perhaps I was ready to listen to rhyme and reason. I have learned many things in a variety of disciplines from Temesgen, but most importantly I have learned the importance of kindness. I would also like to thank the rest of my committee, especially Dr. Hans-Erik Andersen, and Dr. Jim Flewelling for their time, knowledge and support in learning to conduct research. I have still a long ways to go, but they helped me to grow in my capacity to understand and perform scientific investigations.

I would like to thank the many professors in the department of statistics who shaped much of my formal education. It is through their guidance that I learned to doubt every claim that I encounter until satisfied that the methods, analyses, and scope are defensible. This is one of the most important lessons I have learned, and it affects how

I filter knowledge in every aspect of my life. Most relevantly, it has pushed me to challenge the validity of my own work, enabling me to slowly but steadily grow as a researcher.

There is one individual who has been a constant support through nearly my entire academic career. I am grateful to Stephen E. Reutebuch for his technical advice, mentoring, support, occasional good-natured lambasting, and the entertainment value of his frequent battles with oft-automated prone-to-disconnect prone-to-place-on-hold prone-to-redirect phone support. I also appreciate the good will and technical advice provided by Robert J. McGaughey, Petteri Packalen, Robert E. Kennedy, and Justin Braaten.

The PhD journey would not have been nearly as pleasant without my fellows and predecessors along the way including Bianca Eskelson, Michael Goerndt, Brian Wing, Donald Gagliasso, David McClung, Will Pollock, Joonghoon Shin, Krishna Poudel, Zane Haxton, and Junhui Xao. Too many to name, I am also indebted to my fellows in the statistics department who allowed me to join in their revelry.

Last but not least I would like to express my appreciation to my mother, my father, my step-father and my siblings for (in no particular order) loving, raising, and putting up with me.

CONTRIBUTION OF AUTHORS

Dr. Temesgen Hailemariam, Dr. Hans-Erik Andersen, Dr. Jim Flewelling, and Dr. Lisa Madsen provided technical and statistical advice, analytical critiques, and extensive revisions.

TABLE OF CONTENTS

Page

TABLE OF CONTENTS (Continued)

TABLE OF CONTENTS (Continued)

TABLE OF CONTENTS (Continued)

LIST OF FIGURES

LIST OF TABLES

Estimation and Modeling of Selected Forest Metrics with Lidar and Landsat

Jacob L Strunk

1 Introduction

1.1 Background

1.1.1 Forest inventory

Forest resources are often distributed over vast areas, and the measurement, monitoring and mapping of forest resources can prove quite difficult and costly. Strategies for sampling and estimation of these are quite mature (e.g. Gregoire and Valentine, 2004; Schreuder et al., 2004; Shiver and Borders, 1995; Johnson, 2000), and forest inventory procedures play a role in nearly every forest manager's operations. However, traditional sampling and estimation strategies commonly used for forest inventory may not be feasible or efficient in all areas (e.g. Alaska: Barrett et al., 2011, p.1). The utilization of modern remote sensing may improve the efficiency of estimation, enabling forest inventory and monitoring even in remote areas (Andersen et al., 2011a) or improving spatial products and potentially reducing costs where traditional forest inventory strategies are already implemented. Mapping is an area where standard forest sampling, inventory, and estimation strategies are likely to prove deficit. For example, fine-scale Information about how the forests and terrain vary spatially may prove important for representing and understanding ecological processes that drive some management decisions (Russel et al., 2007). Field measurements alone may not reflect spatial variability on the landscape at a resolution that is suitable to monitor the phenomenon (Hinsley et al., 2006). This is an area where leveraging remote sensing data is likely to provide benefit (Mutlu et al., 2008).

1.1.2 Remote sensing

Remote sensing data has an advantage over in-the-field measured data in that it can most often be collected for large areas at a fraction of the cost per unit area relative to the cost of field measurements. Remote sensing data has a disadvantage in that the information represented often does not correspond exactly with the variables that we wish to measure, map, or monitor. From this perspective, it is may be necessary to collect remote sensing in conjunction with field measurements. The field measurements can provide a bridge between remote sensing data and what the data represents on the ground. This "bridge" is formalized through the development of an empirical (typically) model linking the sources of data. Clearly there will be some loss in information (errors or residuals) in using the model instead of measurements when the model is applied. However, depending upon the variable of interest and the remote sensing data source, it is sometimes possible to increase the precision of estimates (e.g. the total and mean) and predictions (e.g. mapped values) over those made without leveraging remotely sensed information. However, the information contained within remote sensing data differs depending upon the system, and the data from some systems do not have the capacity to provide the information desired by the user. And, clearly there are some field measurements that are not likely to ever be measured with remote sensing, such as soil biomass or wood density.

1.1.3 Aerial photos in forest inventory

Aerial photos are still the most common source of remote sensing data for forest inventory, often used for delineation and classification (Hall, 2003). For industrial

forest inventory, delineation and classification is typically performed by a skilled photo interpreter using aerial photos with resolutions commonly ranging from 1:10,000 to 1:20,000 (Ahern and Leckie, 1987). Aerial photos can also be used to measure forest structure directly (photo measurements taken as truth) or photo measurements can be adjusted by double sampling. In a double-sampling approach a large number of measurements from aerial photos are calibrated using a model(s) fitted to corresponding field measurements for a small subsample of photo measurements (Howard, 1991, 307–314). Aerial photos provide some advantages in forestry over other remote sensing data sources in that they are high resolution (> 0.2 m), can be used with some success for species differentiation, and provide context that is evident to the naked eye, and they can be easily transported to and used in the field. A primary downside of aerial imagery is that some variables, such as volume a key requirement of many inventories, may not be attainable without time intensive user interpretation or additional information (Hall, 2003).

1.1.4 Space borne sensors

Satellite-based imagery has been available for use in mapping forest resources at least since the launch of the Landsat 1 platform in 1972 (Garner, 2012). Studies which used Landsat data to map forest resources were published shortly thereafter (Kirvida and Johnson, 1973; Jobin and Beaubien, 1974). Images from medium resolution (e.g. 30 m), satellite-based sensors are a source of data that can be used to classify and predict forest resources for large areas. Satellite-based sensors provide much higher temporal resolution than is feasible from aerial platforms and the cost of data is lower, although

the spatial resolution that is feasible from a satellite platform is also lower. Landsat is a data source that is frequently used for mapping over large areas because it has a long collection history, has a frequent re-measurement cycle, and is of reasonably high resolution (Huang et al., 2003, 389–390). Landsat TM data (from Landsat 4 and Landsat 5 platforms, which are no longer operational) are 30 m resolution data collected using scanning sensors which are sensitive to seven spectral bands. This data was passed to ground stations where it was processed and distributed as georeferenced grids of digital numbers. However, while the cost, coverage and temporal data density represent advantages of Landsat, and derivatives on a regional scale may be adequate, the quality of individual mapped predictions and classifications may be quite low (DeVelice, 2012; Hyyppä et al., 2000). There are sensors in orbit capable of acquiring much higher resolution imagery (>1m), but for large areas these sensors have many of the same feasibility and cost constraints as imagery collected from aerial platforms (Huang et al., 2003, 389–390). Higher temporal resolution data are also available, but typically have reduced spatial resolution, and may have a variety of technical issues associated with their use (Cihlar et al., 2003).

1.1.5 Lidar

Airborne near-infrared scanning light detection and ranging (lidar) systems are a source of auxiliary data that have grown in importance in forestry in recent years. While lidar is primarily collected to enable accurate representation of the terrain surface, it was early on recognized by the natural resource community that the vertical distributions of lidar data corresponding to laser reflections from vegetation can be

used to quantify vegetation properties (Maclean and Krabill, 1986; Nelson et al., 1988). Lidar sensors use a laser pulse and a sensor, in addition to various positioning equipment to actively measure three-dimensional structure. The combination of an accurate digital terrain model (DTM) which can be derived from lidar points and the vertical distributions of lidar points above the estimated surface make it possible to make inference about vegetation height and canopy cover. These in turn can be used to predict forest metrics like biomass and volume (e.g. Strunk et al., 2012). It should not, however, be assumed that lidar directly provides information about every individual tree (e.g. a tree list) or that lidar-derived height and cover are the same as field measured height and cover. The strength of the reflected lidar pulse (intensity) can also be used with some success for prediction and classification (Donoghue et al., 2007; Hudak et al., 2006).

Fortunately, the application of lidar aided techniques in forestry and forest inventory is quite similar to the techniques which are already in use with aerial imagery. Much like the double sampling approach previously described for use with aerial photo measurements, corresponding lidar and field metrics can be used to train models for prediction of field metrics in locations where only lidar is available (Andersen et al., 2005) or for estimation (Corona and Fattorini, 2008; Opsomer et al., 2007). An advantage of lidar in this context is that it is fairly easy to automate the calculation of lidar metrics. Using photo plots as an analogy, it is equivalent to automating the measurement of hundreds of thousands to millions (and perhaps even billions) of photo plots – or the complete area covered by the lidar. Lidar can also be used to

identify potential tree crowns, although sub-canopy trees are likely to be omitted and interconnected trees may be lumped together (Ene et al., 2012; Peuhkurinen et al., 2011). The height, cover, and intensity information could potentially even be used simply as the basis for automated stand or stratum delineation and classification(Sullivan et al., 2009) while using traditional forest inventory plots for estimation – an approach which is similar to how aerial imagery is most often used in practice for forest inventory.

In the forestry literature lidar is most often studied in a wall-to-wall capacity, and for good reasons. This type of acquisition is the most flexible with respect to potential because it is possible to develop complete maps of the study area including DTMs, canopy height, and predicted forest metrics in addition to performing estimation. The alternate uses may in fact have greater influence on the decision to acquire lidar than estimation, especially for DTMs. However, in some instances it will not be feasible to acquire lidar over an entire study area due to cost and estimation may be the primary motivation to acquire lidar. A number of recent studies looked at estimation with strips of lidar collected as a sample over their respective study areas (Andersen et al., 2011b; Parker and Evans, 2007; Gregoire et al., 2011; Ståhl et al., 2011). Collecting lidar as a sample of strips will negate many of the mapping benefits of lidar when strips of lidar are used alone, but may yield a better cost for precision ratio for large areas. For small areas the approach will not yield sufficient cost reduction to warrant obtaining lidar as a sample of strips.

1.1.6 Lidar limitations

As with satellite and aerial based passive sensing systems, lidar is not without limitations. A primary limitation currently is the cost of a lidar acquisition. To guarantee that reflected lidar pulses have enough energy to register with the systems sensor, flying heights must be relatively low, less than 4000 to 5000 m typically – although the flying height is frequently much lower, ≈1000 m, to achieve a desired pulse repetition frequency (PRF). This is much lower than for aerial photography and means that the number of passes required over a target area is high – driving up costs to on the order of approximately $0.70 per acre in contrast $0.35 per acre for aerial imagery. An additional limitation of lidar is that it may provide less information which is useable for species differentiation. Lidar is typically flown using a single near-infrared (1064 nm) laser which provides less spectral information than is available from a multi-band sensor under optimal conditions. Additionally, since a lidar pulse has a non-negligible footprint, information on reflectance properties may be confounded by the size of the object which registers a return, or may represent multiple objects with quite different reflectance properties (e.g. foliage and branches).

1.1.7 Adoption of lidar aided inventory approaches

While there have been a large number of studies that explored the use of lidar for mapping, estimation, and classification, whether there is sufficient impetus to adopt new these techniques which take advantage of lidar depends in large part upon the success of existing methodologies to satisfy information needs, and the perceived benefits from adopting new methodologies. In the experience of the first author from

interacting with private industry users of forest inventory data across the United States, existing plot and aerial imagery based methodologies are perceived to be satisfactory, if costly, and whether lidar approaches provide sufficient benefits to warrant adoption is unclear. In light of the lack of clarity on the tradeoffs between traditional forest inventory monitoring and measurement approaches and new remote sensing approaches (especially with lidar), it is important that benefits of modern approaches be provided with context. One way to do this is to provide results in a format that is comparable to existing inventory outputs – when possible (some lidar products, such as a 1m DTM, are simply not available except with lidar). This is not meant to diminish the importance of exploratory analyses that do not immediately translate into applicable and comparable methodologies. Lidar aided techniques, for example, are sufficiently advanced today to enable straightforward prediction and estimation of volume for complete forests, but this may have seemed a distance pipe dream to early researchers in this area.

1.2 Research problems

Lidar is recognized as a powerful tool in the prediction of forest attributes such as volume and biomass, but there is a knowledge gap that impedes using lidar as an auxiliary data source for many potential users. Users must be able to assess the tradeoffs between how the data is collected and the resulting estimation precision or feasibility before they can critically assess adoption. For example, in an estimation strategy in which relationships between forest and lidar metrics on plots are empirically modeled, changing the number of field plots and the lidar pulse density

can also greatly affect the cost. To select a configuration that meets the requirements of the users, it is also important to understand how components of the configuration affect estimation precision.

The issues of pulse density and sample size have been examined in a number of studies (e.g. Gobakken & Næsset, 2008; Magnusson et al., 2007), however they typically do not place the effects of density and sample size in the context of estimation, an important basis for inference, and typically do not consider wide variation in pulse density and sample size in combination. In chapter 2 we focus on the properties of estimation of forest metrics with lidar for a case study when lidar was acquired for the entire study area. The precision of estimates was described for various lidar pulse densities and different numbers of training plots. The analysis was performed using a simulation approach for a range of parameters that include the lower end of sampling and acquisitions parameters that are likely to be considered. Both the lidar and field plots were sub-sampled, and the effect on finite-population parameters was empirically demonstrated using bootstrap simulations. As one would expect, the number of field plots was found to have a pronounced effect on estimator precision. Less intuitively, but in line with previous studies, pulse density had almost no effect on estimator precision. The results from this analysis contribute to forest inventory with lidar by providing a thorough description of the relationship between pulse density, sample size, and estimator precision.

Clearly lidar can be used for both mapping and estimation purposes when it is collected wall-to-wall, but for large areas when considered for estimation purposes alone, it may also prove beneficial to consider lidar in a sampling mode. Long narrow strips of lidar dispersed over the study area are likely to capture much of the variability in the study area, potentially achieving much of the gains possible with wall-to-wall lidar. This is an important area of inquiry with lidar that has been examined in a several studies (Parker and Evans, 2007; Gregoire et al., 2011; Andersen et al., 2011a; Ståhl et al., 2011), however it is an area that is still relatively unexplored and deserving of further attention. Much as with wall-to-wall lidar, the performances of estimators for different configurations of estimation strategies with lidar in a sampling mode need to be reported with context to enable critical assessment of their merits prior to adoption. If strategies are reported relative to alternate estimation strategies, any advantages from using samples of lidar strips are more likely to be apparent. Landsat is another source of auxiliary information which may work well for estimation of forest metrics over large areas. For prediction of forest metrics like volume and biomass and classification, Landsat variables are likely to have less predictive power than lidar (DeVelice, 2012; Hyyppä et al., 2000). However, since Landsat provides frequent and expansive medium resolution coverage for free, if it can provide any aid in estimation it may prove to be useful in increasing the efficiency of an estimation strategy. The cost to inventory and monitor natural resources in large regions in remote locales can prove to be prohibitive, and any reasonable means to increase the viability of an estimation strategy is worth pursuing.

In chapter 3 we investigate of the precision of lidar aided estimation for a scenario in which lidar is collected as a sample of strips, in addition to considering several Landsat assisted and plot-only approaches. This chapter can be seen as an extension of the concepts investigated in chapter 2 to scenarios in which lidar cannot be used for complete coverage due to the high cost. However, as a sample it was hypothesized that for some forest metrics, lidar aided estimation can improve upon estimation efficiency with respect to the number of required field plots to achieve a given level of precision. As previously discussed, the spatial properties of lidar strips make them ideally suited for estimation because the long narrow strips will include much of the variability on the landscape, a desirable condition which is likely to enable relatively small variances for the appropriate estimators (Lohr, 2009, 173–178) . In our analysis this proved to be the case, and the lidar-assisted estimator used for a two-stage sample performed quite well, especially when used together with a Landsat- assisted estimator as part of a composite estimator. We additionally identified the number of lidar strips that are necessary for the lidar-assisted estimator to achieve the same precision as the estimator for a plot-only simple random sampling strategy. In a future study we plan to investigate the reduced number of strips that would be necessary for the lidar and Landsat composite estimator to achieve the same precision.

An approach that is able to use both lidar and Landsat as sources of auxiliary data for estimation was shown to fare better than an approach which uses either source alone. The addition of Landsat when lidar is collected in a sampling mode may also yield advantages with respect to modeling. Due to rectification errors and differences

between the size of a Landsat pixel and the size of the field plot, it may prove difficult to model forest metrics with Landsat values. If lidar were used to aid in training a Landsat model, some of the modeling difficulties with Landsat may be overcome because the area used to model could be increased substantially, increasing the area that is likely to overlap between response and auxiliary variables. In chapter 4 we implemented a number of multi-phase modeling strategies and for several strategies we were able to achieve improved results with respect to residual variability over those achieved by modeling Landsat directly as was done in chapter 2. We also found that the resolution of the data used to model with Landsat was important, with larger areas faring better, and identified modeling approaches which appear to work better than others.

1.3 Citations

Ahern, F.J. and Leckie, D.G. 1987. Digital remote sensing for forestry: Requirements and capabilities, today and tomorrow. Geocarto International **2**(3): 43–52.

Andersen, H.E., McGaughey, R.J. and Reutebuch, S.E. 2005. Estimating forest canopy fuel parameters using LIDAR data. Remote Sensing of Environment **94**(4): 441–449.

Andersen, H.E., Strunk, J. and Temesgen, H. 2011a. Using Airborne Light Detection and Ranging as a Sampling Tool for Estimating Forest Biomass Resources in the Upper Tanana Valley of Interior Alaska. Western Journal of Applied Forestry **26**(4): 157–164.

Andersen, H.-E., Strunk, J., Temesgen, H., Atwood, D. and Winterberger, K. 2011b. Using multilevel remote sensing and ground data to estimate forest biomass resources in remote regions: a case study in the boreal forests of interior Alaska. Canadian Journal of Remote Sensing **37**(6): 596–611.

Barrett, T.M., Christensen, G.A. and Pacific Northwest Research Station (Portland, O.. 2011. Forests of Southeast and South-central Alaska, 2004-2008: Five-year Forest Inventory and Analysis Report. US Department of Agriculture, Forest Service, Pacific Northwest Research Station.

Cihlar, J., Latifovic, R., Beaubien, J., Trishchenko, A., Chen, J. and Fedosejevs, G. 2003. National scale forest information extraction from coarse resolution satellite data, Part 1. Data processing and mapping land cover types. In Remote Sensing of Forest Environments: Concepts and Case Studies, Springer, p. 552.

Corona, P. and Fattorini, L. 2008. Area-based lidar-assisted estimation of forest standing volume. Can. J. Forest. Res. **38**(11): 2911–2916.

DeVelice, R.L. 2012. 10 Accuracy of the LANDFIRE Alaska Existing Vegetation Map over the Chugach National Foreset. LANDFIRE. Assessments.

Donoghue, D.N.M., Watt, P.J., Cox, N.J. and Wilson, J. 2007. Remote sensing of species mixtures in conifer plantations using LiDAR height and intensity data. Remote Sensing of Environment **110**(4): 509–522.

Ene, L., Næsset, E. and Gobakken, T. 2012. Single tree detection in heterogeneous boreal forests using airborne laser scanning and area-based stem number estimates. International Journal of Remote Sensing **33**(16): 5171–5193.

Garner, R. 2012. NASA - Landsat Overview.

Gobakken, T. and Næsset, E. 2008. Assessing effects of laser point density, ground sampling intensity, and field sample plot size on biophysical stand properties derived from airborne laser scanner data. Can. J. Forest. Res. **38**(5): 1095–1109.

Gregoire, T.G., Stahl, G., Naesset, E., Gobakken, T., Nelson, R. and Holm, S. 2011. Model-assisted estimation of biomass in a LiDAR sample survey in Hedmark County, Norway. Canadian Journal of Forest Research **41**(1): 83–95.

Gregoire, T.G. and Valentine, H.T. 2008. Sampling Strategies for Natural Resources and the Environment. 1st ed. New York: Chapman and Hall/CRC. 474 p.

Hall, R.J. 2003. The roles of aerial photographs in forestry remote sensing image analysis. (Pages 47-75 in Wulder MA,Franklin SE. Methods and Applications for Remote Sensing of Forests: Concepts and Case Studies.). Kluwer Academic Publishers, Boston/Dordecht/London.

Hinsley, S.A., Hill, R.A., Bellamy, P.E. and Balzter, H. 2006. The application of lidar in woodland bird ecology: climate, canopy structure, and habitat quality.

Howard, J.A. 1991. 621 Remote sensing of forest resources: theory and application. Chapman & Hall.

Huang, C., Homer, C. and Yang, L. 2003. Regional forest land-cover characterizations using medium spatial resolution satellite data. (Pages 47-75 in Wulder MA,Franklin

SE. Methods and Applications for Remote Sensing of Forests: Concepts and Case Studies.). Kluwer Academic Publishers, Boston/Dordecht/London.

Hudak, A.T., Crookston, N.L., Evans, J.S., Falkowski, M.J., Smith, A.M.S., Gessler, P.E. and Morgan, P. 2006. Regression modeling and mapping of coniferous forest basal area and tree density from discrete-return lidar and multispectral satellite data. Canadian Journal of Remote Sensing **32**(2): 126–138.

Hyyppä, J., Hyyppä, H., Inkinen, M., Engdahl, M., Linko, S. and Zhu, Y.-H. 2000. Accuracy comparison of various remote sensing data sources in the retrieval of forest stand attributes. Forest Ecology and Management **128**(1-2): 109–120.

Jobin, L. and Beaubien, J. 1974. Capability of ERTS-1 imagery for mapping forest cover types of Anticosti Island. The Forestry Chronicle **50**(6): 233–237.

Johnson, E.W. 2000. Forest sampling desk reference. CRC.

Kirvida, L. and Johnson, G.R. 1973. Automatic interpretation of ERTS data for forest management.

Lohr, S.L. 2009. Sampling: design and analysis. Thomson.

Maclean, G.A. and Krabill, W.B. 1986. Gross-merchantable timber volume estimation using an airborne LIDAR system. Canadian Journal of Remote Sensing **12**: 7–18.

Magnusson, M., Fransson, J.E.S. and Holmgren, J. 2007. Effects on estimation accuracy of forest variables using different pulse density of laser data. Forest Sci. **53**(6): 619–626.

Mutlu, M., Popescu, S.C., Stripling, C. and Spencer, T. 2008. Mapping surface fuel models using lidar and multispectral data fusion for fire behavior. Remote Sensing of Environment **112**(1): 274–285.

Nelson, R., Krabill, W. and Tonelli, J. 1988. Estimating forest biomass and volume using airborne laser data. Remote Sensing of Environment **24**(2): 247–267.

Opsomer, J.D., Breidt, F.J., Moisen, G.G. and Kauermann, G. 2007. Model-assisted estimation of forest resources with generalized additive models. Journal of the American Statistical Association **102**(478): 400–409.

Parker, R.C. and Evans, D.L. 2007. Stratified light detection and ranging double-sample forest inventory. South. J. Appl. For. **31**(2): 66–72.

Peuhkurinen, J., Mehtätalo, L. and Maltamo, M. 2011. Comparing individual tree detection and the area-based statistical approach for the retrieval of forest stand characteristics using airborne laser scanning in Scots pine stands. Canadian Journal of Forest Research **41**(3): 583–598.

Russel, R.E., Saab, V.A. and Dudley, J.G. 2007. Habitat-Suitability Models for Cavity-Nesting Birds in a Postfire Landscape. Journal of Wildlife Management **71**(8): 2600–2611.

Schreuder, H.T., Ernst, R. and Ramirez-Maldonado, H. 2004. Statistical techniques for sampling and monitoring natural resources. Rocky Mountain Research Station.

Shiver, B.D. and Borders, B.E. 1995. Sampling Techniques for Forest Resource Inventory. Wiley.

Ståhl, G., Holm, S., Gregoire, T.G., Gobakken, T., Næsset, E. and Nelson, R. 2011. Model-based inference for biomass estimation in a LiDAR sample survey in Hedmark County, NorwayThis article is one of a selection of papers from Extending Forest Inventory and Monitoring over Space and Time. Can. J. For. Res. **41**(1): 96–107.

Strunk, J.L., Reutebuch, S.E., Andersen, H.-E., Gould, P.J. and McGaughey, R.J. 2012. Model-Assisted Forest Yield Estimation with Light Detection and Ranging. Western Journal of Applied Forestry **27**(2): 53–59.

Sullivan, A.A., McGaughey, R.J., Andersen, H.E. and Schiess, P. 2009. Object-oriented classification of forest structure from light detection and ranging data for stand mapping. Western Journal of Applied Forestry **24**(4): 198–204.

2 Manuscript 1

Effects of Lidar Pulse Density and Sample Size on a Model-Assisted Approach to Estimation of Forest Inventory Variables

Jacob Strunk, Hailemariam Temesgen, Hans-Erik Andersen, James P. Flewelling, and Lisa Madsen

Canadian Journal of Remote Sensing

Canadian Aeronautics and Space Institute

350 Terry Fox Drive, Suite 104

Kanata, ON K2K 2W5, Canada

(Manuscript Submitted April 2012)

Abstract

Using lidar in a model-assisted approach to forest inventory has the potential to increase estimation precision for some forest inventory variables. This study documents the bias and precision of a model-assisted regression estimator approach to forest inventory with lidar-derived auxiliary variables relative to lidar pulse density and the number of sample plots.

For managed forests on the Lewis portion of the Lewis-McChord Joint Base (35025 ha, 23290 forested) in western Washington state, we evaluated a regression estimator for combinations of pulse density (.05 - 3 pulses / m^2) and sample size (15 – 105 plots) for estimation of the five forest yield variables basal area, volume, biomass, number of stems, and Lorey's height. The results indicate that there is almost no loss in precision in using as few as .05 pulses / m^2 relative to 3 pulses / m^2. In contrast, precision for reduced sample sizes declines quickly and even affects the validity of inference; simulations indicate that central limit theorem based confidence intervals were too small on average for sample sizes smaller than 45.

The results from this study can aid in selecting an appropriate pulse density and sample size.

2.1 Introduction

Over the last several decades many studies have used models to relate forest variables to variables derived from airborne scanning lidar (lidar metrics) including basal area (Lefsky et al., 1999), stem volume (Næsset, 1997b), stand height (Næsset, 1997a), biomass (Lefsky et al., 1999; Means et al., 1999), and others. The many studies documenting the relationship between lidar and forest variables are important because they indicate that there is a strong association between the two types of variables, although the studies may provide limited descriptions of how the models should be used for practical inference. The most common approach to inference in forest inventory and survey sampling in general is design-based inference. In the design-based context a probability sample is used to make inference about parameters of a finite population (e.g. the population mean or total). If a forest analyst wished to estimate the carbon present in a forest and achieve a level of confidence in the estimate, the analyst would most often use a design-based estimator. Lidar metrics and a model can be leveraged in a design-approach by using a model-assisted approach (Parker and Evans, 2007; Corona and Fattorini, 2008). For the same number of plots a model-assisted approach with lidar can for some variables increase estimation precision over a plot-only approach.

As with planning a traditional design-based inventory, it is desirable to quantify the effect that inventory design parameters have on estimation precision. Increasing the number of ground plots is one possible way to modify a design to increase estimation precision. In the case of model-assisted forest inventory with lidar (FIWL), lidar pulse

density is a lidar acquisition parameter that must be specified in addition to the number of ground plots. The effects of lidar pulse density have been examined in a forestry setting using at least three approaches, including by thinning the data (Holmgren, 2004; Gobakken and Næsset, 2008; Maltamo et al., 2006), performing multiple lidar acquisitions for the same area (Parker and Glass, 2004; Næsset, 2004), and by generation of synthetic lidar data (Lovell et al., 2005). There appears to be a consensus among findings that reduction in pulse density increases the variability in lidar metrics (sometimes this is expressed implicitly in studies, such as in increased standard error (SE) estimates for model coefficients for reduced pulse density) which is in accordance with the consistency property (asymptotically approaches the true value as the sample size increases) of statistics which are used to summarize lidar height values, but studies differ in whether there is an effect on the variability of residuals around the regression line. The study by Gobakken and Næsset (2008) additionally details the effects of number of ground plots and the size of ground plots. Both of these had an effect on residual bias and root mean square error (RMSE). While these studies have exclusively focused on model behavior, they are highly relevant for estimation of population parameters in the model-assisted context because model behavior plays an important role in the estimation of variance for model-assisted estimators.

The objective of this study is to look at the effects of pulse density and sample size on regression estimator precision for selected forest attributes, biases of estimators of the standard deviations of regression estimators, and on 95% confidence interval coverage

probabilities for a model-assisted regression estimation approach. We pursue our aim with a simulation approach. We simulate sampling distributions of model-assisted mean and mean variance estimators for different combinations of pulse density and sample size. The performance of estimators for a given pulse density and sample size is assessed by looking at properties of the sampling distributions of estimators, and by contrasting model-assisted and simple random sampling (SRS) estimators. The related study by Strunk et al. (2012) provides a practical demonstration of inference for an entire forest using regression estimation with lidar metrics as auxiliary variables. This study extends the work of previous studies that have looked at the effects of pulse density and sample size on residual variability by looking at the implications of pulse density and sample size for design-based estimation. Our inference here is restricted to cases where wall-to-wall lidar is used, but our results concerning the effect of sample size and pulse density on estimation can be easily extended to other approaches (e.g. lidar strip sampling as in Andersen et al., 2011).

2.2 Methods

2.2.1 Study Site

This study was conducted on the forested areas of the Fort-Lewis military installation (47^0 30' 58" N 122^0 35' 11" W) in western-Washington state, USA (Figure 2.1). Managed forests are dominated by conifer trees, especially Douglas-fir with interspersed western hemlock (*Tsuga heterophylla (Raf.*) Sarg.), western red cedar (Thuja plicata Donn ex D.Don) and very limited amounts of Sitka spruce (*Picea sitchensis* (Bong.) Carrièr) and pacific yew (*Taxus brevifolia* Nutt.). Hardwood trees

are also present on managed sites, mostly in the wet areas, including red alder (*Alnus Rubra* Bong.), big leaf maple (*Acer Macrophyllum* Pursh) and black cottonwood (*Populus balsamifera ssp. Trichocarpa* (Torr. & A. Gray ex Hook.) Brayshaw).

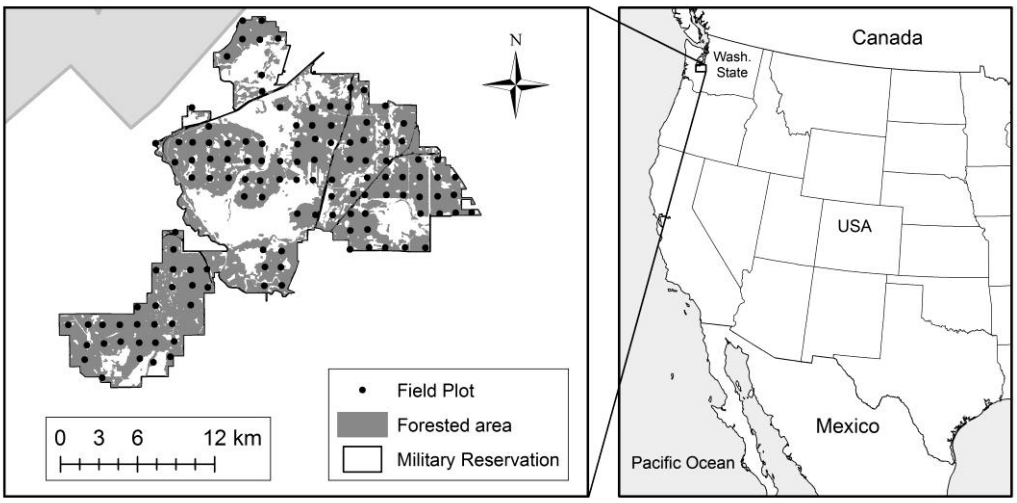

Figure 2.1 Location of study area in central western-Washington state

2.2.2 Data Description

2.2.2.1 Forest inventory variables

Values of forest inventory variables were calculated for 120 circular 809 m^2 (0.2 acres) continuous forest inventory plots measured between May of 2004 and January of 2005. The plots are distributed on a 1.28 × 1.28 km grid within forested areas of the study site. Field measurements recorded for each tree that we used include diameter at breast height (dbh) measured at 1.37 m, and species. Because measurements were not consistently taken on trees less than 20.32 cm in diameter, trees with dbh's less than 20.32 cm were excluded from plot tabulations. Tree heights were measured for a subset of trees on plots, approximately 2.5 trees per plot.

Unmeasured Douglas-fir heights were estimated using a non-linear mixed effects model (Temesgen et al., 2008) developed specifically for this study using Fort Lewis inventory data. There were insufficient numbers of trees from other species to model heights in this way. Heights for other species were estimated using the Wykoff et al. (1982) model form with Eugene-area (Oregon state, USA) parameter estimates from the Pacific Northwest Coast Variant Overview for the Forest Vegetation Simulator (Keyser, 2010). The values for five variables were calculated for each plot (Table 2.1) including basal area (ba), total stem volume including top and stump (vol), mean height weighted proportional to ba – Lorey's height (lor), total aboveground biomass (bm) and number of trees (stems). Vol was estimated using the allometric models included with the National Volume Estimator Library plug-in for excel (USFS, 2008) and bm was estimated using the models provide by Jenkins et al. (2004).

Table 2.1 Summary of plot level variables.

variable	mean	min.	max.	st. dev.
ba (ft^2 / ha)	35.1	0	130.9	21.1
vol (ft^3 / ha)	453	0	2376	334
stems (/ha)	220	0	864.9	156
bm (kg / ha)	294	0	1508	205
lor (m)	35.1	0	59.27	9.42

2.2.2.2 Precision plot positioning

Coordinates for plot centers were collected between September 2007 and May 2008. Survey-grade differential global navigation satellite system (GNSS) receivers were used to survey plot centers marked with stakes. GNSS data were post-processed,

including differentially corrected, using the Ensemble processing suite from Javad Navigation Systems (now Javad GNSS) to achieve the desired level of accuracy, approximately 1m horizontal RMSE, under dense northwestern USA forest canopy (Andersen et al., 2009; Clarkin, 2007).

2.2.2.3 Lidar data and variables

The lidar data used for this study were acquired in September 2005 (leaf on) within one growing season from when field measurements were performed. Lidar data were collected from a fixed wing aircraft. The airplane flying height was approximately 1000m above ground, the scan angle was +/- 14 degrees, and the laser beam divergence was 0.3 mrad. The pulse repetition frequency (PRF) was approximately 71 kHz and the nominal pulse density was 4 pulses / m^2. The vendor collected the data with an Optech ALTM 3100.

The lidar metrics used in this study are a series of statistics calculated on the lidar height data. The statistics were computed on first return lidar heights above 1m, including the mean, standard deviation, and percentiles (e.g. ht_5 and ht_{95} represent 5^{th} and 95^{th} percentile heights). We also computed the ratio of the number of first returns above a given height relative to the total number of first returns for a plot (e.g. $cover_1$ and $cover_2$ are the proportions of returns above 1 and 2 m respectively). Lidar heights were estimated by subtracting ground elevations from lidar elevations. Ground hit designation and interpolation to a raster processing were performed with FUSION (McGaughey, 2012) in addition to other lidar processing tasks.

2.2.3 Regression estimation

In this study we make use of a regression estimator (Särndal et al., 1992, 225–238) for the mean

$$\hat{\mu}_y = \mu_X^T \hat{\beta} \quad \textbf{(1)}$$

where

$\hat{\mu}_y$ is the regression estimate of the response mean

$\hat{\beta}$ is a vector of regression coefficients fitted with OLS including the intercept,

μ_X^T is the transpose of a vector of means of auxiliary variables including a 1.0 corresponding to the intercept.

An accompanying SE is

$$SE_{\hat{\mu}} \approx \sqrt{\frac{s_{reg}^2}{n}} \quad \textbf{(2)}$$

where

$SE_{\hat{\mu}}$ is the standard error of the regression estimate of the mean,

n is the size of the sample,

s_{reg}^2 is the variance of the regression residuals.

This formulation of a regression estimator is appropriate when the auxiliary variables are available for the entire finite population of interest, and the sample was collected using an SRS design (Lohr, 1999; Gregoire and Valentine, 2008; Särndal et al., 1992). Using SRS estimators for a systematic sample will yield unbiased mean estimates, but SEs under a systematic design will tend to be conservative (too large) when using SRS estimators unless periodicity of the attribute of interest matches the interval of the systematic sample. This bias of the variance estimator is typically ignored because there is not a design-unbiased estimator for systematic designs. In the model-assisted approach to estimation, inference is dependent upon having a probability sample, and does not require that the model fits the data – which is a requirement for model based inferences with an OLS model. We contrast this aspect of model-assisted inference with model-based inference because of the practical result that we need not assume linearity, homogenous variance, and correct specification of the model to make inference from an OLS model – although a model that fits the data well is likely to have lower residual variance.

2.2.4 Simulations

2.2.4.1 General description

In this study we use resampling to approximate the sampling distributions of estimators for given pulse densities and sample sizes. The resampling approach that we use for inference in this study is methodologically very similar to bootstrap variance estimation (Efron and Tibshirani, 1993). However, for convenience we defined our population as our complete sample, all 120 observations collected in the

field. This approach is similar to the approach used by Andersen and Breidenbach (2007) to contrast several approaches to estimation with lidar. We elected to treat our sample as the population because we were not attempting to estimate parameters of the original population; we were attempting to describe general behavior of an estimation strategy relative to pulse density and sample size. This is not to say that our results will hold everywhere, but they can serve to highlight general trends and issues and can be indicative of their behavior for similar areas and sampling designs.

2.2.4.2 Lidar thinning

To assess the effect of pulse density on inference in model-assisted estimation the original lidar point cloud was thinned repeatedly to reduced pulse densities. The pulse densities examined are .05, .3, .45, .6, .85, 1, 2, and 3 pulses / m^2. Thinning, along with other lidar processing, was performed using FUSION. The first step in the thinning procedure was to thin the original lidar dataset for large (relative to the plots) 314m wide squares centered on the ground plots. The large squares contain both the plots and buffer regions around the plots to eliminate edge effects within field plots when creating digital elevation models (DEMs) and thinning the lidar. Reduced pulse density data on the 314 x 314 m squares were then used to select ground returns and create bare-earth digital elevation models. A 3m median smoother was applied to each ground DEM. DEM elevations were then subtracted from lidar elevations to calculate lidar height values. The reduced density elevation-corrected lidar data was then clipped to the extents of the precisely geo-referenced ground plots. Finally, lidar metrics were calculated for each thinned lidar dataset.

2.2.4.3 OLS regression

The relationship between measures of forest yield (e.g. ba) and lidar metrics was modeled using OLS regression. OLS models were fitted using a two step procedure: 1) prior to the simulations predictor variables were selected to include in the models 2) model parameters were re-estimated using the fixed set of predictors for each of 5000 random resamples. Model RMSE values were calculated for each of the 5000 models (fit to the 5000 resamples of data). We initially considered inclusion of an automated variable selection algorithm in the simulations to allow different variables for each simulation, but found that the choice of model-selection algorithm highly influenced the results.

The sets of predictor variables used for regression were selected by comparing the RMSEs of a variety of models using all 120 observations and comparing their Bayesian information criterion (BIC) scores – one of several common bases for variable selection (Schwarz, 1978). Additionally, we preferred simple models that included at least one height quantile metric and one cover metric. Interactions between variables selected for inclusion were also explored. No transformations of the responses were used because there was only very mild heteroskedasticity, and model-assisted inference does not require equal variance. The same set of predictors was used for ba, vol, stems, and bm (ht_{25}, $cover_{1.37}$, and $cover_{1.37} \times ht_{70)}$ with a slightly different set used for lor (ht_{70}, ht_{95}, $cover_{1.37}$, and $cover_{1.37} \times ht_{95}$). It should be noted that many different sets of predictors fared comparably in terms of BIC, RMSE, and simplicity,

and that the selection of one of the many comparable sets of variables is somewhat arbitrary, but that this has no effect on our ability to make inference.

2.2.4.4 Estimator performance

We used a straightforward basis to evaluate the mean estimator for different combinations of pulse density and sample size. First, we sampled from our population of 120 elements to a reduced sample size 5000 times with replacement. For each sample we estimated the population mean using the regression estimator (1) and calculated deviations (or residuals) of mean estimates from the known population mean

$$\varepsilon_{\hat{\mu},i} = \hat{\mu}_i - \mu \,. \qquad \textbf{(3)}$$

The empirical distribution of mean residuals was evaluated using the mean (or bias)

$$B_{\hat{\mu}} = \frac{\sum_{i=1}^{5000} \varepsilon_{\mu,i}}{5000} \qquad \textbf{(4)}$$

and standard deviation

$$\sigma_{\hat{\mu}} = \sqrt{\frac{\sum_{i=1}^{5000} \left(\varepsilon_{\mu,i} - B_{\hat{\mu}}\right)^2}{5000-1}} \,. \qquad \textbf{(5)}$$

A smaller bias and standard deviation of mean residuals indicates superior performance for a given configuration of pulse density and sample size.

We used a two step procedure to evaluate the performance of SEs relative to pulse density and sample size. Our first step was to approximate the sampling distribution of the regression estimates of the mean. An approximate sampling distribution of means estimates was generated by taking 5000 samples with replacement from our population of 120 elements and applying the regression estimator to each sample. Because we have taken 5000 repeated samples from our population it allows us to unbiasedly estimate the standard deviation of the regression estimator by taking the standard deviation of the 5000 estimates. And since the number of samples is large, 5000, the variability of our estimate will be very small. This value was treated as if it was the actual standard deviation of mean estimates, $\sigma_{\hat{\mu}}$, a population parameter. The second step to our evaluation was to approximate the sampling distribution of SEs using the 5000 samples. For each of the 5000 samples we estimated the SE in addition to the mean. The SEs for each sample, $SE_{\hat{\mu}}$, were then differenced from $\sigma_{\hat{\mu}}$

$$\varepsilon_{\hat{\sigma}} = SE_{\hat{\mu}} - \sigma_{\hat{\mu}}. \quad \textbf{(6)}$$

Again, a small bias

$$B_{\hat{\sigma}} = \frac{\sum_{i=1}^{5000} \varepsilon_{\hat{\sigma},i}}{5000} \quad \textbf{(7)}$$

and small variance

$$\sigma_{\hat{\sigma}} = \sqrt{\frac{\sum_{i=1}^{5000}\left(\varepsilon_{\hat{\sigma},i} - B_{\hat{\sigma}}\right)^2}{5000-1}} \quad \textbf{(8)}$$

of residuals indicates superior performance for the analytical variance estimator. We then used the distribution of SE estimates and looked at coverage probability, the proportion of confidence intervals developed from SE estimates for a given confidence level that cover the population mean.

For each combination of pulse density and sample size we also calculated the relative precision

$$RP_{nk} = \frac{\sigma^2_{\hat{\mu}}}{\sigma^2_{SRS,120}}, \quad \textbf{(9)}$$

where

RP_{nk} is the relative precision of the regression estimator for n_k observations,

$\sigma^2_{SRS,120}$ is the variance of 5000 SRS sample mean estimates for 120 plots.

Relative precision is analogous to design effect (Särndal et al., 1992, 53–55) which is used to roughly indicate the efficiency (precision relative to sample size) of an estimation strategy. Multiplication of relative precision reported in this study by the

ratio $\frac{n_k}{120}$ will yield a value that is equivalent to design effect for a given pulse density and sample size.

2.3 Results and Discussion

2.3.1 Model performance

The magnitudes of percent RMSE differed by response variable, but the general behavior relative to pulse density and sample size was similar for the five response variables examined (ba, vol, bio, stems, and lor). Reduction in sample size caused a noticeable increase in the median model RMSE and had a pronounced effect on the variability of the distribution of RMSEs, shown for ba in Figure 2.2, and for all of the variables for a fixed pulse density in table 2.2. The shaded curves in Figure 2.2 are empirical densities created from 5000 simulations for each of the combinations of pulse density and sample size. The effect of sample size was slight for samples with as few as 45 observations. Below this threshold the median of the simulation distribution of model RMSE's and the widths of the simulation distributions increased more rapidly. The effect of reduced pulse density on RMSE was slight. The behavior shown for ba relative to pulse density in Figure 2.2 is typical of the behavior for the remaining response variables. The median of the simulation distribution of RMSEs does not appear to change as a result of reduction in pulse density until pulse density is reduced to .05 pulses / m^2. The variances of the simulation distributions of RMSE values do, however, increase slightly for reductions in pulse density.

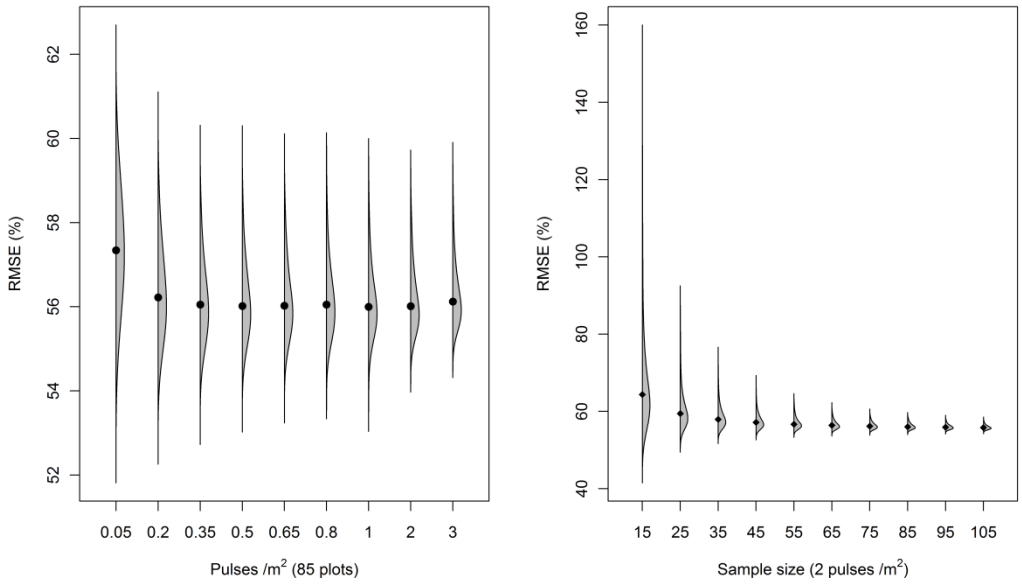

Figure 2.2 Simulation distributions of model RMSEs in percent of the mean by sample size and pulse density for ba. Black dots indicate the medians RMSEs and the horizontal lines indicate bounds of 95% empirical confidence intervals.

Table 2.2 Model RMSEs for different sample sizes using lidar with 1 pulse / m^2.

	Sample size									
Resp.	**15**	**25**	**35**	**45**	**55**	**65**	**75**	**85**	**95**	**105**
ba	11.6	10.8	10.6	10.4	10.3	10.3	10.2	10.2	10.1	10.1
stems	139.4	129.2	126.1	124.4	123.5	122.9	122.5	122.1	121.9	121.7
vol	200.3	190.3	186.4	183.8	181.8	180.4	179.4	178.4	177.6	177.1
bm	130.7	124.1	121.4	119.6	118.3	117.4	116.6	116.1	115.6	115.2
lor	5.3	4.9	4.8	4.7	4.7	4.6	4.6	4.6	4.6	4.6

2.3.2 Mean estimator

The behavior of the regression estimator of the mean relative to pulse density and sample size, shown in Figure 2.3 for lor, was similar to that observed for the remaining response variables. The sampling distributions of mean residuals indicate that the mean estimator is nearly unbiased and that, as we would expect, the variability of mean residuals increases for smaller sample sizes. However the decline in performance is slight for as few as 45 observations. Below this threshold the widths of 95% CIs increase more rapidly. Reduction in pulse density does not appear to affect the bias or variance of the regression mean estimator.

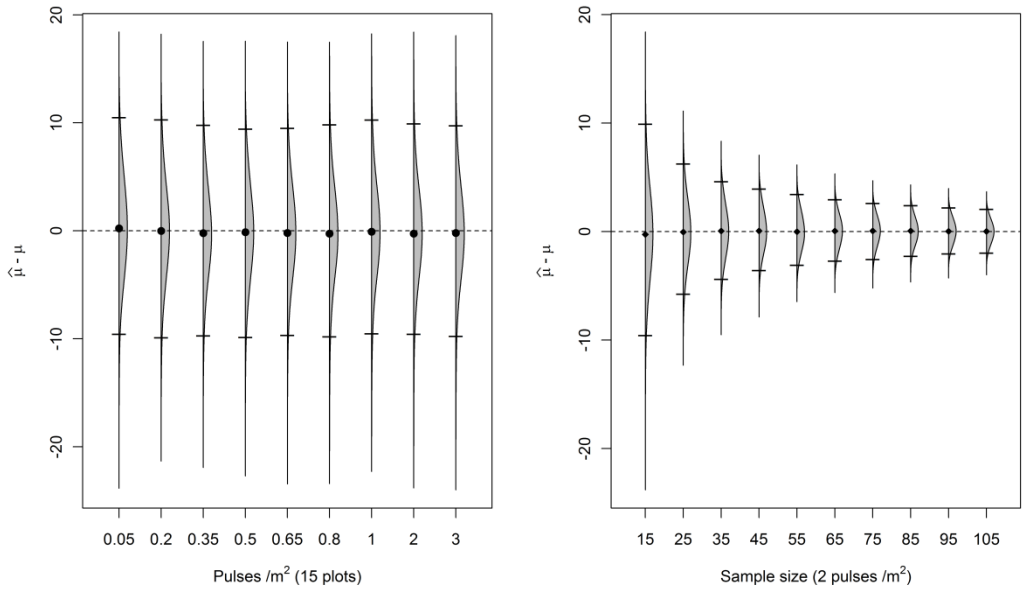

Figure 2.3 Simulation distributions of differences between estimates of mean lor and the population mean. Black dots indicate the medians of differences and the horizontal lines indicate bounds of 95% empirical confidence intervals.

2.3.3 SE performance

SEs varied methodically from negative to positive bias as sample sizes ranged from 15 to 105 plots. The trends in SE behavior displayed in Figure 2.4 when used to estimate bm is very similar to the trend observed when the estimator was used for the other variables, except that the point where median bias crossed from negative to positive bias ranged from 75 for stems to 75 for bm and vol. For bm, SEs were positively biased for 55 or more observations, approximately unbiased for 45 observations, and gradually increasingly negatively biased, to a maximum of -1%, for fewer than 45 observations. No effect from pulse density was detected on the SEs.

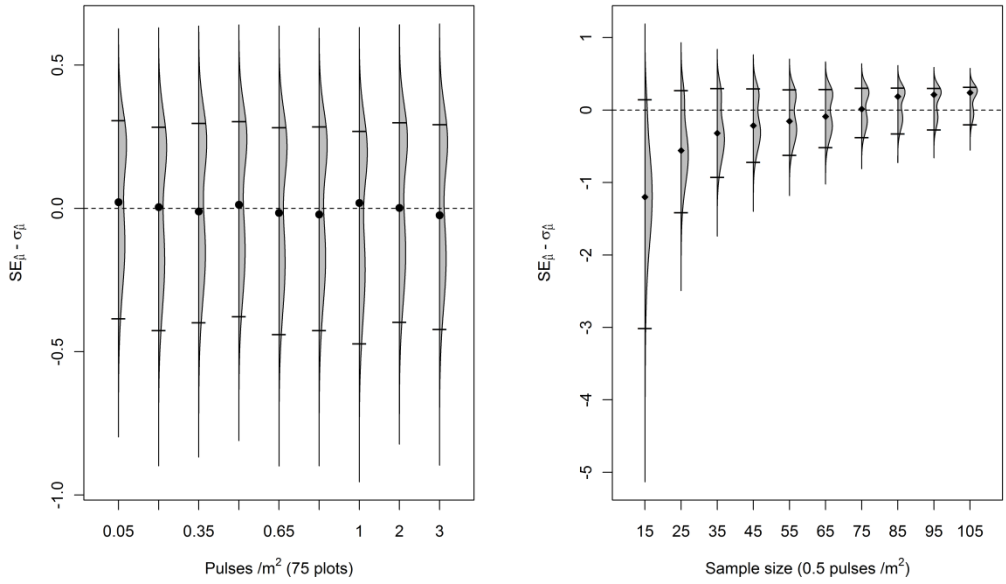

Figure 2.4 Simulation distributions of differences between sample SEs and the standard deviations of the sampling distributions of mean estimates for bio. Black dots indicate the medians of differences and the horizontal lines indicate bounds of 95% empirical confidence intervals.

The effect of variance estimator bias on analytical confidence intervals as a result of sample size was more dramatic. There was a sharp decline in the percentage of 95% asymptotic confidence intervals that cover the population mean following reductions in sample size to fewer than 35 observations (Table 2.3). This is perhaps not surprising since asymptotic properties are dependent upon having a reasonably large sample size, although it is important to demonstrate what is "reasonably large". Coverage probabilities were nearly unchanged for different pulse densities (not shown).

Table 2.3 Coverage probabilities by sample size for 1 pulse / m^2 for analytical two-side 95% confidence intervals.

	Coverage Probability				
sample size	**ba**	**stems**	**vol**	**bm**	**lor**
15	0.81	0.80	0.80	0.79	0.81
25	0.90	0.89	0.88	0.88	0.89
35	0.92	0.91	0.91	0.91	0.91
45	0.94	0.94	0.93	0.92	0.93
55	0.95	0.95	0.94	0.93	0.95
65	0.95	0.96	0.94	0.94	0.95
75	0.96	0.97	0.95	0.94	0.96
85	0.97	0.97	0.95	0.95	0.97
95	0.98	0.97	0.96	0.96	0.97
105	0.97	0.98	0.96	0.96	0.97

2.3.4 Relative precision

Relative precision varied for a given sample size amongst the response variables (Table 2.4), but were not affected by pulse density (not shown). Our primary interest in relative precision is the region where relative precision is equal to or smaller than 1.0. This is the region where the regression estimator provides greater estimation precision than with plots alone with 105 plots. Each of the response variables was sufficiently correlated with lidar metrics to yield some gain in precision from using the regression estimator. The threshold at which design effect was 1.0 or smaller varied from 35 to 75 plots. For sample sizes of 75 observations or more, regression estimation was more precise than SRS estimation on average for the forest inventory variable stems, the variable that fared poorest. The results for pulse density were not reported because they do not appear to have an effect on relative precision for the densities examined.

Table 2.4 Relative precision for regression estimates by sample size for 1 pulse / m^2

	Relative Precision				
sample size	**ba**	**stems**	**vol**	**bm**	**lor**
15	4.01	10.53	4.79	5.49	5.14
25	1.47	3.70	1.80	2.17	1.90
35	0.93	2.15	1.09	1.23	1.09
45	0.63	1.55	0.78	0.87	0.75
55	0.48	1.20	0.61	0.67	0.57
65	0.39	0.93	0.49	0.53	0.45
75	0.32	0.79	0.40	0.45	0.35
85	0.27	0.64	0.33	0.37	0.30
95	0.23	0.55	0.28	0.32	0.25
105	0.20	0.45	0.24	0.26	0.23

Note: The denominator sample size for relative precision calculations was fixed at 120.

2.4 Discussion

2.4.1 Pulse density

The effect of reduction in pulse density on estimation and inference in a model-assisted inventory with lidar was assessed in several ways. We looked at the effect of pulse density on model RMSE, on mean estimation precision, and on the precision of the SEs. The reduction in information present in lower density data caused model RMSE to increase slightly. However, the effect of reduction in pulse density was so small that it did not carry through to impact inference. There was no observed effect of pulse density on mean estimators.

The empirical study by Parker and Glass (2004) performed with .5 and 1m lidar pulse spacing corroborates our results in that they did not find an effect of pulse density on

estimation precision when using a double sampling estimator – although they looked at a much smaller range of densities. We are not aware of any other studies that detail the performance of model-assisted estimators relative to pulse density. As previously mentioned, there are a number of studies that have looked at model precision relative to pulse density for forest yield variables. In four studies of particular relevance, two of the studies found increased RMSE as a result of lower pulse density (Magnusson et al., 2007; Gobakken and Næsset, 2008), while two others did not (Holmgren, 2004; Maltamo et al., 2006). We found that there was a slight but negligible effect of pulse density on model RMSE. The discrepancy between our findings and others' may result from the fact that there are substantial methodological differences between our study and other studies. The differences in results highlight the constraint that results from this study may not extend to implementations of model-assisted forest inventories with lidar that deviate from our methodology.

The first methodological difference we noted between this and other studies was that we created highly smoothed DEMs. Smoothed DEMs have less detail, but they appear to be less susceptible to irregularities like pits and spikes. Secondly, our plot size was larger than the plots used in the studies that found a noticeable density effect. For the lowest pulse density we examined there were on average 40 pulses per plot, double or more the number of returns for alternate studies which encountered a density effect. The sample statistics used for this study, including percentiles (Serfling, 1980) and ratios, are consistent statistics; this means they asymptotically approach the true population parameter as the sample size increases. It is likely then that sample

statistics calculated for our plots with greater area achieved greater stability for a given pulse density than observed in studies which detected a density effect with smaller area plots.

The absence of a density effect on precision is an important result because it indicates that airplanes may fly higher and faster to achieve the same precision in estimation as achieved for narrower pulse spacing. Flying higher and faster may save both time and energy in the acquisition of lidar for forest inventory purposes. The savings from flying low-density lidar may make it feasible for more forest land managers to fly their forests, or to fly greater proportions of their land base if they are acquiring lidar in a sampling context (Andersen et al., 2011; Gregoire et al., 2011; Ståhl et al., 2011). However, the cost savings from choosing a reduced pulse density will depend upon details specific to each acquisition. Mobilization of the aircraft to the forest can be a major, or *the* major cost in acquiring lidar. If the distance to the forest is great, or the forest is small, then selection of a pulse density may have little impact on the cost of the acquisition. The cost of mobilization can be reduced if the timing of the acquisition is not critical; the vendor may be able to schedule a lidar acquisition over a forest when they are planning to be in the vicinity of the forest for another acquisition.

An important consideration with regards to lidar is that forest inventory is only one of many potential applications of lidar. In some instances lidar may be used for a great number of applications including detailed DTM extraction, individual tree segmentation, canopy surface modeling, and others. For alternative uses a reduced

pulse density may have drastic repercussions on what is feasible. For example, it is highly unlikely that accurate individual tree segmentation is feasible with 1 pulse / 20 m^2. However, for large acquisitions when forest inventory is the primary concern and the cost of mobilization is not the bulk of the acquisition cost, acquiring reduced pulse density wall-to-wall lidar appears to be a highly viable option to reduce the cost of the acquisition without affecting estimation precision for the variables we examined.

2.4.2 Sample size

The effects of sample size on model-assisted estimation and inference were evaluated by looking at resampling distributions of model RMSE, the regression mean estimator, and the SE for the regression mean estimator. Unlike reductions in pulse density, reductions in sample size clearly had a deleterious effect on performance, and for small samples biased the SE. The bias was small, but coverage probabilities were appreciably biased for small samples. This result indicates that for small sample sizes the analytical SE may provide misleading results. Ideally we prefer unbiased SEs, but even conservative (too large) variance estimators can be acceptable, within reason. However, with a negatively biased (too small) variance estimator, the probability that a confidence interval covers the true population parameter will be less than is expected. Also, there is no guarantee that the sample size thresholds for which the variance estimator is unbiased or conservative for this study will hold for other variables or other study areas –especially given alternative measurement and sampling protocols. It may prove useful to compare analytical and simulation confidence

intervals. This would help assess the bias of analytical variance estimators as well as non-normality and skewness in the resampling distribution of mean estimators.

The precision of the regression estimator for the variable stems, the variable that performed the poorest amongst the response variables examined, was superior with greater than 75 observations than the SRS estimator with 120 observations, as indicated by having a relative precision of approximately 1.0. From an estimation standpoint there would be no precision gain from using the regression estimator with lidar using 75 plots over performing SRS estimation with 120 plots, if stems is a critical variable. Practically speaking, a forest inventory may use a design which is more precise than with SRS. This means that 75 observations serve as a lower bound to achieve the same precision with the regression estimator as is achieved with 120 observations with the SRS estimator. To evaluate (roughly) the sample size that is required to realize a precision gain from using model-assisted estimation with lidar over another inventory requires that the design effect of the alternative design must also be estimated. However, presenting variance estimates for alternative designs is beyond the scope of this study. The results that we present are instead general so as to enable such comparisons for planning purposes.

A caveat is that if comparison between the precisions of regression estimates and estimates from another design and estimator are required for a forest type that is quite different from our study site, then the model variances from this study may not be appropriate. Instead, it should prove feasible to take advantage of the model variances

reported for a study site that is more similar to the forest of interest. SE estimates for the regression estimator for a variety of sample sizes can then be obtained by inserting a model variance estimate reported in the literature into equation (2) and then varying n_k across a range of sample sizes. Unfortunately, there is a sample size effect on model RMSE, but so long as the sample size contemplated is greater than 45 observations the effect is slight.

2.4.3 Limitations

A weakness in this study which is common to studies which estimate forest inventory variables is that some variables which were treated as if they were measured, such as volume and biomass, were actually estimated with allometric models. The effect of using predicted biomass and volume on variance estimators is not something that this or other similar studies take into consideration when estimating variability. However, the variables estimated with allometric models are highly correlated with ba. The results for ba can serve in some sense as a reality check on results for bm and vol.

A characteristic of this study that differs from some other studies using lidar to estimate forest attributes is that relatively few heights were measured for each plot. This is the result of using data from an operational forest inventory with a set measurement protocol instead of tailoring a new set of field measurements for this study. This resulted in larger model RMSEs for vol, bm, and lor than we see for ba even though vol, bm, and lor are more closely related to height – the forest characteristic represented by lidar predictors. If we measured each tree height it would likely reduce models' residual variability and increase the precisions of total and mean

estimators for vol, bm, and lor. As a result the standard errors reported here are likely conservative for a given pulse density and sample size relative to what could be obtained using data from inventories in which more tree heights were measured – although this will not introduce bias for this analysis.

Additionally, our field data does not include trees smaller than 8 inches. While this is problematic for management reasons, if only merchantable trees are considered the effect on variance estimates and hence our inference relative to pulse density and sample size is negligible. As the values ba, vol, bm are exponentially related to height and diameter (which are relatively small for these trees), the magnitude of the contribution of small trees to these variables (and lor, a function of ba and height) is also very slight. If there is interest in representing numbers of small trees, then clearly the effect on stems is very pronounced because small trees are weighted equally with large trees for this response variable.

2.5 Conclusions

Lidar is a tool that has gained popularity for remote measurement and monitoring of natural resources. Whether there is benefit to using lidar for forest inventory depends in large part on characteristics specific to each forest. This study should facilitate examination of whether using lidar will provide a gain in precision over an alternative estimation strategy for a specific forest and provide indication of an appropriate sample size and pulse density. Fortunately, almost no effect of pulse density was observed on model precision. We saw equivalent precision with 0.05 pulses / m^2 as with 3 pulses / m^2. In contrast, a sample size effect on residual variability was evident,

but the majority of the influence of sample size on the precision of the regression estimator of the mean is introduced by central limit theorem; as the sample size increases the variability of mean estimates declines proportional to n_k. The expected influence of n_k can be seen in the denominator of the variance estimator.

Unfortunately for inference for small samples, we found that central limit theorem based confidence intervals were too narrow for small samples (fewer than 35 to 45 observations). If fewer than 45 observations are used, caution should be taken with respect to inference from analytical confidence intervals.

2.6 Acknowledgements

We would like to acknowledge the USFS PNW research station (Alaska and Seattle offices) for funding and support for data collection and analyses. We would like to thank the public works department of the Fort Lewis military installation, especially Jeff Foster, for providing data and logistical support. Finally, we would like to thank four anonymous reviewers who provided valuable insights and critiques.

2.7 Citations

Andersen, H.E. and Breidenbach, J. 2007. Statistical properties of mean stand biomass estimators in a LIDAR-based double sampling forest survey design. In Proceedings of the ISPRS Workshop Laser Scanning 2007 and SilviLaser 2007, Espoo Finland: IAPRS, p. 8–13.

Andersen, H.E., Clarkin, T., Winterberger, K. and Strunk, J.L. 2009. An Accuracy Assessment of Positions Obtained Using Survey-and Recreational-Grade Global Positioning System Receivers across a Range of Forest Conditions within the Tanana Valley of Interior Alaska. West. J. Appl. For. **24**(3): 128–136.

Andersen, H.E., Strunk, J. and Temesgen, H. 2011. Using Airborne Light Detection and Ranging as a Sampling Tool for Estimating Forest Biomass Resources in the Upper Tanana Valley of Interior Alaska. Western Journal of Applied Forestry **26**(4): 157–164.

Clarkin, T. 2007. Modeling global navigation satellite system positional error under forest canopy based on LIDAR-derived canopy densities. M.Sc. thesis, Univ. of Washington, Seattle, Washington, USA. 99 p.

Corona, P. and Fattorini, L. 2008. Area-based lidar-assisted estimation of forest standing volume. Can. J. Forest. Res. **38**(11): 2911–2916.

Efron, B. and Tibshirani, R. 1993. An introduction to the bootstrap. CRC Press. 456 p.

Gobakken, T. and Næsset, E. 2008. Assessing effects of laser point density, ground sampling intensity, and field sample plot size on biophysical stand properties derived from airborne laser scanner data. Can. J. Forest. Res. **38**(5): 1095–1109.

Gregoire, T.G., Stahl, G., Naesset, E., Gobakken, T., Nelson, R. and Holm, S. 2011. Model-assisted estimation of biomass in a LiDAR sample survey in Hedmark County, Norway. Canadian Journal of Forest Research **41**(1): 83–95.

Gregoire, T.G. and Valentine, H.T. 2008. Sampling Strategies for Natural Resources and the Environment. 1st ed. New York: Chapman and Hall/CRC. 474 p.

Holmgren, J. 2004. Prediction of tree height, basal area and stem volume in forest stands using airborne laser scanning. Scand. J. Forest. Res. **19**(6): 543–553.

Jenkins, J.C., Chojnacky, D.C., Heath, L.S. and Birdsey, R.A. 2004. Comprehensive database of diameter-based biomass regressions for North American tree species. Gen. Tech. Rep. NE-319. Newtown Square, PA: US Department of Agriculture, Forest Service, Northeastern Research Station **45**.

Keyser, C.E. 2010. 49 Pacific Northwest Coast (PN) Variant Overview – Forest Vegetation Simulator. Fort Collins, CO: WO-Forest Management Service Center, USDA-Forest Service. Internal Report.

Lefsky, M.A., Harding, D., Cohen, W.B., Parker, G. and Shugart, H.H. 1999. Surface Lidar Remote Sensing of Basal Area and Biomass in Deciduous Forests of Eastern Maryland, USA. Remote Sensing of Environment **67**(1): 83–98.

Lohr, S.L. 1999. Sampling: Design and Analysis. Pacific Grove, CA: Duxbury Press. 494 p.

Lovell, J.L., Jupp, D.L.B., Newnham, G.J., Coops, N.C. and Culvenor, D.S. 2005. Simulation study for finding optimal lidar acquisition parameters for forest height retrieval. Forest Ecol. Manag. **214**(1-3): 398–412.

Magnusson, M., Fransson, J.E.S. and Holmgren, J. 2007. Effects on estimation accuracy of forest variables using different pulse density of laser data. Forest Sci. **53**(6): 619–626.

Maltamo, M., Eerikainen, K., Packalen, P. and Hyyppa, J. 2006. Estimation of stem volume using laser scanning-based canopy height metrics. Forestry **79**(2): 217.

McGaughey, R.J. 2012. FUSION/LDV: Software for LIDAR Data Analysis and Visualization, Version 3.01. USFS.

Means, J.E., Acker, S.A., Harding, D.J., Blair, J.B., Lefsky, M.A., Cohen, W.B., Harmon, M.E. and McKee, W.A. 1999. Use of large-footprint scanning airborne LiDAR to estimate forest stand characteristics in the western cascades of Oregon. Remote Sensing of Environment **67**(3): 298–308.

Næsset, E. 1997a. Determination of mean tree height of forest stands using airborne laser scanner data. Remote Sens. Environ. **52**(2): 49–56.

Næsset, E. 2004. Effects of different flying altitudes on biophysical stand properties estimated from canopy height and density measured with a small-footprint airborne scanning laser. Remote Sensing of Environment **91**(2): 243–255.

Næsset, E. 1997b. Estimating timber volume of forest stands using airborne laser scanner data. ISPRS. J. Photogramm. **61**(2): 246–253.

Parker, R.C. and Evans, D.L. 2007. Stratified light detection and ranging double-sample forest inventory. South. J. Appl. For. **31**(2): 66–72.

Parker, R.C. and Glass, P.A. 2004. High-versus low-density LiDAR in a double-sample forest inventory. South. J. Appl. For. **28**(4): 205–210.

Särndal, C.E., Swensson, B. and Wretman, J. 1992. Model assisted survey sampling. New York: Springer-Verlag. 694 p.

Schwarz, G. 1978. Estimating the Dimension of a Model. The Annals of Statistics **6**(2): 461–464.

Serfling, R.J. 1980. Approximation theorems of mathematical statistics. Wiley. 402 p.

Ståhl, G., Holm, S., Gregoire, T.G., Gobakken, T., Næsset, E. and Nelson, R. 2011. Model-based inference for biomass estimation in a LiDAR sample survey in Hedmark

County, NorwayThis article is one of a selection of papers from Extending Forest Inventory and Monitoring over Space and Time. Can. J. For. Res. **41**(1): 96–107.

Strunk, J.L., Reutebuch, S.E., Andersen, H.-E., Gould, P.J. and McGaughey, R.J. 2012. Model-Assisted Forest Yield Estimation with Light Detection and Ranging. Western Journal of Applied Forestry **27**(2): 53–59.

Temesgen, H., Monleon, V.J. and Hann, D.W. 2008. Analysis and comparison of nonlinear tree height prediction strategies for Douglas-fir forests. Can. J. Forest. Res. **38**(3): 553–565.

USFS. 2008. National Volume Estimator Library (NVEL).

Wykoff, W.R., Crookston, N.L. and Stage, A.R. 1982. User's guide to the stand prognosis model, USDA Forest Service, Intermountain Forest and Range Experiment Station, Ogden, Utah. Gen. Tech. Rep. INT-133 **112**.

3 Manuscript 2

Two-Stage Regression Estimation of Biomass with Multi-Temporal Landsat and a Sample of Lidar Strips - A Case Study on the Kenai Peninsula, Alaska

Jacob Strunk, Hailemariam Temesgen, Hans-Erik Andersen

Remote Sensing of Environment

Elsevier Journals Customer Service
3251 Riverport Lane
Maryland Heights, MO 63043, USA

(Submitted April 2012)

Abstract

In this study we examined whether regression estimators appropriate for a two-stage design using Landsat and a sample of 7 lidar strips as auxiliary data were more precise for estimation of biomass than Horvitz-Thompson (HT) estimators appropriate for simple random sample (SRS) and two-stage designs. Estimators appropriate for two-stage designs were compared with each other and with estimators appropriate for SRS designs. We additionally examined a composite estimator which combined Landsat and lidar-assisted estimators for a two-stage design. The study was carried out for our study site, a portion of the western lowlands of the Kenai Peninsula AK, USA.

Both the lidar and Landsat-assisted estimators for a two-stage design were estimated to be equivalently precise to the HT estimator for the SRS design with the same numbers of plot, with standard errors (SEs) on the order of 9-10 Tg. However, the composite estimator combining the two regression estimators for the two-stage design fared better than the HT estimator for the SRS design for the same number of sample plots. Additionally, we briefly demonstrate that by increasing the number of lidar strips it should be possible to reduce the SE without greatly affecting the number of sample plots required. This will also improve the precision of the composite estimator, but we did not analytically explore this relationship.

3.1 Introduction

Estimation of finite population parameters for a forest is not always feasible using traditional design-based estimators found in a standard forest measurements textbook. This is especially the case for remote areas with limited transportation infrastructure. Such remote areas may be extremely difficult to access to establish ground plots for inventory purposes. Sampling in remote areas may require more sophisticated sampling and estimation techniques, including composite and model-assisted approaches that can leverage remote-sensing information. While we emphasize these approaches for remote areas because traditional approaches are simply not feasible in many cases, these approaches are also likely to provide benefits even in areas with existing road-based transportation infrastructure.

Remote sensing data, such as stereo imagery, interferometric synthetic aperture radar (IfSAR or InSAR), and airborne lidar can be used to measure or estimate three-dimensional (3D) forest structure. These advanced remote sensing technologies have been shown to enable more precise estimators of forest inventory parameters which are highly correlated with vegetation height and cover, such as tree biomass and volume. Manual interpretation of stereo imagery was the preferred method to leverage 3D auxiliary information in forestry until scanning airborne lidar became well-known and widely available. Automated extraction of canopy surface is feasible with digital stereo imagery, but vegetation heights may require an accurate digital terrain model (DTM). There are few examples of estimation of forest variables like biomass with auxiliary variables automatically extracted from stereo images (St-Onge et al., 2008). In contrast, estimation of forest variables with lidar data, where lidar data are intrinsically 3D, is a field that is quite well developed. Lidar-assisted estimates of biomass and volume (e.g.) are precise and estimation is straightforward (Tonolli et al., 2011; Woods et al., 2011). An internet search for scholarly articles with keywords “lidar”, “biomass”, and “volume” yielded 980 records for 2011 alone. A similar search for “radar” instead of “lidar” yielded over a thousand records. In contrast to lidar,

IFSAR can provide 3D elevation data for large areas very quickly, making it much more cost effective than lidar for large areas, although the resolution of IFSAR data is usually much lower than the resolution of lidar. Using IFSAR data may be a highly viable approach to measuring 3D forest structure information and estimating biomass (Solberg et al., 2010).

While estimation of forest variables with lidar is now commonly described in research papers, most studies describe the use of wall-to-wall lidar for mapping or estimation (Strunk et al., 2012). This is not, however, always tenable – especially for large and remote areas. Attempting to obtain complete coverage with lidar over a large area may often prove prohibitively expensive. Instead, for large areas it may prove more realistic to obtain lidar as a sample (e.g. Parker and Evans 2004, Gregoire et al. 2011, Andersen et al. 2011). The most convenient strategy to adopt with lidar is to select a systematic sample of strips of lidar because it is relatively straightforward for an airplane mounted with a lidar sensor to fly parallel lines over a target area. Field plots within the lidar strips can then be used to estimate model parameters relating lidar derived variables and field plot derived variables. A two-stage estimator is necessary to estimate the total, with the first stage sampling units being lidar strips and the second stage sampling units being field plots.

Several studies have examined the synergy between lidar and other remote sensing data sources (Hyde et al., 2007; Kennaway et al., 2008). Currently it appears there is a single study which lidar strips with Landsat for estimation (Andersen et al., 2011b). The study by Andersen et al., (2011b) uses a nearest neighbor model with Landsat and IFSAR auxiliary information to apportion lidar strip based estimates of biomass to areas not sampled with lidar. In this study we consider a design-based alternative approach to examine whether it is possible to improve the precision of total estimates by compositing distinct lidar-assisted and Landsat-assisted biomass estimator. Composite estimation is an approach that takes advantage of multiple estimators to create a new estimator with increased precision. In the forestry context the estimators

could, for example, be based on a combination of current and previous inventories (Särndal et al., 1992, 368–379), separate estimators (McTague, 2010), or take advantage of different inventories performed for different reasons or by separate agencies (Lund and Schreuder, 1980). In the context of this study, we are interested in the estimated improvement in estimator precision that is obtained by combining multiple remote-sensing based estimators relative to a single estimator. This is a particularly enticing approach because in some instances it is fairly cheap and easy to obtain multiple estimators. Estimators that take advantage of the large body of free Landsat data as well as previous inventory data are examples that would be inexpensive to implement (although we do not look at previous inventory data in this study).

The primary objective of this study is to examine whether a two-stage lidar-assisted approach to estimation of biomass can be more efficient than a plot-only based approach using an estimator appropriate for a simple random sample (SRS) design. And, since Landsat is free and readily available, we are also secondarily interested in testing whether Landsat can be easily and beneficially incorporated into a model-assisted approach to augment lidar-assisted estimation. We examine individual model-assisted estimators with auxiliary lidar and Landsat, as well as a composite estimator which is a weighted combination of the two-stage lidar and Landsat-assisted estimators. The tradeoff between precision and number of sample strips is examined, and several additional estimation strategies are explored as an aside to provide context to the estimators of primary interest.

3.2 Methods

3.2.1 Study site

Our study site was located in the western lowlands of the Kenai Peninsula in south-central Alaska (Figure 3.1). The western Kenai lowlands cover approximately 8200 km^2. To facilitate the use of Landsat for this investigation, the extent of the study site was restricted to the portion of the lowlands that fall within a single Landsat scene,

approximately 7400 km^2. A variety of forest types are present including black spruce (Picea mariana) predominating in poorly drained areas, and mixed stands populated by paper birch (Betula papyrifera), white spruce (Picea glauca), and quaking aspen (Populus tremuloides) predominating in upland areas. This study site was selected because it is the only boreal forest area in Alaska that is covered by the US Forest Service (USFS) Forest Inventory and Analysis (FIA) program's annual inventory (Bechtold and Patterson, 2005). FIA has established a 10-panel inventory design on the Kenai lowlands. The western Kenai Peninsula is more accessible than other boreal forests due to the relatively gentle terrain and the presence of several communities connected by an extensive road system, reducing the cost of plot access.

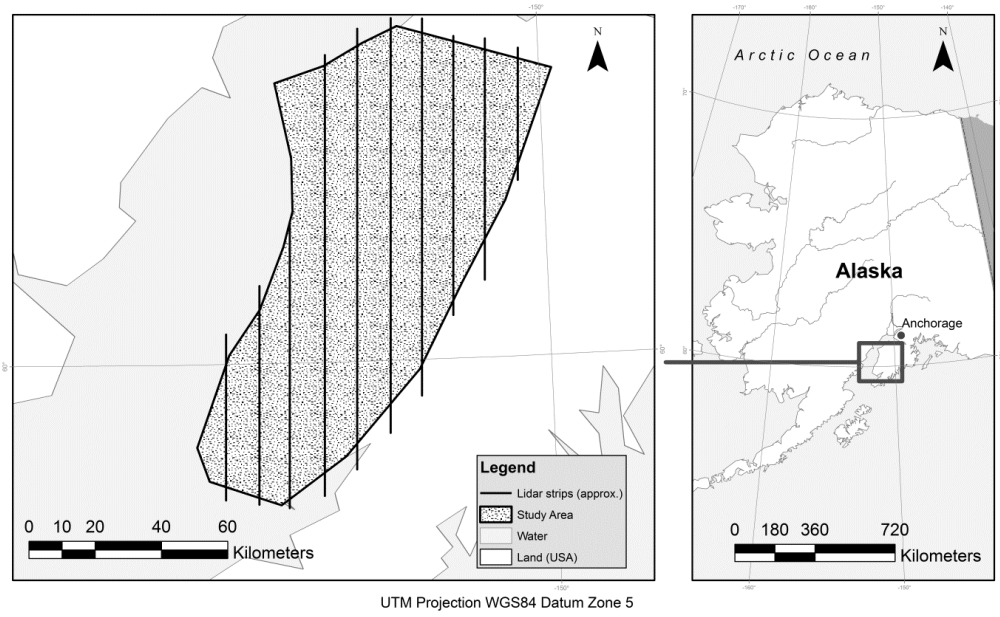

Figure 3.3.1 Overview of study area on the Kenai Peninsula, Alaska

3.2.2 Data

3.2.2.1 FIA plots

Forest inventory data were compiled from the database of United States Forest Service (USFS) Forest Inventory and Analysis (FIA) individual tree measurements for the Kenai Peninsula, Alaska. The measurements were taken on FIA plot clusters containing four circular sub-plots each (Bechtold and Patterson, 2005). Under the FIA sampling design, Alaska is divided into inter-penetrated panels consisting of equilateral hexagonal polygons of equal area. While in the lower 48 contiguous states field plots are randomized within each hexagon, on the western Kenai peninsula of Alaska the entire grid of field plots was randomized a single time – thus adjacent plot are approximately a fixed distance apart. Each plot consists of 4 subplots 168.11 m^2 in area. The 4 subplots include 3 satellite plots 36.578 meters from a center plot, placed 120 degrees apart, and aligned with magnetic north (Bechtold and Patterson, 2005).

The ground data used in this study were collected between 2005 and 2009 as part of the annual inventory program. We compiled biomass for each subplot from individual tree records in the FIA database (The Forest Inventory and Analysis Database: Database Description and Users Manual Version 3.0 for Phase 2, n.d.). The biomass values in the FIA database were predicted by FIA using species-specific allometric equations – an important contribution error but one that we do not treat explicitly. The minimum biomass observed (predicted by allometry) biomass at a subplot was 0.0 Mg / ha, the maximum was 281.6 Mg / ha, the median was 41.8 Mg/ha, the mean was 59.3 Mg / ha, and the first and third quartiles were 11.7 and 87.6, with a standard deviation of 60.5 Mg / ha.

Subplot data are typically averaged prior to an analysis by FIA; however we maintained separate records for each subplot for modeling purposes. Our analyses required fitting regression models between response variables (measured on the field plots) and remotely sensed auxiliary variables (lidar, Landsat, and DEM derived). The regression analyses were performed at the subplot level, but prior to computing

landscape estimates, subplot response predictions and corresponding residual error predictions in per hectare units were averaged (separately) for each plot.

3.2.2.2 Plot coordinates

For a random subset of plots on the Kenai peninsula, subplot coordinates were precisely georeferenced using survey grade L1/L2 GPS/GLONASS global navigation satellite system (GNSS) receivers. Receiver antennas were raised to 3 meters using a bipod and the receiver was allowed to collect positions at a 1hz epoch rate throughout the subplot measurement period, which can require a substantial (hours) amount of time, with a minimum of 15 minutes of 1hz data recorded. The precise coordinates were obtained to enable precise spatial alignment of remotely-sensed data with field measurement data. A study performed in an interior boreal forest in Alaska indicated that the horizontal precision for coordinates collected with these survey-grade GNNS units and 20 minutes of data (1 hertz) is on average better than 0.5 m RMSE (Andersen et al., 2009).

3.2.2.3 Lidar

Small-footprint discrete-return airborne lidar data (lidar) were collected in strips (Figure 3.1) over the Kenai Peninsula in the spring of 2009 with and Optech Gemini sensor. A total of 10 strips were collected for the peninsula, although only 7 of the strips were used in this study. The 7 strips cover 4.3% of the forested area in our study area. Lidar data were collected in the spring of 2009 leaf-off for the Kenai Peninsula. The arrangement of the lidar strips corresponds to alternate strips of systematic FIA field plots. The lidar data was collected from a fixed wing aircraft fly at an average height of 1,150 m. The maximum scan angle was limited 7.5 degrees. The aircraft speed average 130 Knots. The lidar system scan rate was 71 kHz .The flight configuration yielded a nominal pulse density of ~4 pulses / m^2.

Lidar data consists of a series of records corresponding to locations where pulses within laser scan lines intersected the ground or objects above the ground. We are

specifically interested in the 3D lidar point cloud data that represent measurements of forest canopy structure. Raw lidar coordinate data are first summarized using statistics computed on lidar heights (the lidar statistics are henceforth referred to as "lidar metrics"). Lidar heights are lidar point elevations minus ground elevations for the same positions. The point data were processed to extract lidar structural metrics both at the subplot level and within each grid cell of a raster layer (GIS grid). The subplot level variables are statistics calculated on the lidar points falling within the spatial bounds of each 168.11 m^2 subplot. A grid of lidar metrics was calculated by tessellating the study area into 12.96 by 12.96 m grid cells and calculating the lidar metrics for the lidar data falling within the grid cells.

Lidar metrics considered in our analysis include height percentiles (e.g. ht_{95},ht_{50}, and ht_{30}) and cover ratios (e.g. $cover_1$ and $cover_2$) which are described in detail below. Both percentile and cover metrics are calculated using only lidar first returns. Only heights greater than 1m (a cutoff for "ground" and low vegetation returns) in height are considered for height quantile metrics. As an example, if ht_{95} for a given pixel is 17 m, then 95 percent of lidar point heights within the pixel fall below 17 m (excluding ground returns). Cover metrics correspond to the percentage, or equivalently proportion, of first returns above a given height. $Cover_1$, for example, indicates the proportion of first returns on a plot or a pixel that are greater than 1m in height. Lidar data were processed, including creation of a DTM, using freely-available FUSION software (McGaughey, 2012).

3.2.2.4 Landsat and elevation data (excluding lidar)

National Elevation Dataset (NED) elevation raster data were downloaded from the National Map Seamless Server website (http://seamless.usgs.gov/). Five tiles of elevation data were necessary to cover the entire study area. Data with approximately 10 m resolution (1/3 arc second) were available for nearly the entire peninsula. Elevation data were processed to estimate slope, aspect, and 24-hour solar irradiance.

Landsat images were downloaded from the GLOVIS website (http://glovis.usgs.gov/). As mentioned previously, the extent of our study area within the Kenai lowlands was restricted to fall within a single Landsat image. This was to simplify the analysis and reduce artifacts from mosaicked images. The Landsat archive from 2005 through 2009 (these years match the range of years of field data collection) was browsed for relatively cloud-free images between June and September. Unfortunately, cloud-free images are difficult to find for the Kenai Peninsula. Only 6 images with large cloud-free portions of the landscape exposed were found for the indicated period. All of the selected images had some cloud cover over the study area – despite the 0% cloud cover reported for one image by the GLOVIS website. Cloudy pixels were treated as noise in this analysis and included in the analysis without modification. The images were not processed to correct for atmospheric and sensor effects; we used the raw digital numbers (DNs) assigned to each image pixel.

Values for subplots were calculated by using a bilinear interpolation of grid values to the locations of subplots.

3.2.3 Strata

Our target population, forested areas in the Kenai lowlands, was identified using LANDFIRE data (Rollins, 2009). Forested and un-forested regions were defined based upon the layer specifying vegetation height by vegetation type. Any pixels classified as either as having tree heights greater than 0.0 m were considered within our target population. LANDFIRE products for Kenai include vegetation type, vegetation height by type, cover by type, and maps of disturbance areas by year. The accuracy of LANDFIRE classification products was estimated to be between 46% and 57% for a region of the Kenai Peninsula in an assessment using multiple sources of field measurements (DeVelice, 2012).

3.2.4 Estimation

3.2.4.1 Inference

In this study we use design-based inference for estimation (Gregoire, 1998). Design-based inference refers to inference about the estimation of parameters such as the mean or the total of a realized finite population. The design-based properties of estimators (e.g. bias and variance) are with respect to the finite sampling distributions of the estimators (Särndal et al., 1992, 40). For example, if an estimator is design-unbiased for the total, it means that if it were possible to take every possible unique sample from the population, then the mean of all estimates would equal the population mean. Common assumptions for this type of inference include that all of the elements in the population have non-zero probability of selection, and that the first order inclusion probability for sampled elements is known or approximately known. Commonly used estimators for design-based inference typically exhibit the desirable consistency (Särndal et al., 1992, 166–169) property that the expected difference between the estimator and the parameter of interest decreases for an increased sample size. However, even if an estimator is unbiased for a population parameter, a single estimate from the estimator may differ considerable from the population parameter. We selected this mode of inference because it most accurately reflects our objective in practice – which is to estimate what is currently present on the landscape, and is not dependent upon correct specification of a model for the population.

In this study we perform estimation using both asymptotically design-unbiased regression estimators and design-unbiased estimators. Regression estimators are asymptotically unbiased estimators which are able to leverage the explanatory power of a regression model for estimation fitted to a sample of data. This can prove very useful, as models can contribute to estimation efficiency, and although the estimators are biased, the bias is minimal for a sufficiently large sample (Särndal et al., 1992, 235). We would also like to note that the properties of regression estimators are not subject to common modeling assumptions that one *might* require for model-based

inference (Särndal et al., 1992, 227) – where model-based inference is an alternate mode of inference in which we suppose the data arise from a super population model (e.g. for a regression model fitted by ordinary least squares (OLS) it is common to assume that regression residuals are approximately normally distributed with mean 0 and variance σ^2), and we attempt to make inference about the super-population model parameters (Gregoire, 1998).

3.2.4.2 Preliminary notation

Table 3.1 Definitions of symbols

Symbol	Definition
U	Population of elements
U_i	A cluster of elements
i	A cluster
j	An element
N	Number of clusters in the population
n	Number of clusters in the sample
G	Set of sampled clusters
s	Set of sampled elements
s_i	Set of sampled elements in cluster i
M	Number of elements in the population
M_i	Number of elements in a given cluster
m	Total number of elements in the population sampled
m_i	Number of elements sample in a cluster
t	The total of some attribute for the population
t_y	The total of a response attribute for the population
t_x	The total of an auxiliary attribute for the population
A_U	The area (ha) of the study region

Symbol	Definition
A_i	The area (ha) of a cluster
A_0	The area (ha) of a single element
y_j	The response value for a single element
μ_y	The mean response value of all elements in U
π_i	The first order inclusion probability (probability of selection) of a cluster
$\pi_{j\|i}$	The conditional probability of selection for element j given cluster i
π_j	The first order inclusion probability for an element

Let U be a finite population consisting of M elements for which we wish to estimate the sum of response values y_j associated with each element; this parameter of interest, t, is defined for y as $t_y = \sum_{j \epsilon U} y$ or as $t_y = M \times \mu_y$where μ_y is the mean of the M elements in U. Let *s* denote a random sample of *m* elements, where $m_i \in s$ is the number of elements from *s* falling within a cluster $U_i \in \{(U_1, \ldots, U_N) = U\}$, where cluster U_i consists of M_i elements, and where $G = (U_1, \ldots, U_n)$ is the set of n sampled clusters containing the m sampled elements. The first order inclusion probability (the probability of selecting a sampling unit as a result of the sampling design) for cluster U_i is π_i, and the first order inclusion probability for element j is $\pi_j = \pi_i \pi_{j|i}$ where $\pi_{j|i}$ is the conditional probability that element $j \in s$ given that $i \in G$.

With respect to our case study, U is a tessellated irregular polygon with M elements that approximately bounds the western lowlands of the Kenai Peninsula. A systematic sample of north-south lidar strips, G composed of 7 clusters ($G = U_1, \ldots, U_7 \in U$), transect U. The plots within G were originally laid out as a systematic sample of elements. For this study we obtained a random subsample of 32 plots which are a subset of the original plot layout which were precisely positioned. Both G and *s* are treated as simple random samples, which provides unbiased two-stage estimators of *t* and μ_y, but can result in biased estimators of the variance for two-stage t and μ_y estimators (typically positively biased (Gregoire and Valentine, 2008, 55)). The area

of the study region U is A_U, the area of a lidar strip U_i is A_i and the area of an element j is A_0. M is defined as A_U/A_0, and M_i as A_i/A_0. For the inclusion probability $\pi_i = \pi_{i'}$ for cluster i we use $\sum_{Ui \in G} M_i/M$, and m_i/M_i for the conditional inclusion probability $\pi_{j|i}$ for elements $j \in U_i$.

The M elements that compose U correspond to a 13 x 13 m grid overlaid on the boundary of U where each cell had approximately the same area as a subplot (168.11 m^2). Although sample plots do not fall precisely on grid cells, and their shapes do not conform to the shape of a grid cells, for estimation we perform a simplification by treating the center subplot as an element in the population of grid cells, where the response value y_j for a given center subplot is defined as the average of attributes on all four subplots. If a subplot did not fall within a forested area it was not included, thus the response for plot y_j can represent the average of from 1 to 4 subplots. Lidar and Landsat values used to predict biomass were also calculated for the location of the precisely georeferenced subplots. Lidar metrics were calculated for each cell in the 13 x 13 m grid overlaid on U. For total and means of auxiliary variables, t_x and $\bar{x}$, auxiliary variables for lidar and Landsat values are also arranged on a fixed grid, but the grid differs in resolution (30 m) from the grid of 13 x 13 m cells which compose U. However, the parameters of the finite population of an auxiliary variable, e.g. t_x, are approximately equal for the original grid or for an alternate grid with a slightly different resolution.

The model-assisted estimators used in this study, described in the next section, use models fitted by the OLS method for estimation with auxiliary data. The models were fit between field measured variables and remote sensing derived variables for sub-plots. Predictions and residuals for the subplots were then averaged and assigned to the center sub-plot.

3.2.4.3 Estimators

The Horvitz-Thompson (HT) design-unbiased estimators for the total for an SRS sample and an unbiased estimator of its variance are (Lohr, 2009, 37)

$$\hat{t}_{SRS} = M * \bar{y} \quad \textbf{(1)}$$

$$\bar{y} = \frac{1}{m}\sum_{j \in U} y_j$$

$$\hat{V}(\hat{t}_{SRS}) = \frac{M^2}{m}\left(1 - \frac{m}{M}\right)\frac{\sum_{j \in s}\left(y_j - \bar{y}_s\right)^2}{m-1}. \quad \textbf{(2)}$$

The regression estimator for the total for an SRS design is (Särndal et al., 1992, 231)

$$\hat{t}_{regSRS} = \sum_{j \in s}^{M} \hat{y}_j \quad \textbf{(3)}$$

$\hat{y}_j$ = regression estimate of y_j.

An approximate variance estimator for $\hat{t}_{regSRS}$ is (Särndal et al., 1992, 237)

$$\hat{V}(\hat{t}_{regSRS}) = \left(\frac{M^2}{m}\right)\frac{\sum_{j \in s}\left(y_j - \hat{y}_j\right)^2}{m-1}. \quad \textbf{(4)}$$

The HT estimator for the total from a two-stage sample is given by (Lohr, 2009, 183)

$$\hat{t}_{2S} = \sum_{i \in G}\frac{\hat{t}_i}{\pi_i} \quad \textbf{(5)}$$

$$\hat{t}_i = \sum_{j \in si}\frac{y_j}{\pi_{j\,|\,i}}.$$

The variance of (5) can be unbiasedly estimated by (Lohr, 2009, 185)

$$\hat{V}(\hat{t}_{2S}) = N^2\left(1-\frac{n}{N}\right)\frac{s_t^2}{n} + \frac{N}{n}\sum_{i\in G} M_i^2\left(1-\frac{m_i}{M_i}\right)\frac{s_i^2}{m_i}$$

$$s_t^2 = \frac{1}{n-1}\sum_{\mathrm{i}\in \mathrm{G}}\left(\hat{t}_i - \frac{\hat{t}_{2S}}{N}\right)^2$$

s_i^2 = variance of $\mathrm{m_i}$ SSUs in PSU i.

The Durbin with-replacement estimator for the variance of $\hat{t}_{2S}$ in (7) is slightly biased for without-replacement sampling (for a small sampling fraction), but the variance estimator has smaller variance than (6), is always positive definite, and is simple to compute.

$$\hat{V}_D(\hat{t}_{2S}) = \frac{n}{n-1}\sum_{i\in G}\left(\frac{t_i}{\pi_i} - \frac{\hat{t}_{2S}}{n}\right)^2 \qquad \textbf{(6)}$$

Estimators (8) and (10) are regression estimators which we used with regression models fitted by OLS to relate our response variable to predictor variables. The first two-stage model-assisted total estimator, $\hat{t}_{reg1}$ (Särndal et al., 1992, 322–327), is appropriate when auxiliary data are available for every element in the population

$$\hat{t}_{reg1} = \sum_{i\in U}\hat{y}_i + \sum_{j\in s}\frac{e_j}{\pi_j} \qquad \textbf{(7)}$$

k = number of elements in the population

$\mathrm{y_i}$ = the response corresponding to a single element

$\hat{y}_j$ = regression estimate of $\mathrm{y_j}$

m = total number of sampled elements

$e_j = y_j - \hat{y}_i$

π_j = sampling probability for element j.

Because of its extreme simplicity and the near equivalence between with-replacement and without replacement two-stage estimators, for the regression estimators we

adapted the Durbin variance estimator (7) for use with (8) and (9). The variance of (9) was estimated with (6) by replacing y_j values with regression residuals e_j

$$\hat{V}_D(\hat{t}_{reg1}) = \frac{n}{n-1}\sum_{i\in G}\left(\frac{t_{i,e}}{\pi_i} - \frac{\hat{t}_{2S,e}}{n}\right)^2 \quad \textbf{(8)}$$

$$\hat{t}_{2S,e} = \sum_{i\in n}\frac{\hat{t}_{i,e}}{\pi_i}$$

$$\hat{t}_{i,e} = \sum_{j\in si}\frac{\hat{y}_j - y_j}{\pi_{j\,|\,i}}$$

The second two-stage model-assisted estimator, $\hat{t}_{reg2}$, is appropriate when auxiliary information is available for every element in sampled PSUs but is not available otherwise

$$\hat{t}_{reg2} = \sum_{i\in G}\frac{\hat{t}_i}{\pi_i} \quad \textbf{(9)}$$

$$\hat{t}_i = \sum_{j\in Ui}\hat{y}_j + \sum_{j\in si}\frac{e_j}{\pi_j}$$

$$e_j = y_j - \hat{y}_j$$

y_j = the response corresponding to a single element

$\hat{y}_j$ = OLS prediction of element y_j

The variance of (10) was firstly estimated with

$$\hat{V}_D(\hat{t}_{reg2}) = \frac{n}{n-1}\sum_{i\in G}\left(\frac{t_i}{\pi_i} - \frac{\hat{t}_{reg2}}{n}\right)^2. \quad \textbf{(10)}$$

The variance of (12) was also estimated using a bootstrap estimator. Bootstrap variance estimators are a non-parametric, resampling-simulation based approach to estimation of variance. In the simplest approach to bootstrap variance estimation

(Efron and Tibshirani, 1993, 47) a large number of resamples are taken with replacement from the original sample, then the estimator of interest is applied to each resample. The resulting empirical distribution of resample-based estimates is then used to approximate the properties of the sampling distribution of the estimator. The standard error, for example, can be estimated by taking the standard deviation of the resampling distribution of estimates, or confidence intervals for the estimator can be calculated directly by calculating quantiles from the resampling distribution.

Our bootstrap simulations for an estimator for a two-stage design proceeded as follows: in a given bootstrap simulation $k \in \{1,...,N_k\}$ we select a bootstrap resample s_k^* of m elements. We first took a resample of n clusters with replacement (G*) from our original sample G of n clusters. Within each resampled cluster, U_i^*, m_i plots, s_i^*, were resampled with replacement from the m_i elements original from U_i^* in s. If multiple U_i^* were present in G*, then plots in s_i^* were sampled independently for each copy. This resampling procedure follows from Rao and Wu (1988). The N_k bootstrap resamples were then used to estimate the variance,

$$\hat{V}_{bs}(\hat{t}_{reg2}) = \left(\frac{n}{(n-1)N_k}\right)\sum_{k\in Nk}\left(\hat{t}^*_{reg2,k} - \bar{\hat{t}}^*_{reg2}\right)^2 \qquad \textbf{(11)}$$

$$\hat{t}^*_{reg2,k} = \frac{N}{n}\sum_{i\in n} t^*_{k,i}$$

$$t^*_{k,i} = \sqrt{m_i/m_i - 1}\left(\sum_{j\in Mi}\hat{y}^*_j + \sum_{j\in mi}\frac{e^*_j}{\pi_j}\right)$$

$$\pi_j = \pi_{j|i}\pi_i \ ,$$

where the inflation factors, $\frac{n}{(n-1)}$ and $\sqrt{m_i/m_i - 1}$, arise in (12) because the bootstrap variance estimator is negatively biased (decreasing for larger n and m_i; Antal and Tillé, 2011). The variables included in the model to predict $\hat{y}^*_j$ were selected

using the full dataset, but the model coefficients were estimated uniquely with OLS for each resample.

3.2.5 Composite estimation

Multiple estimators can be combined to create a composite estimator which can reduce the variance over the contributing estimators. We consider a composite estimator which is a linear combination of two correlated estimators. A restriction is typically placed on the weights such that the variance estimate of the composite estimator is at most equal to variance of the less precise of the contributing estimators. This means that the estimator will at worst perform equally to the more precise of the two estimators. For two estimators, the composite estimator is (Green and Strawderman, 1986; Gregoire and Walters, 1988)

$$\hat{t}_{y,c} = \theta \hat{t}_1 + (1-\theta)\hat{t}_2 \qquad \textbf{(12)}$$

$0 \le \theta \le 1$

$\hat{t}_{y,c}$ = composite estimator

$\hat{t}_1$ and $\hat{t}_2$ are any two estimators of the population total

θ is an estimated weight treated as a constant

with variance estimator

$$\hat{V}(\hat{t}_{y,c}) = \theta^2 \hat{V}(\hat{t}_1) + (1-\theta)^2 \hat{V}(\hat{t}_2) + 2\theta(1-\theta)\hat{C}(\hat{t}_1, \hat{t}_2) \qquad \textbf{(13)}$$

where we estimate the covariance, $\hat{C}$, between $\hat{t}_1$ and $\hat{t}_2$ by calculating the covariance between 5000 simultaneous bootstrap estimates of $\hat{t}_1$ and $\hat{t}_2$. To estimate a θ that on average minimizes the variance we use (McTague, 2010)

$$\theta = \frac{\hat{V}(\hat{t}_2) - \hat{C}(\hat{t}_1, \hat{t}_2)}{\hat{V}(\hat{t}_1) + \hat{V}(\hat{t}_2) - 2\hat{C}(\hat{t}_1, \hat{t}_2)}. \qquad \textbf{(14)}$$

3.2.6 Design effect

Design effect, a specific case of relative efficiency, indicates the performance of a sampling and estimation strategy relative to that of the HT estimator for an SRS design. Algebraically, design effect is the ratio of the variance estimate for an estimator to the variance of the SRS estimator

$$DE = \frac{\hat{V}(\hat{t}_{.})}{\hat{V}(\hat{t}_{SRS.})}. \quad \textbf{(15)}$$

Design effect indicates the performances of an estimator and design relative to the SRS design and estimator. The variance of a total estimator using an estimator other than the HT estimator for an SRS will depend upon characteristics specific to each design, making it difficult to interpret whether a variance estimate is large or small. The variance of the SRS estimator, in contrast, can be estimated in nearly every case. By comparing the variance of an estimate with the variance of the SRS estimator, a more general indication of performance is provided.

3.3 Results

3.3.1 Model Selection

Models were selected using the leaps and bounds best subsets selection algorithm, a computationally efficient subset selection algorithm pioneer by Furnival and Wilson Jr (1974), followed by manual interaction by the user to select meaningful combinations of variables. The coefficients and selected variables for final models are provided in Table 3.2. Lidar models explained more variability in biomass as indicated by the RMSE and R^2 values than Landsat models. The final lidar model included two explanatory variables, a height percentile and a cover variable, and their interaction. The Landsat model included six variables. The Landsat variables selected are two of the longer of the Landsat wavelengths (bands 5 and 6) and come from three image dates, one image in 2005 and two images in 2009. None of the elevation derivatives

(elevation, slope, aspect) or coordinate variables ($x,y,x^2,y^2,x:y$) were selected for inclusion.

Table 3.2 OLS model coefficients and fit statistics for lidar and Landsat models

Lidar		Landsat	
Predictor	Coefficients	Predictors	Coefficients
intercept	-18.928310	intercept	1228.6031
Ht_{99}	6.588540	B5 (2005/06/28)	-0.01478
$Cover_1$	-0.081450	B6 (2005/06/28)	-2.72055
Ht_{99}:$Cover_1$	0.073560	B5 (2009/07/09)	3.49811
		B6 (2009/07/09)	-1.46667
		B5 (2009/08/10)	-3.94418
		B6 (2009/08/10)	-5.10074
RMSE (Mg / ha):	33.18		48.65
$R^{2:}$	0.69		0.34

3.3.2 Estimation

For inference estimates of the standard deviations of estimators, or standard errors $SE = \sqrt{\hat{V}(\hat{t}_{.})}$, are often easier to interpret, compare and report than variance estimates. However, for clarity of notation we provided formulas for *variance* estimators instead of standard error estimators. For the remainder of the paper we make inference about standard error estimates while referencing corresponding variance estimators with the intention that the standard error estimate may be obtained by taking the square root of the variance estimate calculated using the referenced variance estimator. We also provide mean estimates, and corresponding standard errors. These are obtained by dividing total estimates and total estimator standard errors by M, the number of elements in the population. The mean estimates are more easily compared to the values obtained for other forests without need to account for the size of the area being studied.

Total and standard error estimates in Table 3.3 were calculated for our study area using formulas (1) – (15) in addition to design effect (16). Estimates are provided for the subset of 32 FIA plots for all of the estimators, but only with SRS HT estimators for the full set of 145 plots from which our subset was sampled. SRS estimates were obtained by ignoring the clustering of plots within PSUs. SRS estimates were calculated to provide an indication of the efficiency (number of elements sampled relative to precision) that is lost with the two-stage design relative to the SRS design. The remaining estimators were applied consistently with the arrangement of the sample as a two-stage design.

For the HT total estimator for a two-stage design (5) and the second regression estimator for a two stage design (10), standard errors were calculated twice with separate estimators. The standard error of (5) was estimated twice, with both (6) and (7), to demonstrate that the Durbin estimators provide similar estimates to (6). This was to validate our use of Durbin-type standard error estimators for two-stage regression estimators of the total (8) and (10). The bootstrap estimator was used similarly to validate the Durbin-type estimator for the standard error of (10). In Table 3.3 we see that in fact, for both of these cases, the pairs of estimators provided equivalent estimates.

Table 3.3 Total and mean parameter estimates for the finite population and estimates of the standard deviations of parameter estimators in addition to design effect and sample size

Estimator	t (Tg)	t sd (Tg)	mu (Mg/ha)	mu sd (Mg/ha)	DE(%)*	n
SRS HT	30.7	2	60.2	4	-	145
SRS HT	31.2	5	61.3	9	100	32
SRS Reg lidar	32.8	2	64.3	4	46	32
SRS Reg Lands.	38.7	3	76.0	7	73	32
2S Plots	34.2	8	67.1	15	159	32
2S Plots Durb.	34.2	8	67.1	15	161	32
2S Reg1 Durb.	38.7	4	76.0	9	94	32
2S Reg2 Durb.	32.7	5	64.3	10	102	32
2S Reg2 BS	32.7	5	64.3	10	105	32
2S Reg Comp.	35.7	3	70.1	6	63	32

*Design effect was calculated relative to the "SRS HT" for n=32. "t" and "mu" are the population total and mean in teragrams (Tg) and megagrams (Mg) respectively, and "t sd" and "mu sd" are the standard deviations of "t" and "mu" estimators.

The two most precise estimators according to SEs were provided by the HT estimator for the SRS design (1) with 145 observations, and the regression estimator (3) for the SRS design with auxiliary lidar, with both of them yielding equivalent precisions (≈2 Tg). The standard errors of the regression estimator (3) with Landsat for the SRS design and the composite estimator which combines two-stage regression (8) with Landsat and (10) with lidar were slightly larger (~3 Tg), with the composite estimator providing a dramatic increase in precision over either contributing two-stage regression estimator. The regression estimators (8) and (10) Landsat and lidar had lower precision by ~ 3 Tg relative to regression estimators (3) with Landsat and lidar, but were equivalent to the HT estimator (1) for 32 observations.

The reason for the difference between standard error estimates in Table 3.3 from two-stage estimators (5) and (10) can be explained by the corresponding PSU mean estimates in Table 3.4. The variability of these estimators is driven by the variability between PSU totals, unlike the variability of (8) which is not a function of PSU totals.

As a result of the long narrow north-south running regions of our study area spanned by the PSUs, we would expect that variability within strips would be high and the variability between strips would be low. This is an ideal scenario for two-stage sampling, resulting in lower variance than if the PSUs encompassed less geographic variability. However, the efficiency gain from using long narrow strips is better realized with regression estimator (10) than with HT estimator (5). This is because increased variability in PSU total estimators increases the precision of these two-stage total estimators. Regression estimators of PSU totals, applied for element predictions for every element in the PSUs, are very precise, while HT PSU total estimators, applied to the relatively few sampled elements per PSU, are much less precise. The difference in variability between regression and HT estimators is evident from the PSU means shown in Table 3.4. HT mean estimates range from 30 to 105 megagrams (Mg), while regression estimates range from 56 to 76 Mg.

Table 3.4 PSU mean estimates used for 2S HT and 2S Reg2 variance estimators

	Mean Estimates (Mg) for PSUs						
Estimator	**1**	**2**	**3**	**4**	**5**	**6**	**7**
2S HT	77.2	49.6	95.9	105.5	68.1	42.7	29.7
2S Reg2	53.4	60.0	73.8	76.3	60.4	64.2	56.0

In addition to being easy to implement and comparable to without-replacement estimators, the Durbin estimators are also convenient because they enable straightforward investigations of the effect of the number of sampled PSUS. We can look at alternate sample sizes, n, by multiplying the standard error estimate by the ratio of the number of PSUs in the observed sample to the target number of sampled PSUs. In Figure 3.2 we can see standard error estimates for various sample sizes for (10). The standard errors for the observed number of PSUs (n=7) occurs where dramatic increases in precision are still possible for modest increases in the number of PSUs.

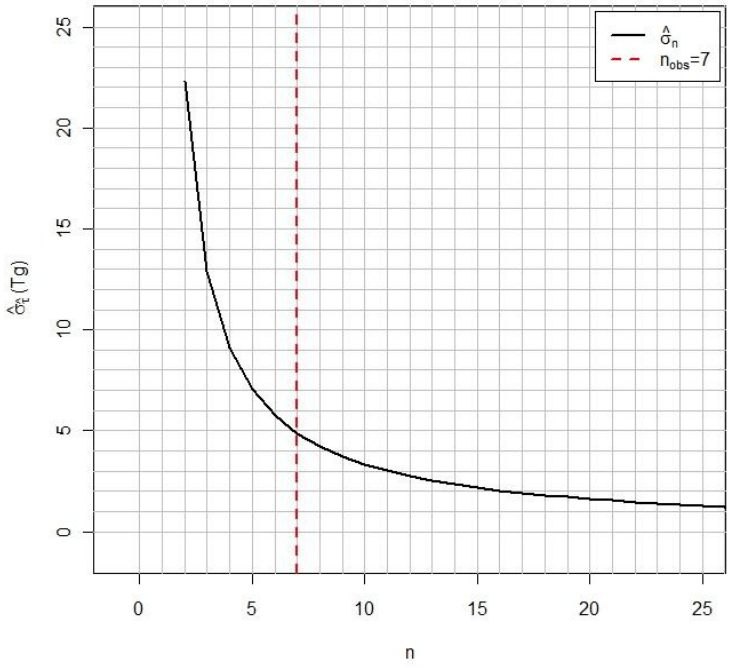

Figure 3.3.2 Two-stage lidar-assisted standard errors (10) relative to different numbers of sampled PSUs

3.4 Discussion

3.4.1 Total estimation

The results from this study indicate that lidar and Landsat can play a beneficial role in estimation of some forest metrics. Under the two-stage design, model-assisted estimation with Landsat (8) was competitive with respect to precision to the HT estimator under the SRS design (1). And for the SRS regression estimator (3) with Landsat, the estimator was at least 20% more precise than the SRS HT estimator for the same number of sampled elements. The SRS regression estimator was more precise with lidar than either the SRS HT estimator or the SRS Landsat-assisted estimator, although the standard error for SRS lidar-assisted estimator was presented only as an indication of an upper bound on precision for a two-stage lidar-assisted approach, because the high cost of obtaining lidar makes wall-to-wall lidar collection likely too expensive to be viable as part of a standard FIA annual inventory protocol.

The lidar and Landsat-assisted two-stage estimators were much more precise than the two-stage HT estimator (5), but it is unlikely that this two-stage design would be used in practice if a lidar strip sample were not collected. The precisions of the two-stage lidar-assisted and Landsat-assisted estimators were equivalent– but again, in a scenario where lidar is not collected, a Landsat-assisted approach is most likely to be implemented using a design which legitimately makes use of (3).

From Figure 3.2 we can see that for an increase in the numbers of PSUs to n=15, the two-stage lidar-assisted estimator (10) appears more viable as a stand-alone estimator. This is promising from a practical standpoint because the objective for a two-stage lidar-assisted approach in Alaska is to reduce the number of field plot measurements required because of concerns about cost, safety, and accessibly. For an increase in the number of lidar strips from n=7 to n=15, the two-stage lidar-assisted estimator would be approximately as precise as the SRS HT estimator for biomass for 145 plots. The number of field plots need not increase proportionally because the contribution of within-PSU variance to total estimator variability is small. Also, the relative gain from increasing the number of sample plots in the SRS design (32 plots) falls within a range for which the increase in precision for measuring an additional unit is much less steep – a result from the exponential relationship between sample size and precision.

The use of a composite estimator also yielded highly promising results; by compositing lidar-assisted and Landsat-assisted two-stage estimators we were able to markedly increase the precision over either contributing estimator. The composite estimator with 32 plots did not achieve the precision of the SRS HT estimator for 145 plots, but was able to increase the precision over the more precise contributing two-stage estimator by ~33%, and exceed the SRS HT estimator for the same number of plots by ~33%. While we did not examine the relationship between number of sample strips and precision of the composite total estimator, it is likely that fewer than 15 strips will be necessary for the composite estimator to achieve precision parity with the SRS HT for 145 plots.

While we compared results for alternate designs with the precision of estimators for the original sample, a fair comparison between a lidar-assisted approach and the existing design is not easily performed. The FIA inventory is used to provide detailed information for a wide array of forest attributes (Barrett et al., 2011), and it is likely that application of a lidar-assisted estimator will result in a significant increase in precision for only a subset of these attributes (biomass, merchantable volume, canopy fuels, aboveground carbon).However, it may be determined that obtaining more reliable estimates of these attributes (aboveground carbon in particular) is sufficiently important to justify the additional cost for a supplemental acquisition of lidar sample strips. It should be noted that due to the highly complicated logistics associated with establishing ground plots in interior Alaska, the cost of a lidar acquisition could represent a relatively small proportion of the total inventory cost. For example, plots in interior Alaska cost as much as $8000 each, while the average cost of a lidar strip sample on the Kenai was approximately $5,000.

A similar study to this one was conducted in Norway's boreal forests using a lidar-assisted two-stage estimator for a region roughly five times the area of our study site (Gregoire et al., 2011). It appears that the approach used in the Norway study yielded poorer precision with the model-assisted estimator than for an equivalent sample size with field measurements alone. To compare the SE estimates reported in the Gregoire et al. (2011) study between plot-only and model-assisted estimates, we multiplied the reported SE for the plot-only estimator by $\sqrt{975/445}$ to equalize the sample sizes between the two SEs (treating the plot-only estimate as if it was from an SRS design). The plot based standard error was 2.6 Mg/ ha versus 3.2 Mg/ha for the lidar-assisted estimator. In a model-based analogue to the study described by Gregoire et al. (2011), the companion paper by Ståhl et al. (2011) uses the same dataset as Gregoire et al. (2011) but reported greater precision with the model-based estimator than with the plot-only estimator : 2.2 Mg/ha for the model-based total biomass estimator versus 2.6 Mg/ha for the unbiased total biomass estimator (again adjusted for sample size).

However it is not necessarily reasonable to compare the reported values from the two studies since their bases for inferences differ.

A lidar sampling approach was also by Andersen et al. (2011) for model-based estimation of biomass in a remote region of Alaska. In the study 27 lidar strips were flown over the 2000 km^2 study area, then plots were placed randomly in accessible portions of the lidar strips. In a follow up analysis (Andersen et al., 2011b) the authors leveraged IFSAR and Landsat for stratification to reduce the variability of the total estimator. The standard error of the total estimator was reduced from 7.3% to 5.1%. This compares to a 9.5% standard error if the sample is treated as a simple random sample (the "SRS" standard error estimate, which is not truly appropriate here, is not reported in the paper but can be calculated from the reported mean, sample size, and standard deviation for biomass). A conceptual drawback of the study is that since some sub-regions were not sampled, design-unbiased estimators are not possible. Practically, however, the effect on total estimation is likely to be small as the empirical relationship observed between biomass and lidar is quite strong and is not likely to vary drastically within a region of this size.

3.4.2 Limitations

An important limitation of this study is that forested areas are treated as if they were known. In fact the forest classifications were predicted, which contributes to the variance of total estimates, a source of variation not represented by our variance estimators (McRoberts 2010). If the effect from ignoring this source of error on variance estimators is additive, then the results presented here will still provide a reasonable indication of the relative precision of estimators – although the reported standard errors will be negatively biased.

A second limitation of this study is with respect to the FIA plot design. FIA subplots are quite small, .168 ha, which means that the proportion of tree foliage on a plot which has boundary overlap issues (external trees with foliage falling in the plot, or internal trees with foliage falling outside the plot) may be quite high when attempting

to relate field measurements to lidar. Plot size is a feature of the FIA inventory protocol that is unlikely to change to accommodate lidar, but it is worth noting that the performance of a strip sampling approach with lidar will likely improve if the area of the measurement plot is increased. Plot size may also have an effect on a Landsat assisted approach; if we consider a perfectly spatially co-registered subplot and Landsat pixel, the information represented by the Landsat pixel includes a large buffer around the field plot – reducing the correlation between the two types of data. However, in practice the effect of plot size on a Landsat model may be less because the ability to develop such a model is largely dependent upon spatial correlation between forest characteristics over a short distance; the coordinates associated with a Landsat pixel may be off by 60m on average, thus it is unlikely that the information sensed by Landsat corresponds to the actual plot location.

Finally, there is a temporal limitation to our dataset. The data used for this study were collected as part of the FIA annual inventory, which means measurements are carried out for a subset of plots in a given year. The data collected for this study were collected over a 5 year period. This is problematic for our study area because of the decay and mortality which may have occurred between when plots were measured and when the lidar was collected. As with plot size, this is a limitation which negatively affects the performance of a lidar-assisted approach. Since our results indicated that there is positive potential for using lidar for estimation, it is likely that an alternate field measurement strategy which uses larger plots and temporally matched field and lidar measurements could yield improved results for two-stage estimation with lidar.

While our results were positive with respect to the viability of a Landsat-assisted approach, we should note that our implementation of a Landsat approach was fairly coarse. Landsat processing entailed only the interpolation of Landsat values to the locations of our plots. Adopting a more sophisticated approach which includes histogram matching, atmospheric correction, cloud masking, and temporal pixel trajectories may be a more viable option (Powell et al., 2010).

3.5 Conclusions

In this study we explored the potential of lidar-assisted and Landsat-assisted strategies for estimation of forest metrics measured on the Kenai Peninsula, AK. Because a wall-to-wall lidar collection approach is not considered viable due to the acquisition cost, we primarily compared two-stage regression estimators for use with a sample of lidar strips to the other estimation strategies. We found that a two-stage lidar assisted approach was comparable to SRS estimation with 32 plots, but that by doubling the number of lidar strips it would be feasible to achieve the precision of the existing estimation strategy with 149 plots. Both SRS and two-stage Landsat assisted estimators also compared favorably, exceeding the precisions of plot-based estimators. An estimation strategy with Landsat will be applicable to a variety of scenarios because Landsat data is free and widely accessible. While the use of lidar constitutes an additional cost, there are likely to be scenarios in which the increase in efficiency which is possible with a lidar strip sampling approach, especially in combination with a Landsat, will reduce the cost to achieve a target precision for some forest metrics.

3.6 Citations

Andersen, H.E., Clarkin, T., Winterberger, K. and Strunk, J.L. 2009. An Accuracy Assessment of Positions Obtained Using Survey-and Recreational-Grade Global Positioning System Receivers across a Range of Forest Conditions within the Tanana Valley of Interior Alaska. West. J. Appl. For. **24**(3): 128–136.

Andersen, H.E., Strunk, J. and Temesgen, H. 2011a. Using Airborne Light Detection and Ranging as a Sampling Tool for Estimating Forest Biomass Resources in the Upper Tanana Valley of Interior Alaska. Western Journal of Applied Forestry **26**(4): 157–164.

Andersen, H.-E., Strunk, J., Temesgen, H., Atwood, D. and Winterberger, K. 2011b. Using multilevel remote sensing and ground data to estimate forest biomass resources in remote regions: a case study in the boreal forests of interior Alaska. Canadian Journal of Remote Sensing **37**(6): 596–611.

Antal, E. and Tillé, Y. 2011. A Direct Bootstrap Method for Complex Sampling Designs From a Finite Population. Journal of the American Statistical Association **106**(494): 534–543.

Barrett, T.M., Christensen, G.A. and Pacific Northwest Research Station (Portland, O.. 2011. Forests of Southeast and South-central Alaska, 2004-2008: Five-year Forest Inventory and Analysis Report. US Department of Agriculture, Forest Service, Pacific Northwest Research Station.

Bechtold, W.A. and Patterson, P.L. 2005. The enhanced forest inventory and analysis program: national sampling design and estimation procedures. Asheville, North Carolina: US Department of Agriculture Forest Service, Southern Research Station. 85 p.

DeVelice, R.L. 2012. 10 Accuracy of the LANDFIRE Alaska Existing Vegetation Map over the Chugach National Foreset. LANDFIRE. Assessments.

Efron, B. and Tibshirani, R. 1993. An introduction to the bootstrap. CRC Press. 456 p.

Furnival, G.M. and Wilson Jr, R.W. 1974. Regressions by leaps and bounds. Technometrics: 499–511.

Green, E.J. and Strawderman, W.E. 1986. Reducing sample size through the use of a composite estimator: an application to timber volume estimation. Can. J. For. Res. **16**(5): 1116–1118.

Gregoire, T.G. 1998. Design-based and model-based inference in survey sampling: appreciating the difference. Can. J. Forest. Res. **28**(10): 1429–1447.

Gregoire, T.G., Stahl, G., Naesset, E., Gobakken, T., Nelson, R. and Holm, S. 2011. Model-assisted estimation of biomass in a LiDAR sample survey in Hedmark County, Norway. Canadian Journal of Forest Research **41**(1): 83–95.

Gregoire, T.G. and Valentine, H.T. 2008. Sampling Strategies for Natural Resources and the Environment. 1st ed. New York: Chapman and Hall/CRC. 474 p.

Gregoire, T.G. and Walters, D.K. 1988. Composite vector estimators derived by weighting inversely proportional to variance. Canadian Journal of Forest Research **18**(2): 282–284.

Hyde, P., Nelson, R., Kimes, D. and Levine, E. 2007. Exploring LiDAR-RaDAR synergy--predicting aboveground biomass in a southwestern ponderosa pine forest using LiDAR, SAR and InSAR. Remote Sensing of Environment **106**(1): 28–38.

Kennaway, T.A., Helmer, E.H., Lefsky, M.A., Brandeis, T.A. and Sherrill, K.R. 2008. Mapping land cover and estimating forest structure using satellite imagery and coarse resolution lidar in the Virgin Islands. Journal of Applied Remote Sensing **2**(023551): 1–27.

Lohr, S.L. 2009. Sampling: design and analysis. Thomson.

Lund, H.G. and Schreuder, H.T. 1980. Aggregating inventories. Resources Evaluation Newsletter (4): 1–3.

McGaughey, R.J. 2012. FUSION/LDV: Software for LIDAR Data Analysis and Visualization, Version 3.01. USFS.

McTague, J.P. 2010. New and composite point sampling estimates. Canadian Journal of Forest Research **40**(11): 2234–2242.

Parker, R.C. and Evans, D.L. 2004. An application of LiDAR in a double-sample forest inventory. Western Journal of Applied Forestry **19**(2): 95–101.

Powell, S.L., Cohen, W.B., Healey, S.P., Kennedy, R.E., Moisen, G.G., Pierce, K.B. and Ohmann, J.L. 2010. Quantification of live aboveground forest biomass dynamics with Landsat time-series and field inventory data: A comparison of empirical modeling approaches. Remote Sensing of Environment **114**(5): 1053–1068.

Rao, J.N.K. and Wu, C.F.J. 1988. Resampling Inference With Complex Survey Data. Journal of the American Statistical Association **83**(401): 231–241.

Rollins, M.G. 2009. LANDFIRE: a nationally consistent vegetation, wildland fire, and fuel assessment. International Journal of Wildland Fire **18**(3): 235–249.

Särndal, C.E., Swensson, B. and Wretman, J. 1992. Model assisted survey sampling. New York: Springer-Verlag. 694 p.

Solberg, S., Astrup, R., Gobakken, T., N\aesset, E. and Weydahl, D.J. 2010. Estimating spruce and pine biomass with interferometric X-band SAR. Remote Sensing of Environment **114**(10): 2353–2360.

Ståhl, G., Holm, S., Gregoire, T.G., Gobakken, T., Næsset, E. and Nelson, R. 2011. Model-based inference for biomass estimation in a LiDAR sample survey in Hedmark County, NorwayThis article is one of a selection of papers from Extending Forest Inventory and Monitoring over Space and Time. Can. J. For. Res. **41**(1): 96–107.

St-Onge, Hu, Y. and Vega, C. 2008. Mapping the height and above-ground biomass of a mixed forest using lidar and stereo Ikonos images. International Journal of Remote Sensing **29**(5): 1277–1294.

Strunk, J.L., Reutebuch, S.E., Andersen, H.-E., Gould, P.J. and McGaughey, R.J. 2012. Model-Assisted Forest Yield Estimation with Light Detection and Ranging. Western Journal of Applied Forestry **27**(2): 53–59.

Tonolli, S., Dalponte, M., Neteler, M., Rodeghiero, M., Vescovo, L. and Gianelle, D. 2011. Fusion of airborne LiDAR and satellite multispectral data for the estimation of timber volume in the Southern Alps. Remote Sensing of Environment **115**(10): 2486–2498.

Woods, M., Pitt, D., Penner, M., Lim, K., Nesbitt, D., Etheridge, D. and Treitz, P. 2011. Operational implementation of a LiDAR inventory in Boreal Ontario. The Forestry Chronicle **87**(4): 512–528.

The Forest Inventory and Analysis Database: Database Description and Users Manual Version 3.0 for Phase 2.

4 Manuscript 3

A Multi-Phase Forest Mapping Case Study with Landsat, a Sample of Lidar Strips, and Field Plots on the Kenai Peninsula, Alaska

Jacob Strunk, Hailemariam Temesgen, Hans-Erik Andersen

Abstract

An important value of remotely sensed information is the capacity to model and map forest variables like biomass and volume. Mapped values can provide insight into the spatial distribution of forest resources, facilitating analyses not feasible with point estimates. In this study we leverage data from a lidar strip sample (collected for more efficient point estimation) to better match the resolution of forest structure information to the resolution of Landsat for model development and prediction, and to increase the number of training observations. Both of these are important for modeling, as Landsat values are only weakly related to forest inventory and analysis (FIA) plot measurements when modeled directly. We also leverage pre-processing outputs from the novel LandTrendr approach which can make use of a Landsat time-series, including partly cloudy images and SLC off ETM+ data to generate noise dampened, cloud free, images for any year in the range of the archive.

The results from this study indicate that a three phase approach with plots, lidar, and Landsat could provide more precise predictions than those made from field data alone or with a two-phase (Landsat) approach. For the best three-phase strategy, model RMSEs for tree volume, biomass, and trees per hectare were 61%, 64%, and 81% respectively.

4.1 Introduction

Studies that demonstrate techniques to incorporate lidar in forest inventory, mapping and monitoring are now fairly common. Investigators often report modeling and estimation of forest attributes(Tonolli et al., 2011) including classification by forest type (Pascual et al., 2008), species (Kim et al., 2009a), or condition(Kim et al., 2009b) , delineation of stand boundaries(Sullivan et al., 2009), and segmentation of upper canopy tree crowns (Hyyppa et al., 2001). The examinations typically rely on empirical relationships between lidar and field measurements developed for sample plots to train a process or approach for use with lidar covering the entire area of interest (AOI). However, the acquisition of lidar for an entire AOI is not always justifiable due to high costs, especially for large AOIs. Recently interest has increased in approaches to estimation that use strips (or swaths) of scanning lidar data instead of complete lidar coverage (Parker and Evans, 2007; Gregoire et al., 2011; Ståhl et al., 2011; Andersen et al., 2011a). The lidar strip sampling approach is not, however, directly suited to the development of mapped forest attributes. Lidar-based maps are feasible within the lidar strips, but since the lidar is not available elsewhere, direct predictions are not available for locations without lidar. Prediction of values for gaps between lidar strips would require additional auxiliary information for those areas, possibly lower cost spectral information acquired with a passive measurement device.

A number of studies have examined integrated lidar and spectral approaches to model forest attributes. Many of these previous efforts describe using lidar and spectral information in unison, where lidar and spectral information are available for the same areas (Packalen and Maltamo, 2006; Hudak et al., 2006; Popescu et al., 2004). Lidar-based approaches to modeling forest attributes improve slightly with the addition of spectral information, although spectral information can prove more useful for species differentiation. There have also been examples of mapping exercises in which lidar is only available for a subset of the study area, while spectral information was available over a broader area. Wulder et al. (2007) used Landsat ETM+ data and profiling lidar in concert. The Landsat data were used to classify the region into forest types, and the

lidar was used to assign height data for those classes. In a similar approach by (Andersen et al., 2011b), Landsat and IFSAR were used to classify the landscape using a nearest neighbor approach, then scanning lidar data was used to estimate average biomass for the classes. The approach described by (Andersen et al., 2011b) was aimed at estimation (e.g. the population mean or total) rather than prediction (e.g. mapping). In another study, Hudak et al. (2002) used simulations to look at estimation of canopy height from Landsat ETM+ and samples of lidar data for different numbers and configurations of lidar samples. Wall-to-wall lidar was resampled systematically in strips and small circles. Landsat data and spatial correlation were used to predict heights for areas omitted in a particular resample simulation. The study found that it was possible to sample the landscape with lidar and still predict forest height information for areas not covered with lidar. A primary advantage of such an approach is that if it can be used successful, then Landsat, the auxiliary spectral data used in the study which has a frequent return interval (>1 month) and is available for free could be used to support forest mapping at little or no cost. However, the sampling densities examined exceed those that have been considered in practice (Andersen, 2009, 2009; Andersen et al., 2011a; Gregoire et al., 2011; Parker and Glass, 2004; Ståhl et al., 2011).

Whether a multi-scale approach with lidar strips can succeed is also dependent upon the modeling strategy. For example, one of the simplest strategies, taking the mean of sample plot data within a landscape segment and applying it to every pixel within the segment, will in many instances not be sufficiently precise for mapping or efficient for estimation. Preferably a more efficient strategy can better reflect the range of response values observed within the segment. Two of the most common approaches to modeling forest attributes with lidar include ordinary least squares (OLS) (Means et al., 2000b; Strunk et al., 2012) and nearest neighbors (Maltamo et al., 2006; Packalén and Maltamo, 2007). Ordinary least squares has proven to work well for prediction of a variety of continuous forest attributes including basal area (Means et al., 2000a; Jensen et al., 2006), volume (Næsset, 1997; Lim et al., 2003), and biomass (Drake et

al., 2003; Hall et al., 2005). Nearest neighbor approaches also appear to work well for these variables, and depending upon the implementation, also have the flexibility to simultaneously predict attributes by trees species including diameter distributions (Packalén and Maltamo, 2008).

While lidar can be quite effective for modeling some forest attributes, complete lidar coverage can be prohibitively expensive, and for a lidar sample strip estimation strategy, high-precision lidar-based mapped products are not available over the majority of the AOI. The objective of this study is to develop and evaluate modeling approaches for prediction of forest attributes using Landsat for an AOI in which lidar strips are available as a sample. We evaluate selected approaches to "fill in" areas not covered with lidar by using lidar to train models with Landsat as auxiliary variables. We demonstrate that using lidar strip data to train Landsat in a multi-step modeling procedure improves predictions of forest attributes. OLS and nearest neighbor approaches are explored for modeling, and both 30m and 90m data resolutions for training Landsat with lidar are explored. Prediction performance is evaluated in our investigations for a subset of the overlap between lidar and Landsat for our AOI, ~1500 points.

4.2 Methods

4.2.1 Study site

Our study was conducted for the boreal forests located in the western lowlands of the Kenai Peninsula Alaska (Figure 4.1). The western lowlands are an area of approximately 8200 km^2 on the Kenai Peninsula. The extent of our study area was restricted to the portion of the western lowlands which falls within a single Landsat image, approximately 7400 km^2. Prevalent forest types for this area include black spruce (Picea mariana) in wet lower parts of drainages, and mixed paper birch (Betula papyrifera), white spruce (Picea glauca), and quaking aspen (Populus tremuloides) in well drained areas.

FIA has an annual inventory design in operation for this area. They were able to implement an inventory for this portion of Alaska because it is relatively accessible: the weather in this region is relatively mild, there is a road system connecting communities, and the peninsula is surrounded by water enabling helicopter access from a helipad located on a boat even in roadless areas.

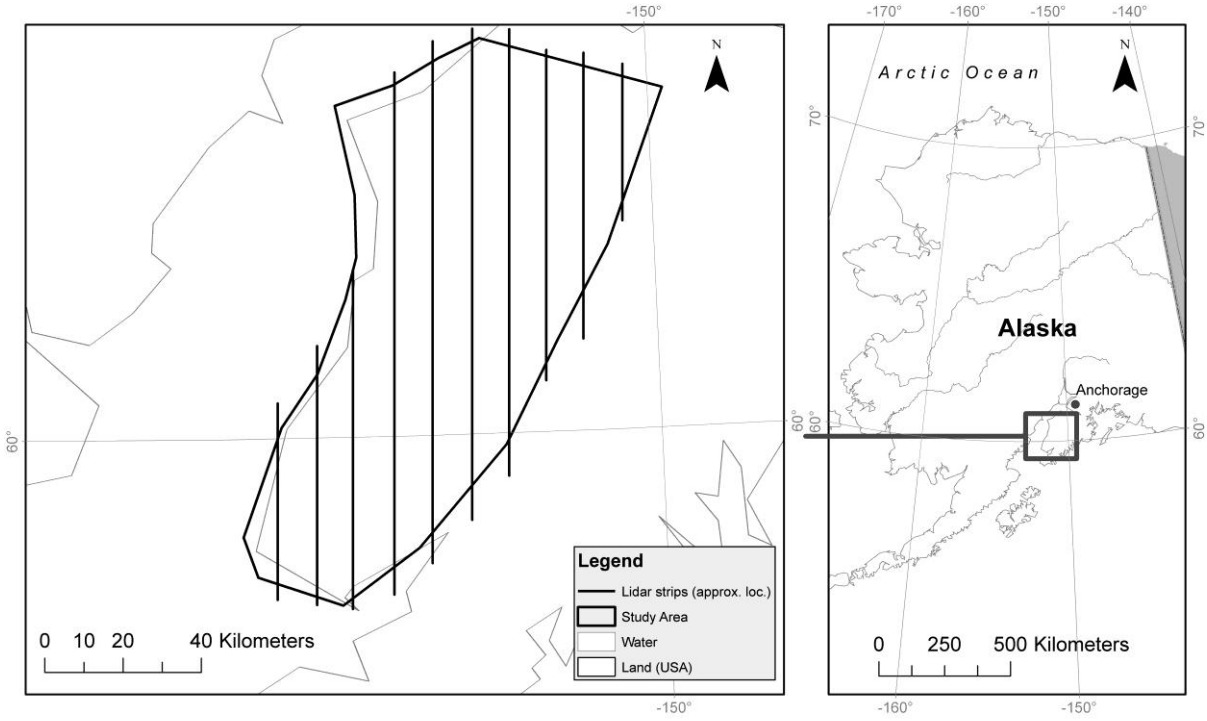

Figure 4.3 Location of study area on the Kenai Peninsula, Alaska

4.2.2 Forest measurement data

Data for this study were collected as part of the United States Forest Service (USFS) Forest Inventory and Analysis (FIA) annual inventory program. While the field plots are organized as part of a 10 panel design, for our purposes the relevant design components are that field plots are arranged systematically, and each field plot consists of four circular .017 ha subplots arranged in a fixed manner with respect to distance and orientation (Bechtold and Patterson, 2005). The systematic sample of field plots on the Kenai Peninsula has a single randomization for the entire grid, unlike

other parts of the country where individual plots are randomized within approx. 6000 ha hexagonal tessellations. The field measurements used in this study were collected between 2005 and 2009 for trees greater than 12.7 cm in diameter. A subset of 32 plots including 80 (Table 4.1) subplots from the systematic grid of field plots covering our AOI was used for our analyses. These are plots for which precise GPS coordinates (better than .5 m HRMSE, (Andersen et al., 2009)) were obtained with a survey-grade GPS unit. Tree height, diameter, species, condition class (live or dead), and biomass from the FIA database were used. Plot-level values were calculated from the individual tree records including biomass per hectare (bio), basal area per hectare (ba), and stems per hectare (stems).

Table 4.2 Summary of response data for 80 subplots used in analyses

	bio kg/ha	ba m^2/ha	stems /ha
min	0	0.0	0
max	179,002	32.9	1,130
mean	35,421	8.3	227
st. dev.	45,572	9.1	242

4.2.3 Lidar

Airborne discrete-return scanning lidar data (lidar) were collected leaf-off for the Kenai Peninsula in the spring of 2009. Lidar data were collected in a systematic sample of strips over the locations of a subset of the grid of FIA field sample plots on the peninsula. The average flying height was 1,150 m above ground, the maximum scan angle was 7.5 degrees, the average flying speed was 130 Knots, and the pulse repetition frequency was approximately 71 kHz .The flight configuration yielded a nominal pulse density of ~4 pulses / m^2.

Lidar data consists of a series of records corresponding to locations (“returns”) where pulses within laser scan lines intersected the ground or objects above the ground. We are specifically interested in the vertical distribution of lidar returns within an area (e.g. a plot) which provide a sample of the vertical arrangement of stems, branches,

and foliage. Lidar data were summarized using statistics computed on lidar heights (these lidar statistics are henceforth referred to as "lidar metrics"). Lidar heights are lidar point elevations minus ground elevations for the same horizontal coordinates. The point data were processed to extract lidar metrics for circles with 13m, 30m, and 90m radii. Lidar metrics considered in our analyses include height percentiles (for example, ht_{95} is the 95 percentile lidar height computed from all of the first-return lidar heights in the plot greater than 1m) and cover ratios (for example, $cover_1$ is the proportion of first returns above 1m). Lidar data were processed using the freely-available FUSION software (McGaughey, 2012) including identification of ground returns and interpolation of a digital terrain model.

4.2.4 Landsat

Our analyses made use of the historical archive of Landsat TM and Landsat ETM+ imagery available from the GLOVIS website (http://glovis.usgs.gov/). Landsat images were selected for the period spanning 1984 to 2009. For this range of years images were selected for dates between late spring and early fall that had cloud-free areas intersecting our AOI. Landsat ETM+ images were used from both SLC on (1999-2003), and SLC off (after May 2003) periods.

The Landsat data were used in this study by taking advantage of the trajectories of individual pixel values over time. Ideally, we expect to relate the value recorded for a pixel to static (constant over a short period such as a year) vegetation properties for the corresponding location on the ground. However, the value recorded for a given pixel is influenced by a wide variety factors including phenology, atmospheric conditions, solar incidence angle, sensor properties, and others. For our purposes, effects from these factors are all considered noise. If we assume these sources of noise are random, then for a pixel representing a static ground condition we can average values from multiple years to obtain a more representative, less noisy pixel value. The LandTrendr process (Kennedy et al., 2010) takes this one step further and empirically models the trend in values for a single pixel over time using iterated piecewise regression. This is

useful because it essentially allows us to average out noise over a lengthy period of time despite potential changes in the structural characteristics of vegetation that we are interested in measuring. The rate of incline, decline, and the occurrence of drastic changes in the pixel trajectory over time can also be indicators of the physical processes taking place on the ground (Meigs et al., 2011; Pflugmacher, 2011; Powell et al., 2010). However, for this initial analysis, we only investigate the predictive properties of the noise-dampened fitted pixel values. Because the model will tend to be less stable near the bounds of the data (1984 and 2009 in our case) we used fitted values for 2007 as predictors for our analysis. We fitted pixel-based time-series models for Landsat bands 1-5, and 7, as well as the derivative vegetation indices normalized burn ratio (NBR), and normalized difference vegetation index (NDVI). Pixel values were interpolated to points from surrounding cells by taking the averages of cells with center points within 30m and 90m radii.

4.2.5 Model development

A model can be defined as a mathematical or statistical representation of a relationship between variables which may represent processes or attributes of interest(Ford, 2009). Or, more generally as a mechanism which accepts data as an input, processes the data, and outputs modified data (MacKay, 2012). We use models in this study to bridge a relationship between response variables and auxiliary variable. However, the models taken without appropriate context are non-parametric, and cannot necessarily be ascribed useful properties. Typically, however, we develop models in a way that they are useful for scientific inference and we make inference from and about the models by relying on statistical theory. But, fitting a model does not automatically imply that we are using model-based statistics. Ordinary Least Squares (OLS) regression, which includes simple linear regression and multiple regression, does not imply a model-based analysis or an attempt at model-unbiasedness – although this may be the case and it is often useful to do so. An OLS model, for example, is at its simplest simply an explicit mathematical link between variables until we attempt to assign theoretical properties to the model.

It is in the sense of explicitly linking inputs and outputs that we proceed to examine OLS and several nearest neighbor (kNN) modeling approaches. In both of these approaches, algorithms are used to develop model(s) relating response and predictor variables. The models are then used to predict response values for locations where only predictor information is available. The primary advantage of models in the mapping context is the ability to predict values for every location on the landscape. We do not, however, claim that the prediction strategies are unbiased for what is present at a given location from either a model-based or design-based perspective. The predictions are still useful however, even if they are, for example, biased towards the mean (noise in the explanatory variables with OLS causes coefficients to be biased towards zero (Kmenta, 1997b, 348–352), because they may still describe a sufficient portion of the variability that is present on the landscape to be useful for inference from mapped outputs. We do claim that our sample of field plots can be used to represent the variability of predictions relative to their true values.

By convention in discussions of nearest neighbor models for forestry, "reference" or "training" observations are data points for which both explanatory and response variables are available, and "target" observations are observations for which only explanatory variables are available and for which we wish to make a prediction. "Imputation" is commonly used with nearest neighbor approaches instead of the word "prediction". Formally the word "imputation" means to substitute for missing values, although practically the word is used synonymously with "prediction" – except that it denotes that a nearest neighbor strategy was employed for the prediction. These same conventions are equally applicable to alternate modeling approaches. The model used to predict a new value using the nearest neighbor approach is a linear function of the response values from the K (an integer > 0) nearest training observations as measured by some distance metric in explanatory space – thus it is referred to as the k nearest neighbors (kNN) approach. The k nearest neighbors imputed to a new location are referred to as "donors" for obvious reasons. In predicting a new value from a linear function of donor values it is common to weight donors inversely to their relative

distance from the target observation in explanatory space, or to simply average the k nearest neighbors. In preliminary investigations with the dataset used for this study, the performance of prediction (model RMSE) was largely insensitively to the choice of k in the range of 3 to 15 neighbors when there were sufficient numbers of training observations. We arbitrarily set k to 5 neighbors and used inverse distance weighting for imputations. The kNN approach is simplest to apply when used for continuous response variables, although a variety of approaches are feasible to reflect multiple donors of categorical variables (not discussed here). In this study only continuous variables were considered.

The choice of a distance metric plays an important role in the kNN model, and has a significant role in performance. We examined four measures of distance for nearest neighbor approaches in this study. The first distance approach was Euclidean distance based on normalized predictors (kNN-EU). The second was weighted Euclidean distance with weights assigned according to the magnitudes of the coefficients when canonical correlation was used to relate normalized response and predictor variables (kNN-MSN). The third approach was based upon distances calculated from a random forest proximity matrix (kNN-RF). The final approach used Mahalanobis distance (kNN-MH).

4.2.6 Modeling strategies

Selected strategies were examined to link Landsat to field metrics using both two-phases and three-phases of data. In the two-phase scenario a vector of field measured forest attributes **Y** was linked directly to a vector of 30m auxiliary Landsat variables, $\boldsymbol{X_{30,ls}}$, with fitted model $\hat{f}_1$

$$\boldsymbol{Y} = \hat{f}_1(\boldsymbol{X}_{30,ls}) + \hat{\boldsymbol{e}}_1 \quad (1)$$
$$\widehat{\boldsymbol{Y}}_{\boldsymbol{30,ls}} = \hat{f}_1(\boldsymbol{X}_{30,ls}),$$
$$\hat{\boldsymbol{e}}_1 = \widehat{\boldsymbol{Y}}_{\boldsymbol{30,ls}} - \boldsymbol{Y}$$

where the resolution of the forest attribute(s) and the Landsat differ.

Two distinct three-phase procedures were examined. In three-phase procedure A, third phase field metrics were linked to second phase auxiliary (13m) lidar data, $\boldsymbol{X_{13,lid}}$ using fitted model $\hat{f}_2$. Then estimates from second-phase data were linked to first phase Landsat data at 30m, $\boldsymbol{X_{30,ls}}$, and 90m resolutions, $\boldsymbol{X_{90,ls}}$, using fitted model $\hat{f}_3$

$$\boldsymbol{Y} = \hat{f}_2\left(\boldsymbol{X}_{13,lid}\right) + \hat{\boldsymbol{e}}_2 \tag{2}$$

$$\widehat{\boldsymbol{Y}}_{\boldsymbol{30,lid}} = \hat{f}_2\left(\boldsymbol{X}_{30,lid}\right)$$

$$\hat{Y}_{30,lid} = \hat{f}_3\left(\boldsymbol{X}_{30,ls}\right) + \hat{\boldsymbol{e}}_3 \tag{3}$$

$$\hat{\hat{Y}}_{30,ls} = \hat{f}_3\left(\boldsymbol{X}_{30,ls}\right)$$

$\hat{\hat{Y}}_{30,ls}$ *is a prediction of* Y *from the first phase of data where the procedure also used* $\boldsymbol{X}_{90,ls}$.

In three phase procedure B, phases 1 and 2, and phases 2 and 3 are linked separately. First, a model is developed to relate field metrics to lidar as in (2) from procedure A

$$\boldsymbol{Y} = \hat{f}_2\left(\boldsymbol{X}_{13,lid}\right) + \hat{\boldsymbol{e}}_2. \tag{4}$$

But instead of predicting phase 3 values with model $\hat{f}_2$ and auxiliary lidar as in (3), phase two is linked to phase 3 by directly modeling the relationship between phase 2 lidar variables and phase 1 Landsat variables with $\hat{f}_4$

$$\boldsymbol{X}_{30,lid} = \hat{f}_4\left(\boldsymbol{X}_{30,ls}\right) + \hat{\boldsymbol{e}}_3 \tag{5}$$

$$\widehat{\boldsymbol{X}}_{30,lid} = \hat{f}_4\left(\boldsymbol{X}_{30,ls}\right).$$

Then phase 2 predicted values are used to predict forest attributes with the model developed to link phases 2 and 3 with the fitted model $\hat{f}_2$ developed previously

$$\hat{Y} = \hat{f}_2(\hat{\boldsymbol{X}}_{30,lid}). \quad (6)$$

The rationale behind a three phase lidar and Landsat procedure is that Landsat may relate better to field metrics when modeled at the same resolution. Landsat is approximately 30m resolution, while the field metrics are approximately 13m. This means that the information recorded by Landsat includes the area around the field plot. There is also notable error (30m+) in the spatial registration of the Landsat imagery, which would further reduce the correspondence between the two sets of data. The lidar data may also include auxiliary information about the site which is not well represented in response data but may aid in bridging the field data to the first phase of the data. If lidar is used as an intermediate data source, the scales of the data could be matched, and the influence of errors in co-registration would decrease for larger units of area. Additionally, using lidar and an intermediate data source will increase the size of the training set, increasing our power to discerning signal from noise.

4.2.7 Variance estimation

Prediction strategies were evaluated relative to their residual variability using a resampling simulation approach. A resampling simulation approach was adopted because of the simplicity of implementation, the flexibility of such an approach, and the freedom from parametric assumptions – which is especially relevant since we are evaluating non-parametric modeling strategies. Residual variability was estimated using a leave-d-out cross-validation strategy (12) with d=2. Clusters of sub-plots subplots were omitted (2 at a time) in the delete-d simulations to reflect the clustering in the original dataset.

$$\hat{\sigma}_{\hat{\varepsilon}}^2 = \frac{n-d}{k}\sum\left(\hat{Y}_i - Y_i\right)^2 \quad (12)$$

Y_i *is a response variable of interest*

$\hat{Y}_i$ *is a prediction of* Y_i

n *is the number of observations*

d *is the number of observations omitted*

k *is the number of simulations*

A leave-one-out strategy was originally tested, but due to the small number of possible simulations for our sample size, 32 (the number of simulations is equal to the number of observations for a leave-one-out strategy), the leave-one-out estimator did not sufficiently converge. By using a leave-d-out approach the n choose d (where d>1) possible simulation increases the potential to achieve convergence. For example, in Figure 4.2 for one of the modeling scenarios, the leave-3-out (ultimately we used leave-2-out for estimation) residual standard deviation estimator represented by the solid black line does not sufficiently stabilize until approximately 150 simulations for the three-phase strategy, a much greater number of simulations than 32, the number of simulations for a leave-1-out estimator for our dataset. The rate of convergence demonstrated in Figure 4.2 was roughly consistent with results for other modeling scenarios.

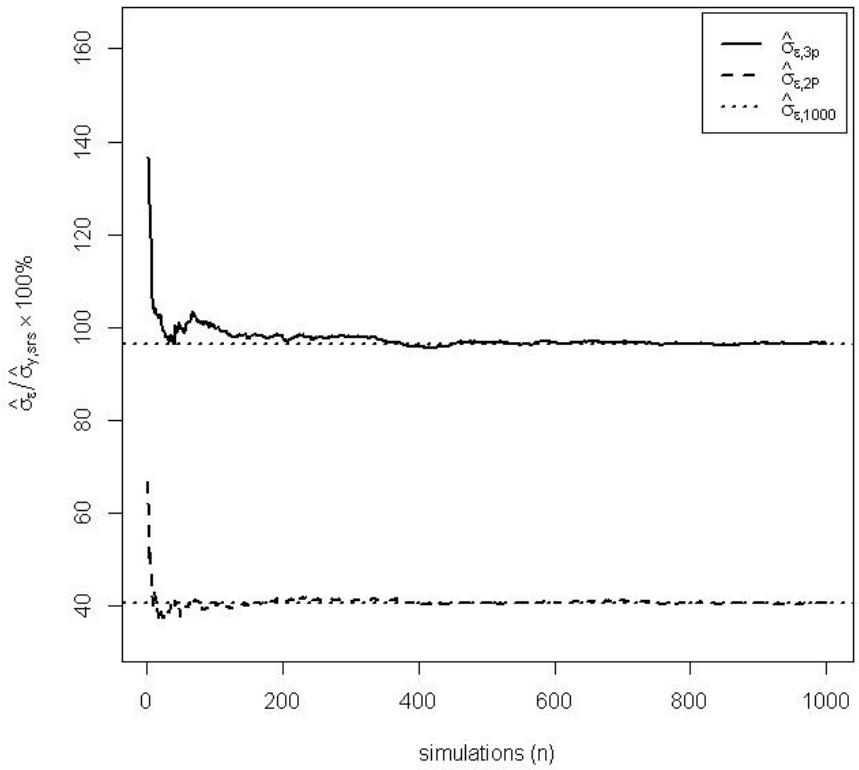

Figure 4.4 Visual diagnostic of convergence relative to number of simulations for an example leave-3-out estimator of residual standard deviation. $\hat{\sigma}^2_{\varepsilon,3p}$ and $\hat{\sigma}^2_{\varepsilon,2p}$ indicate the lines representing estimates of residual standard deviation for different numbers of simulations for three-phase and two-phase modeling strategies respectively. $\hat{\sigma}^2_{\varepsilon,100}$ is a horizontal line indicating the estimate of residual standard deviation following 100 iterations.

Although convergence is less of an issue with bootstrap simulations because samples are taken with replacement, we chose not to not use a bootstrap approach because we found that for our sample size the reduced range of the explanatory variables in bootstrap resamples caused over-estimation of residual variance. In traditional bootstrap simulations (Efron and Tibshirani, 1993) a subsample of observations will have reduced range. This is not a problem for large datasets, but for a dataset as small as the one used in this study, in simulations it contributed extra variability to estimates of regression coefficients.

Because the resolution of phase 1 predictions did not match the resolution of field measurements, residual variability for the 3-phase A approach was estimated using (12)-(16), derived with similar notation to Kmenta (1997, 347–348) for simple linear regression . In (12), ω_i is a residual error from the model linking phase 3 to phase 2 where Y_i is an observed response variable and

$$Y_i = \alpha_1 + \beta_1 X_i - \omega_i \tag{12}$$
$$\hat{Y}_i = \alpha_1 + \beta_1 X_i$$
$$= Y_i + \omega_i$$
$$where\ X_i\ is\ a\ predictor\ and\ \alpha_1 and\ \beta_1\ are\ model\ coefficients\ .$$

Then phase 2 is linked to phase 1 contributing error ε_i

$$Y_i = \alpha_2 + \beta_2 W_i + \varepsilon_i \tag{13}$$
$$where\ \hat{Y}_i\ is\ substituted\ for\ Y_i\ so\ that$$
$$\hat{Y}_i - \omega_i = \alpha_2 + \beta_2 W_i + \varepsilon_i$$
$$\hat{Y}_i = \alpha_2 + \beta_2 W_i + \varepsilon_i + \omega_i$$
$$\hat{\hat{Y}}_i = \alpha_2 + \beta_2 W_i$$

The residual variance for $\hat{\hat{Y}}_i$ is the variance for the sum of the residuals

$$V[\hat{\hat{Y}}_i] = V[\varepsilon_i + \omega_i] \tag{14}$$
$$= \sigma_\varepsilon^2 + \sigma_\omega^2 + 2 * \sigma_{\varepsilon,\omega}^2$$
$$where$$
$$V[\varepsilon_i] = \sigma_\varepsilon^2$$
$$V[\omega_i] = \sigma_\omega^2$$
$$Cov[\varepsilon_i, \omega_i] = \sigma_{\varepsilon,\omega}^2\ .$$

A variance estimator is developed from consistent estimators for the various components

$$V[\hat{Y}_i|W_i] \approx \hat{\sigma}^2_{\hat{\varepsilon}} + \hat{\sigma}^2_{\hat{\omega}} + 2 * \widehat{cov}[\hat{\varepsilon}, \hat{\omega}] \quad (15)$$
$$= \hat{\sigma}^2 \text{ , the estimator of residual variance for } \hat{\hat{Y}} \text{ where}$$
$$\hat{\sigma}^2_{\hat{\varepsilon}}, \hat{\sigma}^2_{\hat{\omega}}, \text{and } \widehat{cov}[\hat{\varepsilon}, \hat{\omega}] \text{ are resample} - \text{based}$$
$$\text{estimators of } \sigma^2_{\varepsilon}, \sigma^2_{\omega}, \text{and } \sigma^2_{\varepsilon,\omega} \text{ when model coefficients in } (12)$$
$$\text{and } (13) \text{ are replaced with OLS estimators.}$$

This approach to variance estimation is applicable generically if we replace the simple linear regression model from (12) (and similarly (13)) as follows

$$Y_i = f(\boldsymbol{X_i}) - \omega_i \quad (16)$$
$$\hat{Y}_i = f(\boldsymbol{X_i})$$
$$= Y_i + \omega_i$$
$$\text{where } f(.) \text{is any generic model that accepts a vector}$$
$$\text{of predictors } \boldsymbol{X_i} \text{ for element i.}$$

A modification to steps (12) – (16) was necessary for the 3-phase B approach since in (4) –(6) we do not have a model that involves the response when relating phases 1 and 2. In the 3-phase B approach residuals $\hat{\omega}_i$ from relating phase 1 and phase 2 in (15) are estimated as

$$\hat{\omega}_i = \hat{f}_2\left(\widehat{\boldsymbol{X}}_{i,lid}\right) - \hat{f}_2\left(\boldsymbol{X}_{i,lid}\right) \quad (17)$$

4.3 Results

Residual variability was quantified using the leave-2-out strategy described in (12)-(17) for the 32 plots (80 sub-plots) used for this analysis. Residual variability was estimated from the 32 choose 2 simulations, or 496, possible unique combinations of 2

plots that can be withdrawn from the training dataset. Residuals were calculated for the subplots corresponding to the 2 omitted plots in each of the 496 simulations per modeling strategy. New models were fit relating forest attributes and auxiliary data for the subplots corresponding to plots not omitted in each of the 496 iterations. Estimates of residual variability, residual root mean square errors (RMSEs), were calculated by taking the standard deviations of residuals for the subplots from the 496 simulations. Although approximately 1500 points were available to model Landsat with lidar – data which could also be used to aid in variance estimation, only the points corresponding to the locations of field plots were used to estimate the variability of residuals for models linking phase 2 lidar to phase 1 Landsat. Simulations (figure 2) indicated that this approach was sufficient for convergence of leave-2-out estimators of residual standard deviations.

RMSEs were calculated for three-phase models developed for a large number of modeling configurations using a subset of the lidar and Landsat datasets, approximately 1500 points including subplot locations. At each of the 1500 points, lidar metrics and Landsat values were calculated as described in the methods section for 13m (lidar only), 30m, and 90m resolutions. A subset of points on the landscape was used instead of the complete lidar and Landsat datasets because calculating RMSEs for the various configurations required extensive processing time. The processing times required for kNN approaches especially were affected by the number of observations used for training and the number of targets for which predictions were desired.

The modeling configurations examined included three general strategies: two-phase strategies with Landsat and field plots, and three-phase strategies A and B with Landsat, lidar, and field data. As an aside we also examined two-phase strategies with field data and lidar to guide our selection of modeling strategies for use with three-phase A and three-phase B approaches. For each of the combinations of multi-phase prediction strategies we examined select combinations of model types including OLS

and the various kNN approaches. We did not attempt every combination of modeling strategy and model type, instead focused on strategies motivated from examining the performance of two-phase strategies.

In two-phase strategies, lidar (Table 4.2) performed much better than Landsat (Table 4.3), which was the expected result - although a two-phase lidar approach is not considered a viable mapping strategy when lidar is collected as a sample of strips. For both auxiliary datasets, OLS models performed better on average than alternate model types. kNN-RF performed only slightly worse in most cases, and both kNN-RF and kNN-EU performed better than OLS for number of stems/ha for lidar. Coarser resolution (90m in this study) auxiliary data was not considered for two-phase strategies. The same sets of predictor variables were available for automated model selection in each strategy.

Table 4.3 Two-phase lidar (13m) model RMSE values for various model types

	$\hat{\sigma}_{\varepsilon,2P}$ ($\hat{\sigma}_{\varepsilon,2P} / \hat{\sigma}_{Y,SRS} \times 100\%$)					
Models	bio kg/ha (%)		ba m^2/ha (%)		stems /ha (%)	
OLS	21061	(44%)	5.0	(52%)	193	(77%)
kNN-MSN	23786	(50%)	5.5	(58%)	213	(85%)
kNN-RF	22395	(47%)	4.9	(52%)	184	(73%)
kNN-EU	23880	(50%)	5.1	(54%)	177	(70%)
kNN-MH	28734	(60%)	6.2	(66%)	219	(87%)

Table 4.4 Two-phase Landsat (30m) model RMSE values for various model types

	$\hat{\sigma}_{\varepsilon,2P}$ ($\hat{\sigma}_{\varepsilon,2P} / \hat{\sigma}_{Y,SRS} \times 100\%$)					
Models	bio kg/ha (%)		ba m^2/ha (%)		stems /ha (%)	
OLS	43115	(92%)	8.4	(90%)	228	(93%)
kNN-MSN	48344	(104%)	9.3	(100%)	243	(99%)
kNN-RF	46053	(99%)	8.8	(95%)	233	(94%)
kNN-EU	48862	(105%)	9.4	(101%)	237	(96%)
kNN-MH	48663	(104%)	9.2	(100%)	237	(96%)

The performances of three-phase A and B strategies were quite different for both 30m and 90m resolutions. For the 30 m resolution (Tables 4.4 and 4.5) the performance for three-phase B was superior to that of three-phase A for biomass and volume for nearly every modeling configuration –especially for biomass, although the poorest three-phase B models were exceeded by the best three-phase A models. For number of stems/ha and 30m resolution, in contrast, the three-phase A strategy appears to be generally superior.

Table 4.5 Three-phase A 30m prediction strategy RMSE values for various model types

	$\hat{\sigma}_{\varepsilon,3P}$ ($\hat{\sigma}_{\varepsilon,3P} / \hat{\sigma}_{Y,SRS} \times 100\%$)					
Models	bio kg/ha	(%)	ba m^2/ha	(%)	stems /ha	(%)
OLS OLS	43159	(90%)	8.3	(88%)	222	(88%)
OLS kNN-MSN	43742	(91%)	8.7	(92%)	222	(88%)
OLS kNN-RF	46336	(97%)	9.2	(98%)	227	(90%)
OLS kNN-EU	46112	(96%)	9.2	(97%)	226	(90%)
OLS kNN-MH	45582	(95%)	9.1	(96%)	221	(88%)
kNN-MSN OLS	45264	(94%)	9.3	(98%)	259	(103%)
kNN-RF OLS	44800	(93%)	8.6	(91%)	216	(86%)
kNN-EU OLS	44053	(92%)	8.7	(92%)	221	(88%)
kNN-MH OLS	39764	(83%)	8.3	(87%)	249	(99%)

Table 4.6 Three-phase B 30m prediction strategy RMSE values for various model types

	$\hat{\sigma}_{\varepsilon,3P}$ ($\hat{\sigma}_{\varepsilon,3P} / \hat{\sigma}_{Y,SRS} \times 100\%$)					
Models	bio kg/ha (%)		ba m^2/ha (%)		stems /ha (%)	
OLS OLS	38288	(80%)	7.8	(82%)	229	(91%)
OLS kNN-MSN	43630	(91%)	8.6	(91%)	241	(96%)
OLS kNN-RF	41474	(86%)	8.3	(88%)	238	(94%)
OLS kNN-EU	42183	(88%)	8.2	(87%)	234	(93%)
OLS kNN-MH	45084	(94%)	8.9	(94%)	249	(99%)
kNN-MSN OLS	39587	(82%)	8.8	(93%)	302	(120%)
kNN-RF OLS	37357	(78%)	8.0	(85%)	268	(106%)
kNN-EU OLS	33652	(70%)	7.6	(81%)	258	(103%)
kNN-MH OLS	33161	(69%)	7.8	(83%)	295	(117%)

The differences between three-phase A and B performances for 90m were even more pronounced in favor of the three-phase B strategy for all three of the response variables (tables 6 and 7). Both strategies saw improvement from using 90m resolution data in linking lidar to Landsat, but the improvement was minimal for three-phase A. For the three-phase B strategy, improvements were substantial for all three of the response variables for several combinations of models.

Table 4.7 Three-phase A 90m prediction strategy RMSE values for various model types

	$\hat{\sigma}_{\varepsilon,3P}$ ($\hat{\sigma}_{\varepsilon,3P} / \hat{\sigma}_{Y,SRS} \times 100\%$)					
Models	bio kg/ha (%)		ba m^2/ha (%)		stems /ha (%)	
OLS OLS	35017	(73%)	7.7	(81%)	218	(87%)
OLS kNN-MSN	39583	(82%)	8.3	(88%)	224	(89%)
OLS kNN-RF	42257	(88%)	8.8	(93%)	224	(89%)
OLS kNN-EU	42409	(88%)	8.8	(93%)	224	(89%)
OLS kNN-MH	41174	(86%)	8.6	(91%)	230	(91%)
kNN-MSN OLS	38191	(80%)	8.6	(91%)	251	(100%)
kNN-RF OLS	37894	(79%)	7.9	(84%)	231	(92%)
kNN-EU OLS	35129	(73%)	7.5	(79%)	209	(83%)
kNN-MH OLS	36697	(76%)	8.2	(87%)	264	(105%)

Table 4.8 Three-phase B 90m prediction strategy RMSE values for various model types

	$\hat{\sigma}_{\varepsilon,3P}$ ($\hat{\sigma}_{\varepsilon,3P} / \hat{\sigma}_{Y,SRS} \times 100\%$)					
Models	bio kg/ha	(%)	ba m^2/ha	(%)	stems /ha	(%)
OLS OLS	28538	(59%)	6.1	(64%)	203	(81%)
OLS kNN-MSN	35550	(74%)	7.3	(77%)	213	(85%)
OLS kNN-RF	36543	(76%)	7.5	(79%)	217	(86%)
OLS kNN-EU	37144	(77%)	7.8	(82%)	222	(88%)
OLS kNN-MH	37347	(78%)	7.8	(82%)	215	(85%)
kNN-MSN OLS	30960	(65%)	7.5	(79%)	258	(103%)
kNN-RF OLS	31044	(65%)	7.1	(75%)	243	(97%)
kNN-EU OLS	29562	(62%)	6.8	(72%)	244	(97%)
kNN-MH OLS	29358	(61%)	6.3	(67%)	238	(95%)

Amongst the RMSE values reported for the various strategies in Tables 4.3 – 4.6 some of the modeling configurations consistently performed better than others. The kNN-MH OLS three phase strategy, for example, was competitive in nearly every case. The OLS OLS strategy also performed well generally, and was the strategy that for three-phase B with 90m resolution performed the best of any of the strategies examined. Excluding OLS OLS, it appears that strategies which used a kNN model followed by OLS performed the best for biomass. There was no clear difference between these two groups for volume, and OLS followed by a kNN approach worked best for number of stems/ha.

4.4 Discussion

4.4.1 Multi-phase modeling strategies

We examined a two-phase approach and two three-phase approaches to modeling selected forest attributes. The two-phase approach with plot and Landsat data performed the poorest amongst the approaches. Based upon what we found with our later analyses, it is likely that plot size played a role in the lack of performance, and that a two-phase Landsat approach would be more successful with larger, and a larger number of plots. Conceivably, if the area covered by four subplots per FIA plot were

consolidated into a single larger plot the performance of Landsat models would be improved for the forest attributes examined here. Consolidation of sub-plot area into a single plot would also likely improve the performance of lidar models as there would be proportionally fewer trees with edge effects (trees in the plot with foliage extending beyond the plot, and trees external to the plot with foliage extending into the plot). However, such a plot design is likely to be less efficient for variables not effectively modeled with lidar and Landsat, and would provide less information about spatial variability. And, since for our study area a lidar strip can be less expensive than a field plot, if performance can be improved for variables associated with forest structure by leveraging lidar at an intermediate stage it could possibly mitigate this weakness.

Our analyses showed that lidar can be of assistance in an intermediate step for prediction of forest attributes ultimately with Landsat. For some configurations of resolutions and model types, both three phase approaches worked much better than a two-phase Landsat approach. Between the two three-phase approaches examined, approach B in which phases 1 and 2 and 2 and 3 are modeled separately performed better than approach A in which phase 3 predictions from phase 2 lidar were modeled with phase 1 Landsat data. Prediction performance for three-phase approaches also improved when we used larger pixels – although the improvement varied considerably. The best overall performance was seen with three-phase B for 90m resolution with OLS models linking the separate phases. The performance may improve even further for modeling strategies using larger areas (>90m) for relating lidar and Landsat, as the proportion of the areas overlapping between lidar and Landsat would increase, reducing the impacts of edge effects and registration errors.

4.4.2 Limitations

In this study there were a variety of limitations with respect to the training dataset restricting our ability to explore different modeling scenarios. As a result, the findings we present here are certainly not the last word on the issues explored in this study, even for our study area. For example, our training data was not collected

simultaneously with the lidar. Field measurements spanned a 5 year period, while lidar was collected in 2009, the 5th year of data collection. Also, the number of training observations was small, and the size of subplots was quite small. As a result we cannot speculate on the performance of our approach under ideal conditions, but given that we were able to explain more variability with a three-phase approach than was feasible in a two-phase approach with Landsat, our results still indicate that using lidar to scale up plot data to the resolution of the Landsat data is an opportunity worth exploiting. This is especially the case if a lidar strip sampling approach is already in place or under consideration for estimation purposes.

4.4.3 Multi-temporal Landsat

The multi-temporal Landsat data available for free from USGS is an under-utilized resource. We were able to make use of this resource to generate atmospherically corrected, cloud free, and temporally normalized Landsat values. By temporally normalized we mean that there is apparent variability in the sensed values for a particular pixel for a particular band which is not associated with changes is the associated vegetative structure. However, this too is an under-utilization of this resource and we envision greater success in the prediction of forest attributes if the trend information, such as intercept for the trend, or the slope or information about large perturbations are taken into consideration as described in Meigs et al. (2011), Robert E. Kennedy et al. (2007), Powell et al. (2010), Pflugmacher, (2011), and others. At this time we also cannot comment on whether using LandTrendr data for image processing improved the performance for cloud-free pixels, but since there are no recent Landsat images available for the Kenai peninsula which are 100% cloud free, we can say that we were able to develop predictions for all areas on the peninsula which would not be possible with a single image. In the future we plan to quantify any gains from using this approach for cloud-free pixels, as well as the potential gains from a more sophisticated interpretation of Landsat time-series information for individual pixels.

4.4.4 High-resolution aerial imagery

The availability of off-the-shelf and publicly available imagery has increased in recent years. In many areas greater than 1 meter resolution aerial imagery is available for free, or at a low cost; USDA NAIP imagery (Gabbott and Officer, 2003), for example. As with Landsat, there is some difficulty in relating forest attributes to aerial imagery. However, with higher resolution data the potential for relating field metrics, especially species, to texture, vegetation indices, and pixel DN values may be higher because the resolution, quality, and quality of spatial reference for aerial orthophotos is generally higher than for medium resolution satellite imagery. This means that with higher resolution imagery there may be even more potential for a three phase approach with lidar as an intermediate data source. It is unlikely that planar information from aerial imagery can achieve the precision achieved with three-dimensional information available from lidar, thus even for very high resolution imagery, using lidar as an intermediate data source may still provide and advantage by increasing the size of the training dataset for modeling with imagery. We did not use high resolution imagery in this study due to availability, complexity, and cost, but when available it is likely to contribute to the viability of a multiphase plot, lidar, and imagery modeling approach.

4.5 Conclusions

Using lidar as a strip sample is an innovative approach to leverage the forest structural information measured by lidar, while collecting the data for a reduced cost relative to a complete area collection. This is chiefly aimed at point estimation, e.g. total biomass for an area, but we demonstrate in this study that lidar strips can also be useful in training coarser resolution and planar Landsat data for prediction of the forest attributes biomass, volume, and trees per hectare. We explored a number of approaches and found that linking plot data to lidar and lidar to Landsat in separate steps before predicting forest attributes with Landsat yielded the most gain with respect to prediction RMSE. And using a 90m resolution yielded better results than when lidar was linked to Landsat at 30m resolution. Moving to an even larger area for modeling lidar to Landsat may also prove beneficial.

While we only performed our analyses for a sample of locations on the peninsula in our exploratory investigations, for mapping applications the use of LandTrendr pre-processing algorithms enables mapping of predictions with a preferred modeling strategy across the entire study area and potentially for any point in the time series. These are important benefits given the difficulty in finding cloud-free images in Alaska, the irregularities in ETM+ data after May 2003 caused by the failure of an important sensor component, the scan line corrector (SLC), for Landsat 7, and the recent (November 2011 to current) difficulties with Landsat 5 data continuity. However, the approach used here did not fully leverage the Landsat pixel trajectories modeled with LandTrendr; we plan to make better use of them in future analyses.

4.6 Acknowledgements

We would like to express our appreciation to Robert E. Kennedy, and Justin Baaten for their time and effort in helping us to process Landsat using LandTrendr pre-processing routines.

Funding for this study was provided by USFS PNW research station FIA.

4.7 Citations

Andersen, H.E. 2009. Using Airborne Light Detection and Ranging (LIDAR) to Characterize Forest Stand Condition on the Kenai Peninsula of Alaska. West. J. Appl. For. **24**(2): 95–102.

Andersen, H.E., Clarkin, T., Winterberger, K. and Strunk, J.L. 2009. An Accuracy Assessment of Positions Obtained Using Survey-and Recreational-Grade Global Positioning System Receivers across a Range of Forest Conditions within the Tanana Valley of Interior Alaska. West. J. Appl. For. **24**(3): 128–136.

Andersen, H.E., Strunk, J. and Temesgen, H. 2011a. Using Airborne Light Detection and Ranging as a Sampling Tool for Estimating Forest Biomass Resources in the Upper Tanana Valley of Interior Alaska. Western Journal of Applied Forestry **26**(4): 157–164.

Andersen, H.-E., Strunk, J., Temesgen, H., Atwood, D. and Winterberger, K. 2011b. Using multilevel remote sensing and ground data to estimate forest biomass resources in remote regions: a case study in the boreal forests of interior Alaska. Canadian Journal of Remote Sensing **37**(6): 596–611.

Bechtold, W.A. and Patterson, P.L. 2005. The enhanced forest inventory and analysis program: national sampling design and estimation procedures. Asheville, North Carolina: US Department of Agriculture Forest Service, Southern Research Station. 85 p.

Drake, J.B., Knox, R.G., Dubayah, R.O., Clark, D.B., Condit, R., Blair, J.B. and Hofton, M. 2003. Above-ground biomass estimation in closed canopy Neotropical forests using lidar remote sensing: factors affecting the generality of relationships. Global Ecology and Biogeography **12**(2): 147–159.

Efron, B. and Tibshirani, R. 1993. An introduction to the bootstrap. CRC Press. 456 p.

Ford, A. 2009. Modeling the Environment, Second Edition. Island Press. 401 p.

Gabbott, W.G. and Officer, C. 2003. The National Agriculture Imagery Program.

Gregoire, T.G., Stahl, G., Naesset, E., Gobakken, T., Nelson, R. and Holm, S. 2011. Model-assisted estimation of biomass in a LiDAR sample survey in Hedmark County, Norway. Canadian Journal of Forest Research **41**(1): 83–95.

Hall, S.A., Burke, I.C., Box, D.O., Kaufmann, M.R. and Stoker, J.M. 2005. Estimating stand structure using discrete-return lidar: an example from low density, fire prone ponderosa pine forests. Forest Ecology and Management **208**(1-3): 189–209.

Hudak, A.T., Crookston, N.L., Evans, J.S., Falkowski, M.J., Smith, A.M.S., Gessler, P.E. and Morgan, P. 2006. Regression modeling and mapping of coniferous forest basal area and tree density from discrete-return lidar and multispectral satellite data. Canadian Journal of Remote Sensing **32**(2): 126–138.

Hudak, A.T., Lefsky, M.A., Cohen, W.B. and Berterretche, M. 2002. Integration of lidar and Landsat ETM+ data for estimating and mapping forest canopy height. Remote Sensing of Environment **82**(2-3): 397–416.

Hyyppa, J., Kelle, O., Lehikoinen, M. and Inkinen, M. 2001. A segmentation-based method to retrieve stem volume estimates from 3-D tree height models produced by laser scanners. Geoscience and Remote Sensing, IEEE Transactions on **39**(5): 969 – 975.

Jensen, J.L.., Humes, K.S., Conner, T., Williams, C.J. and DeGroot, J. 2006. Estimation of biophysical characteristics for highly variable mixed-conifer stands using small-footprint lidar. Canadian Journal of Forest Research **36**(5): 1129–1138.

Kennedy, R.E., Cohen, W.B. and Schroeder, T.A. 2007. Trajectory-based change detection for automated characterization of forest disturbance dynamics. Remote Sensing of Environment **110**(3): 370–386.

Kennedy, R.E., Yang, Z. and Cohen, W.B. 2010. Detecting trends in forest disturbance and recovery using yearly Landsat time series: 1. LandTrendr —

Temporal segmentation algorithms. Remote Sensing of Environment **114**(12): 2897–2910.

Kim, S., McGaughey, R.J., Andersen, H.-E. and Schreuder, G. 2009a. Tree species differentiation using intensity data derived from leaf-on and leaf-off airborne laser scanner data. Remote Sensing of Environment **113**(8): 1575–1586.

Kim, Y., Yang, Z., Cohen, W.B., Pflugmacher, D., Lauver, C.L. and Vankat, J.L. 2009b. Distinguishing between live and dead standing tree biomass on the North Rim of Grand Canyon National Park, USA using small-footprint lidar data. Remote Sensing of Environment **113**(11): 2499–2510.

Kmenta, J. 1997a. Elements of econometrics. Univ of Michigan Pr.

Kmenta, J. 1997b. Elements of Econometrics. 2nd ed. University of Michigan Press.

Lim, K., Treitz, P., Baldwin, K., Morrison, I. and Green, J. 2003. Lidar remote sensing of biophysical properties of tolerant northern hardwood forests. Canadian Journal of Remote Sensing **29**(5): 658–678.

MacKay, B. 2012. What is a Model? URL: http://serc.carleton.edu/introgeo/models/WhatIsAModel.html.

Maltamo, M., Malinen, J., Packalén, P., Suvanto, A. and Kangas, J. 2006. Nonparametric estimation of stem volume using airborne laser scanning, aerial photography, and stand-register data. Canadian Journal of Forest Research **36**(2): 426–436.

McGaughey, R.J. 2012. FUSION/LDV: Software for LIDAR Data Analysis and Visualization, Version 3.01. USFS.

Means, J.E., Acker, S.A., Fitt, B.J., Renslow, M., Emerson, L. and Hendrix, C. 2000a. Predicting forest stand characteristics with airborne scanning lidar. Photogrammetric Engineering and Remote Sensing **66**(11): 1367–1372.

Means, J.E., Acker, S.A., Fitt, B.J., Renslow, M., Emerson, L. and Hendrix, C. 2000b. Predicting Forest Stand Characteristics with Airborne Scanning Lidar. PERS **66**(11): 1367–1371.

Meigs, G.W., Kennedy, R.E. and Cohen, W.B. 2011. A Landsat time series approach to characterize bark beetle and defoliator impacts on tree mortality and surface fuels in conifer forests. Remote Sensing of Environment.

Næsset, E. 1997. Estimating timber volume of forest stands using airborne laser scanner data. ISPRS. J. Photogramm. **61**(2): 246–253.

Packalen, P. and Maltamo, M. 2006. Predicting the plot volume by tree species using airborne laser scanning and aerial photographs. Forest Science **52**(6): 611–622.

Packalén, P. and Maltamo, M. 2008. Estimation of species-specific diameter distributions using airborne laser scanning and aerial photographs. Can. J. For. Res. **38**(7): 1750–1760.

Packalén, P. and Maltamo, M. 2007. The k-MSN method for the prediction of species-specific stand attributes using airborne laser scanning and aerial photographs. Remote Sensing of Environment **109**(3): 328–341.

Parker, R.C. and Evans, D.L. 2007. Stratified light detection and ranging double-sample forest inventory. South. J. Appl. For. **31**(2): 66–72.

Parker, R.C. and Glass, P.A. 2004. High-versus low-density LiDAR in a double-sample forest inventory. South. J. Appl. For. **28**(4): 205–210.

Pascual, C., García-Abril, A., García-Montero, L.G., Martín-Fernández, S. and Cohen, W.B. 2008. Object-based semi-automatic approach for forest structure characterization using lidar data in heterogeneous Pinus sylvestris stands. Forest Ecology and Management **255**(11): 3677–3685.

Pflugmacher, D. 2011. Remote sensing of forest biomass dynamics using Landsat-derived disturbance and recovery history and lidar data.

Popescu, S.C., Wynne, R.H. and Scrivani, J.A. 2004. Fusion of small-footprint lidar and multispectral data to estimate plot-level volume and biomass in deciduous and pine forests in Virginia, USA. Forest Science **50**(4): 551–565.

Powell, S.L., Cohen, W.B., Healey, S.P., Kennedy, R.E., Moisen, G.G., Pierce, K.B. and Ohmann, J.L. 2010. Quantification of live aboveground forest biomass dynamics with Landsat time-series and field inventory data: A comparison of empirical modeling approaches. Remote Sensing of Environment **114**(5): 1053–1068.

Ståhl, G., Holm, S., Gregoire, T.G., Gobakken, T., Næsset, E. and Nelson, R. 2011. Model-based inference for biomass estimation in a LiDAR sample survey in Hedmark County, NorwayThis article is one of a selection of papers from Extending Forest Inventory and Monitoring over Space and Time. Can. J. For. Res. **41**(1): 96–107.

Strunk, J.L., Reutebuch, S.E., Andersen, H.-E., Gould, P.J. and McGaughey, R.J. 2012. Model-Assisted Forest Yield Estimation with Light Detection and Ranging. Western Journal of Applied Forestry **27**(2): 53–59.

Sullivan, A.A., McGaughey, R.J., Andersen, H.E. and Schiess, P. 2009. Object-oriented classification of forest structure from light detection and ranging data for stand mapping. Western Journal of Applied Forestry **24**(4): 198–204.

Tonolli, S., Dalponte, M., Neteler, M., Rodeghiero, M., Vescovo, L. and Gianelle, D. 2011. Fusion of airborne LiDAR and satellite multispectral data for the estimation of timber volume in the Southern Alps. Remote Sensing of Environment **115**(10): 2486–2498.

Wulder, M.A., Han, T., White, J.C., Sweda, T. and Tsuzuki, H. 2007. Integrating profiling LIDAR with Landsat data for regional boreal forest canopy attribute

estimation and change characterization. Remote Sensing of Environment **110**(1): 123–137.

5 Conclusion

5.1 Contributions

The research performed in this dissertation contributes to the body of knowledge which is related to estimation and modeling of forest resources using auxiliary remote sensing data, especially with lidar and Landsat. The research performed also contributes implicitly to the fields of mapping or prediction as a result of our treatment of modeling, but although this is also an important application, it is not an area that we discuss in detail. Remote sensing is a tool that can provide explanatory power for some forest attributes. With an appropriate conceptual framework we can harness this predictive power to make inference about vegetation attributes including lack of vegetation on the landscape. An important distinction regarding use of the word inference in discussing the contributions of this dissertation is that inference may include statistical inference, but the two concepts are not identical. I distinguish two modes of inference that prove useful in my discussion here. I will henceforth refer to the mode of inference which is practically useable but which is not required to be accompanied by statistical properties as *practical inference*, and inference relying on the calculation of statistics as *statistical inference*. For example we can make inference from a lidar derived canopy surface model about the heights of upper canopy trees in the forest which is practically useable for management without performing statistical inference. If we wish to additionally make statistical inferences about the capacity of lidar to distinguish between stand heights, we would need a measure of the accuracy of the lidar-based height measurements of height. This can be obtained by measuring

forest heights in the field and comparing them to the lidar-based measurement. The field measurements could then also be used to improve our height measurements from lidar by adjusting them by an amount indicated by their correspondence with field measurements.

The strategy of making inference from remote sensing data by leveraging the correspondence between field measurements and remote sensing measurements for the same locations, as described in our discussion of inference, is in fact the basis for all of the analyses performed in this dissertation. There are already a large number of studies which examine the correspondences between remote sensing and field measured forest attributes for the same locations. Many of these studies provided statistical inferences which are valuable from a scientific standpoint, but may provide limited practical inference. I believe that an important contribution to this field in its current state, where it is already known that there are strong correspondences between lidar variables and some forest attributes, is to develop, perform, and report statistical inferences in a manner that communicates practical solutions to real world problems (e.g. Corona, 2010).

The research conducted in this dissertation is aimed at communicating inferences that solve problems associated with implementing forest inventory estimation and monitoring strategies that use auxiliary lidar and Landsat. One component of a contribution to the body of knowledge from evaluating a solution is the solution itself, and the second is providing useable inference either by placing the statistical inference

in context or by providing statistical inference that is practically useable. The approach we use to provide useable inference in chapters 1 and 2 is to perform analyses with respect to design-based inference and by comparing the performance of a target strategy with one or more alternate strategies to provide context. Manuscript 3 emphasizes selected multi-phase modeling strategies; context for this section is provided by contrasting the residual variability for a variety of modeling strategies and practical inferences are provided only with respect to the modeling performance.

In manuscripts 1 we used design-based inference to evaluate the effects of pulse density and sample size on estimation. Performing our analyses with respect to design-based estimation had a substantial effect on practical inference regarding the importance of the number of field plots for estimation with wall-to-wall lidar. A number of studies have examined the effects of sample size on modeling (statistical inference) and found that above a certain threshold, the effects of sample size on residual variability was small. This is a valuable scientific contribution that we corroborated. However, by placing this result in the context of estimation we came to a completely different conclusion than one might expect from the result alone. For estimation, the number of field plots was demonstrated to have a substantial effect on precision (a practical application), but chiefly because asymptotic precision of the regression estimator is a function of sample size rather than because of sample size effects on residual variability. If taken without further consideration there is a risk that the statistical inferences provided by previous studies will be interpreted as practical inferences. An incorrect inference from the statistical analysis on sample size and

residual variability is that there is no real benefit from increasing the number of sample plots. Our manuscript obviates the fact that this is not the case.

While we found that modeling errors were immaterial for most sample sizes, accounting for and describing this source of error was an additional component of our contribution to research to this field. We initially estimated the effect of sample size on the variability of model residuals for our study, and did not find a practically worrisome effect of sample size on residual variability for as few as 15 observations, perhaps in part because we used a systematic sample which will yield a greater range of auxiliary values and hence more precise parameter estimates. Accounting for this source of error in estimation also contributes to the defensibility of our practical inferences from the results concerning sample size effects on estimation. The simulation approach that we used to examine reduced sample sizes incorporated both sampling and modeling errors, inflating standard error estimates by an appropriate amount to account for modeling errors.

While the effect of sample size on modeling may have been slight in most cases, it may have influenced the behavior of the variance estimator, contributing to our observation that the formula-based variance estimator for the regression estimator worked poorly for small samples. Even without the effect of sample size on modeling this was not a surprising result given that the properties of the formula-based variance estimator are large sample properties, however it may cause the threshold for reasonable inference from the variance estimator to be greater than if the model

coefficients were not estimated from the sample. Documenting the fact that sample size affects the validity of statistical inference is a particularly important contribution of our research given that many studies modeling forest attributes with lidar were performed with relatively small samples, or reasonable numbers of plots for a single model were stratified yielding too small numbers of plots for stratum models. Our discussion of this issue and providing a warning about the hazard of making inference from a small sample improves the chance that both in applications and in future studies sufficient numbers of observations will be used to make defensible statistical inferences.

In our second manuscript we used design based inference again to support practical inferences about estimation, this time with lidar collected as a sample of strips, Landsat, and lidar strips and Landsat combined. In this manuscript we performed contrasted estimates of precision for a variety of estimation strategies and for multiple approaches to variance estimation. Estimation with strips of lidar is a relatively unexplored area of inquiry and as in the small number of previous studies examining similar approaches, we firstly contributed to this area of research by demonstrating the application and performance of estimation with sample strips for our case study. We secondly contributed to this body of research by suggesting two variance estimators including a bootstrap variance estimator and a Durbin style variance estimator. And finally, we contributed to this body of research by providing extensive context for the precision of estimation with a lidar sample strip approach relative to other estimation strategies. We compared a sample strip approach (which induces a two-stage design)

to an SRS design, to estimation with plots only, and to estimation with and in combination with Landsat. We also examined the effects of the number of lidar sample strips on estimation with lidar. Without contrasting the precision of the lidar sample strip approach to a variety of other estimation strategies it would be difficult to interpret the merits and viability of using lidar in a sampling mode.

As it turns out we were able to demonstrate that there were configurations with a lidar sample strip approach that were highly viable for estimation of biomass, especially when combined with Landsat using a composite estimator. Our results extend the work of previous studies by demonstrating that select configurations with lidar in a sampling mode are viable for estimation by contrasting the relative precisions of alternative estimation strategies including a lidar sampling strip strategy with different numbers of lidar strips. As previously noted, lidar sampling strips have been explored previously, but the relative performances for a variety of related estimation strategies were not provided, hindering the user's ability to interpret whether using lidar as a sample of strips contributed in any way to estimation. Since our study is actually part of a pilot project attempting to develop an approach to more efficiently quantify natural resources (or monitor) in interior Alaska, a region without a complete forest inventory in place, the results from this study may be directly applicable in practice to the development of a sampling strategy for interior Alaska.

Manuscript 3 is slightly different than manuscripts 1 and 2 because the focus is on modeling instead of estimation. We make statistical inferences which are practically

interpretable with respect to estimation, but we do not directly provide statistical results for estimation, although we plan to do so in the future. The objective of manuscript 3 is to develop and evaluate improved strategies for modeling forest attributes with Landsat by using lidar as an intermediary data source. In this analysis statistical inference was provided with estimates of residual variability when for alternate modeling strategies.

The first practical contribution that we made in manuscript 3 was that we identified superior modeling strategies with respect to residual variability. The selection of a superior modeling strategy included as components the approach used to treat lidar as an intermediary step, the order and type of different modeling approaches (KNN and OLS), and the resolution used to train Landsat (30 m or 90 m). There are perhaps innumerable different potential modeling strategies, and we do not claim to have found the best of all possible strategies, but the results indicated strategies that worked well for our case study and should perhaps be tested or implemented with priority over the alternate strategies described. Practically applicable statistical inference with respect to estimation can still be made in a roundabout way from our results by examining the modeling performance in manuscript 3 relative to the modeling performances in manuscript 2 and examining the effect of residual variability on estimation precision – although clearly explicit treatment would be superior, an approach we plan to undertake in future work.

A second contribution from manuscript 3 with practical implications was the development of a strategy to estimate residual variance for a multiphase modeling strategy. This is an important step because the resolution of the field measurements does not match the resolution of the Landsat, especially when Landsat was resampled to 90m resolution. Our estimator of residual variance can then quite easily be plugged into a design-based variance estimator, for example, to make statistical inference that is also of practical value (a step we did not take, but plan to include in future work). We do not claim originality for the concepts or strategy used to develop the residual variance estimator, and in fact leaned heavily on Kmenta (1997) for the derivation, but we are unaware of another study that provides an estimator of residual variance for a multi-phase modeling strategy.

5.2 Limitations

A primary limitation of an approach that uses auxiliary remote sensing information for modeling and estimation of forest attributes is that many field measured variables may have limited or zero useable correspondence with remote sensing variables. Often remote sensing augmented approaches are explored to improve the performance of estimation strategies with the objective to increase the quality of outputs, provide outputs not feasible otherwise, or reduce the cost to achieve the same level of quality. For variables with zero correspondence with remote sensing the addition of remote sensing may provide no benefit, and is likely to require additional cost. Certainly no improved products are feasible for these variables. And if the number of

measurements is reduced to pay for remote sensing then the quality of information for some variables will also be reduced.

For forest inventory applications, acquisition of species information is often mandatory, but is only minimally supported by predictions with lidar or Landsat. For a limited number of applications including where extensive legacy information is available, a single species is dominant, or in rare applications where species is not important, this will not be an issue, but for many cases lack of species information is a deal breaker. In this study, and in many other studies with lidar, the difficulty in acquisition of species information is not addressed. In this dissertation we examined continuous response variables with relatively strong associations with lidar-derived variables. While our analyses provide valuable contributions to scientific and practical inferences, the practical inferences are currently limited in scope to instances where an alternate source of species information is available or species is not needed. Of the variables that we did not address, we especially single out species because in applications it is perhaps the most important attribute which cannot be easily obtained from lidar or Landsat, but the same limitation to our inference is present for any other scenario where an attribute that is required cannot be reasonably captured from these remote sensing sources.

5.3 Future research

Because it provides three dimensional information that is useful in predicting biomass and related variables it is likely that lidar will play an increasing role in forest

inventory and monitoring. However, as previously described, lidar cannot provide species information as easily as forest structure information. Since it is abundantly clear that it is possible to provided volume, biomass, and related variables with lidar, the most important next step in demonstrating the usability of lidar is to develop and describe approaches to retrieve species information. There has been a fair amount of work on predicting species composition from lidar, but it is not clear how the various approaches perform operationally. The effect of these approaches on the quality of practical statistical inference is not described. It is necessary that they are contrasted with existing protocols to acquire forest attributes such as volume by species class, much as we did in chapter 3 by comparing alternate estimation strategies.

Species classification is described in the literature for both individual tree (Holmgren and Persson, 2004) and areal approaches (Donoghue et al., 2007) . An area approach is preferable from a computational perspective, but even an individual tree based approach is highly beneficial so long as it provides additional explanatory power – perhaps in combination with areal estimates of alternate variables. However, lidar may never be the ideal tool for species differentiation by itself. For cases where lidar does not have sufficient explanatory power to differentiate species it will be important to demonstrate alternate sources of species information, such as from aerial photos. Studies in the literature demonstrate that species differentiation is feasible with lidar and aerial imagery. Ideally the approach should be automated, where automation (and vegetation penetration) is one of the primary advantages of using lidar over stereo imagery for height measurements. An approach which relies upon user interpretation

of stereo imagery may be too expensive in many instances. Recently there has also been a fair amount of interest in automated approaches to species differentiation which make use of hyperspectral imagery with promising results (Naidoo et al., 2012; Jones et al., 2010), although the gain relative to multispectral imagery may not warrant the additional cost or effort (Dalponte et al., 2012).

In the same vein as we approached lidar for the research in this dissertation, it is important to demonstrate the effect that various approaches to acquisition of forest variables have on estimation, especially if variables cannot be accessed effectively with remote sensing. Many of the studies in the literature and the research in this dissertation focus on variables accessible with lidar. It is not clear what the implications would be if a large number of variables must be reported, such as for the national FIA program. For example, is there a middle ground where fewer plots are used because of the increased efficiency afforded by remote sensing for variables of primary interest, but more plots than are strictly necessary for biomass (e.g.) to enable adequate (but reduced) precision for variables which are not related to remote sensing variables. Alternatively it may be possible to achieve the desired level of precision at reduced cost by measuring variables at different spatial and temporal frequencies. Understory species composition (e.g.) is unlikely to change rapidly for some forest conditions, so it may prove feasible to acquire this information using a higher spatial sampling intensity measurement protocol with a reduced temporal sampling intensity. Update measurements could even be target to areas with observed remote sensing changes that are indicative of composition changes.

5.4 Citations

Corona, P. 2010. Integration of forest mapping and inventory to support forest management. iForest-Biogeosciences and Forestry **3**(1): 59.

Dalponte, M., Bruzzone, L. and Gianelle, D. 2012. Tree species classification in the Southern Alps based on the fusion of very high geometrical resolution multispectral/hyperspectral images and LiDAR data. Remote Sensing of Environment **123**(0): 258–270.

Donoghue, D.N.M., Watt, P.J., Cox, N.J. and Wilson, J. 2007. Remote sensing of species mixtures in conifer plantations using LiDAR height and intensity data. Remote Sensing of Environment **110**(4): 509–522.

Holmgren, J. and Persson, Å. 2004. Identifying species of individual trees using airborne laser scanner. Remote Sensing of Environment **90**(4): 415–423.

Jones, T.G., Coops, N.C. and Sharma, T. 2010. Assessing the utility of airborne hyperspectral and LiDAR data for species distribution mapping in the coastal Pacific Northwest, Canada. Remote Sensing of Environment **114**(12): 2841–2852.

Kmenta, J. 1997. Elements of Econometrics. 2nd ed. University of Michigan Press.

Naidoo, L., Cho, M.A., Mathieu, R. and Asner, G. 2012. Classification of savanna tree species, in the Greater Kruger National Park region, by integrating hyperspectral and LiDAR data in a Random Forest data mining environment. ISPRS Journal of Photogrammetry and Remote Sensing **69**(0): 167–179.

6 Bibliography

Ahern, F.J. and Leckie, D.G. 1987. Digital remote sensing for forestry: Requirements and capabilities, today and tomorrow. Geocarto International **2**(3): 43–52.

Andersen, H.E. 2009. Using Airborne Light Detection and Ranging (LIDAR) to Characterize Forest Stand Condition on the Kenai Peninsula of Alaska. West. J. Appl. For. **24**(2): 95–102.

Andersen, H.E. and Breidenbach, J. 2007. Statistical properties of mean stand biomass estimators in a LIDAR-based double sampling forest survey design. In Proceedings of the ISPRS Workshop Laser Scanning 2007 and SilviLaser 2007, Espoo Finland: IAPRS, p. 8–13.

Andersen, H.E., Clarkin, T., Winterberger, K. and Strunk, J.L. 2009. An Accuracy Assessment of Positions Obtained Using Survey-and Recreational-Grade Global Positioning System Receivers across a Range of Forest Conditions within the Tanana Valley of Interior Alaska. West. J. Appl. For. **24**(3): 128–136.

Andersen, H.E., McGaughey, R.J. and Reutebuch, S.E. 2005. Estimating forest canopy fuel parameters using LIDAR data. Remote Sensing of Environment **94**(4): 441–449.

Andersen, H.E., Strunk, J. and Temesgen, H. 2011a. Using Airborne Light Detection and Ranging as a Sampling Tool for Estimating Forest Biomass Resources in the Upper Tanana Valley of Interior Alaska. Western Journal of Applied Forestry **26**(4): 157–164.

Andersen, H.-E., Strunk, J., Temesgen, H., Atwood, D. and Winterberger, K. 2011b. Using multilevel remote sensing and ground data to estimate forest biomass resources in remote regions: a case study in the boreal forests of interior Alaska. Canadian Journal of Remote Sensing **37**(6): 596–611.

Antal, E. and Tillé, Y. 2011. A Direct Bootstrap Method for Complex Sampling Designs From a Finite Population. Journal of the American Statistical Association **106**(494): 534–543.

Barrett, T.M., Christensen, G.A. and Pacific Northwest Research Station (Portland, O.. 2011. Forests of Southeast and South-central Alaska, 2004-2008: Five-year Forest Inventory and Analysis Report. US Department of Agriculture, Forest Service, Pacific Northwest Research Station.

Bechtold, W.A. and Patterson, P.L. 2005. The enhanced forest inventory and analysis program: national sampling design and estimation procedures. Asheville, North Carolina: US Department of Agriculture Forest Service, Southern Research Station. 85 p.

Cihlar, J., Latifovic, R., Beaubien, J., Trishchenko, A., Chen, J. and Fedosejevs, G. 2003. National scale forest information extraction from coarse resolution satellite data, Part 1. Data processing and mapping land cover types. In Remote Sensing of Forest Environments: Concepts and Case Studies, Springer, p. 552.

Clarkin, T. 2007. Modeling global navigation satellite system positional error under forest canopy based on LIDAR-derived canopy densities. M.Sc. thesis, Univ. of Washington, Seattle, Washington, USA. 99 p.

Corona, P. 2010. Integration of forest mapping and inventory to support forest management. iForest-Biogeosciences and Forestry **3**(1): 59.

Corona, P. and Fattorini, L. 2008. Area-based lidar-assisted estimation of forest standing volume. Can. J. Forest. Res. **38**(11): 2911–2916.

Dalponte, M., Bruzzone, L. and Gianelle, D. 2012. Tree species classification in the Southern Alps based on the fusion of very high geometrical resolution multispectral/hyperspectral images and LiDAR data. Remote Sensing of Environment **123**(0): 258–270.

DeVelice, R.L. 2012. 10 Accuracy of the LANDFIRE Alaska Existing Vegetation Map over the Chugach National Foreset. LANDFIRE. Assessments.

Donoghue, D.N.M., Watt, P.J., Cox, N.J. and Wilson, J. 2007a. Remote sensing of species mixtures in conifer plantations using LiDAR height and intensity data. Remote Sensing of Environment **110**(4): 509–522.

Donoghue, D.N.M., Watt, P.J., Cox, N.J. and Wilson, J. 2007b. Remote sensing of species mixtures in conifer plantations using LiDAR height and intensity data. Remote Sensing of Environment **110**(4): 509–522.

Drake, J.B., Knox, R.G., Dubayah, R.O., Clark, D.B., Condit, R., Blair, J.B. and Hofton, M. 2003. Above-ground biomass estimation in closed canopy Neotropical forests using lidar remote sensing: factors affecting the generality of relationships. Global Ecology and Biogeography **12**(2): 147–159.

Efron, B. and Tibshirani, R. 1993. An introduction to the bootstrap. CRC Press. 456 p.

Ene, L., Næsset, E. and Gobakken, T. 2012. Single tree detection in heterogeneous boreal forests using airborne laser scanning and area-based stem number estimates. International Journal of Remote Sensing **33**(16): 5171–5193.

Ford, A. 2009. Modeling the Environment, Second Edition. Island Press. 401 p.

Furnival, G.M. and Wilson Jr, R.W. 1974. Regressions by leaps and bounds. Technometrics: 499–511.

Gabbott, W.G. and Officer, C. 2003. The National Agriculture Imagery Program.

Garner, R. 2012. NASA - Landsat Overview.

Gobakken, T. and Næsset, E. 2008. Assessing effects of laser point density, ground sampling intensity, and field sample plot size on biophysical stand properties derived from airborne laser scanner data. Can. J. Forest. Res. **38**(5): 1095–1109.

Green, E.J. and Strawderman, W.E. 1986. Reducing sample size through the use of a composite estimator: an application to timber volume estimation. Can. J. For. Res. **16**(5): 1116–1118.

Gregoire, T.G. 1998. Design-based and model-based inference in survey sampling: appreciating the difference. Can. J. Forest. Res. **28**(10): 1429–1447.

Gregoire, T.G., Stahl, G., Naesset, E., Gobakken, T., Nelson, R. and Holm, S. 2011. Model-assisted estimation of biomass in a LiDAR sample survey in Hedmark County, Norway. Canadian Journal of Forest Research **41**(1): 83–95.

Gregoire, T.G. and Valentine, H.T. 2008. Sampling Strategies for Natural Resources and the Environment. 1st ed. New York: Chapman and Hall/CRC. 474 p.

Gregoire, T.G. and Walters, D.K. 1988. Composite vector estimators derived by weighting inversely proportional to variance. Canadian Journal of Forest Research **18**(2): 282–284.

Hall, R.J. 2003. The roles of aerial photographs in forestry remote sensing image analysis. (Pages 47-75 in Wulder MA,Franklin SE. Methods and Applications for Remote Sensing of Forests: Concepts and Case Studies.). Kluwer Academic Publishers, Boston/Dordecht/London.

Hall, S.A., Burke, I.C., Box, D.O., Kaufmann, M.R. and Stoker, J.M. 2005. Estimating stand structure using discrete-return lidar: an example from low density, fire prone ponderosa pine forests. Forest Ecology and Management **208**(1-3): 189–209.

Hinsley, S.A., Hill, R.A., Bellamy, P.E. and Balzter, H. 2006. The application of lidar in woodland bird ecology: climate, canopy structure, and habitat quality.

Holmgren, J. 2004. Prediction of tree height, basal area and stem volume in forest stands using airborne laser scanning. Scand. J. Forest. Res. **19**(6): 543–553.

Holmgren, J. and Persson, Å. 2004. Identifying species of individual trees using airborne laser scanner. Remote Sensing of Environment **90**(4): 415–423.

Howard, J.A. 1991. 621 Remote sensing of forest resources: theory and application. Chapman & Hall.

Huang, C., Homer, C. and Yang, L. 2003. Regional forest land-cover characterizations using medium spatial resolution satellite data. (Pages 47-75 in Wulder MA,Franklin SE. Methods and Applications for Remote Sensing of Forests: Concepts and Case Studies.). Kluwer Academic Publishers, Boston/Dordecht/London.

Hudak, A.T., Crookston, N.L., Evans, J.S., Falkowski, M.J., Smith, A.M.S., Gessler, P.E. and Morgan, P. 2006. Regression modeling and mapping of coniferous forest basal area and tree density from discrete-return lidar and multispectral satellite data. Canadian Journal of Remote Sensing **32**(2): 126–138.

Hudak, A.T., Lefsky, M.A., Cohen, W.B. and Berterretche, M. 2002. Integration of lidar and Landsat ETM+ data for estimating and mapping forest canopy height. Remote Sensing of Environment **82**(2-3): 397–416.

Hyde, P., Nelson, R., Kimes, D. and Levine, E. 2007. Exploring LiDAR-RaDAR synergy--predicting aboveground biomass in a southwestern ponderosa pine forest using LiDAR, SAR and InSAR. Remote Sensing of Environment **106**(1): 28–38.

Hyyppä, J., Hyyppä, H., Inkinen, M., Engdahl, M., Linko, S. and Zhu, Y.-H. 2000. Accuracy comparison of various remote sensing data sources in the retrieval of forest stand attributes. Forest Ecology and Management **128**(1-2): 109–120.

Hyyppa, J., Kelle, O., Lehikoinen, M. and Inkinen, M. 2001. A segmentation-based method to retrieve stem volume estimates from 3-D tree height models produced by laser scanners. Geoscience and Remote Sensing, IEEE Transactions on **39**(5): 969 – 975.

Jenkins, J.C., Chojnacky, D.C., Heath, L.S. and Birdsey, R.A. 2004. Comprehensive database of diameter-based biomass regressions for North American tree species. Gen. Tech. Rep. NE-319. Newtown Square, PA: US Department of Agriculture, Forest Service, Northeastern Research Station **45**.

Jensen, J.L.., Humes, K.S., Conner, T., Williams, C.J. and DeGroot, J. 2006. Estimation of biophysical characteristics for highly variable mixed-conifer stands using small-footprint lidar. Canadian Journal of Forest Research **36**(5): 1129–1138.

Jobin, L. and Beaubien, J. 1974. Capability of ERTS-1 imagery for mapping forest cover types of Anticosti Island. The Forestry Chronicle **50**(6): 233–237.

Johnson, E.W. 2000. Forest sampling desk reference. CRC.

Jones, T.G., Coops, N.C. and Sharma, T. 2010. Assessing the utility of airborne hyperspectral and LiDAR data for species distribution mapping in the coastal Pacific Northwest, Canada. Remote Sensing of Environment **114**(12): 2841–2852.

Kennaway, T.A., Helmer, E.H., Lefsky, M.A., Brandeis, T.A. and Sherrill, K.R. 2008. Mapping land cover and estimating forest structure using satellite imagery and coarse resolution lidar in the Virgin Islands. Journal of Applied Remote Sensing **2**(023551): 1–27.

Kennedy, R.E., Cohen, W.B. and Schroeder, T.A. 2007. Trajectory-based change detection for automated characterization of forest disturbance dynamics. Remote Sensing of Environment **110**(3): 370–386.

Kennedy, R.E., Yang, Z. and Cohen, W.B. 2010. Detecting trends in forest disturbance and recovery using yearly Landsat time series: 1. LandTrendr — Temporal segmentation algorithms. Remote Sensing of Environment **114**(12): 2897–2910.

Keyser, C.E. 2010. 49 Pacific Northwest Coast (PN) Variant Overview – Forest Vegetation Simulator. Fort Collins, CO: WO-Forest Management Service Center, USDA-Forest Service. Internal Report.

Kim, S., McGaughey, R.J., Andersen, H.-E. and Schreuder, G. 2009a. Tree species differentiation using intensity data derived from leaf-on and leaf-off airborne laser scanner data. Remote Sensing of Environment **113**(8): 1575–1586.

Kim, Y., Yang, Z., Cohen, W.B., Pflugmacher, D., Lauver, C.L. and Vankat, J.L. 2009b. Distinguishing between live and dead standing tree biomass on the North Rim of Grand Canyon National Park, USA using small-footprint lidar data. Remote Sensing of Environment **113**(11): 2499–2510.

Kirvida, L. and Johnson, G.R. 1973. Automatic interpretation of ERTS data for forest management.

Kmenta, J. 1997a. Elements of econometrics. Univ of Michigan Pr.

Kmenta, J. 1997b. Elements of Econometrics. 2nd ed. University of Michigan Press.

Lefsky, M.A., Harding, D., Cohen, W.B., Parker, G. and Shugart, H.H. 1999. Surface Lidar Remote Sensing of Basal Area and Biomass in Deciduous Forests of Eastern Maryland, USA. Remote Sensing of Environment **67**(1): 83–98.

Lim, K., Treitz, P., Baldwin, K., Morrison, I. and Green, J. 2003. Lidar remote sensing of biophysical properties of tolerant northern hardwood forests. Canadian Journal of Remote Sensing **29**(5): 658–678.

Lohr, S.L. 2009. Sampling: design and analysis. Thomson.

Lohr, S.L. 1999. Sampling: Design and Analysis. Pacific Grove, CA: Duxbury Press. 494 p.

Lovell, J.L., Jupp, D.L.B., Newnham, G.J., Coops, N.C. and Culvenor, D.S. 2005. Simulation study for finding optimal lidar acquisition parameters for forest height retrieval. Forest Ecol. Manag. **214**(1-3): 398–412.

Lund, H.G. and Schreuder, H.T. 1980. Aggregating inventories. Resources Evaluation Newsletter (4): 1–3.

MacKay, B. 2012. What is a Model? URL: http://serc.carleton.edu/introgeo/models/WhatIsAModel.html.

Maclean, G.A. and Krabill, W.B. 1986. Gross-merchantable timber volume estimation using an airborne LIDAR system. Canadian Journal of Remote Sensing **12**: 7–18.

Magnusson, M., Fransson, J.E.S. and Holmgren, J. 2007. Effects on estimation accuracy of forest variables using different pulse density of laser data. Forest Sci. **53**(6): 619–626.

Maltamo, M., Eerikainen, K., Packalen, P. and Hyyppa, J. 2006a. Estimation of stem volume using laser scanning-based canopy height metrics. Forestry **79**(2): 217.

Maltamo, M., Malinen, J., Packalén, P., Suvanto, A. and Kangas, J. 2006b. Nonparametric estimation of stem volume using airborne laser scanning, aerial photography, and stand-register data. Canadian Journal of Forest Research **36**(2): 426–436.

McGaughey, R.J. 2012. FUSION/LDV: Software for LIDAR Data Analysis and Visualization, Version 3.01. USFS.

McTague, J.P. 2010. New and composite point sampling estimates. Canadian Journal of Forest Research **40**(11): 2234–2242.

Means, J.E., Acker, S.A., Fitt, B.J., Renslow, M., Emerson, L. and Hendrix, C. 2000a. Predicting forest stand characteristics with airborne scanning lidar. Photogrammetric Engineering and Remote Sensing **66**(11): 1367–1372.

Means, J.E., Acker, S.A., Fitt, B.J., Renslow, M., Emerson, L. and Hendrix, C. 2000b. Predicting Forest Stand Characteristics with Airborne Scanning Lidar. PERS **66**(11): 1367–1371.

Means, J.E., Acker, S.A., Harding, D.J., Blair, J.B., Lefsky, M.A., Cohen, W.B., Harmon, M.E. and McKee, W.A. 1999. Use of large-footprint scanning airborne LiDAR to estimate forest stand characteristics in the western cascades of Oregon. Remote Sensing of Environment **67**(3): 298–308.

Meigs, G.W., Kennedy, R.E. and Cohen, W.B. 2011. A Landsat time series approach to characterize bark beetle and defoliator impacts on tree mortality and surface fuels in conifer forests. Remote Sensing of Environment.

Mutlu, M., Popescu, S.C., Stripling, C. and Spencer, T. 2008. Mapping surface fuel models using lidar and multispectral data fusion for fire behavior. Remote Sensing of Environment **112**(1): 274–285.

Næsset, E. 1997a. Determination of mean tree height of forest stands using airborne laser scanner data. Remote Sens. Environ. **52**(2): 49–56.

Næsset, E. 2004. Effects of different flying altitudes on biophysical stand properties estimated from canopy height and density measured with a small-footprint airborne scanning laser. Remote Sensing of Environment **91**(2): 243–255.

Næsset, E. 1997b. Estimating timber volume of forest stands using airborne laser scanner data. ISPRS. J. Photogramm. **61**(2): 246–253.

Naidoo, L., Cho, M.A., Mathieu, R. and Asner, G. 2012. Classification of savanna tree species, in the Greater Kruger National Park region, by integrating hyperspectral and LiDAR data in a Random Forest data mining environment. ISPRS Journal of Photogrammetry and Remote Sensing **69**(0): 167–179.

Nelson, R., Krabill, W. and Tonelli, J. 1988. Estimating forest biomass and volume using airborne laser data. Remote Sensing of Environment **24**(2): 247–267.

Opsomer, J.D., Breidt, F.J., Moisen, G.G. and Kauermann, G. 2007. Model-assisted estimation of forest resources with generalized additive models. Journal of the American Statistical Association **102**(478): 400–409.

Packalen, P. and Maltamo, M. 2006. Predicting the plot volume by tree species using airborne laser scanning and aerial photographs. Forest Science **52**(6): 611–622.

Packalén, P. and Maltamo, M. 2008. Estimation of species-specific diameter distributions using airborne laser scanning and aerial photographs. Can. J. For. Res. **38**(7): 1750–1760.

Packalén, P. and Maltamo, M. 2007. The k-MSN method for the prediction of species-specific stand attributes using airborne laser scanning and aerial photographs. Remote Sensing of Environment **109**(3): 328–341.

Parker, R.C. and Evans, D.L. 2004. An application of LiDAR in a double-sample forest inventory. Western Journal of Applied Forestry **19**(2): 95–101.

Parker, R.C. and Evans, D.L. 2007. Stratified light detection and ranging double-sample forest inventory. South. J. Appl. For. **31**(2): 66–72.

Parker, R.C. and Glass, P.A. 2004. High-versus low-density LiDAR in a double-sample forest inventory. South. J. Appl. For. **28**(4): 205–210.

Pascual, C., García-Abril, A., García-Montero, L.G., Martín-Fernández, S. and Cohen, W.B. 2008. Object-based semi-automatic approach for forest structure characterization using lidar data in heterogeneous Pinus sylvestris stands. Forest Ecology and Management **255**(11): 3677–3685.

Peuhkurinen, J., Mehtätalo, L. and Maltamo, M. 2011. Comparing individual tree detection and the area-based statistical approach for the retrieval of forest stand characteristics using airborne laser scanning in Scots pine stands. Canadian Journal of Forest Research **41**(3): 583–598.

Pflugmacher, D. 2011. Remote sensing of forest biomass dynamics using Landsat-derived disturbance and recovery history and lidar data.

Popescu, S.C., Wynne, R.H. and Scrivani, J.A. 2004. Fusion of small-footprint lidar and multispectral data to estimate plot-level volume and biomass in deciduous and pine forests in Virginia, USA. Forest Science **50**(4): 551–565.

Powell, S.L., Cohen, W.B., Healey, S.P., Kennedy, R.E., Moisen, G.G., Pierce, K.B. and Ohmann, J.L. 2010. Quantification of live aboveground forest biomass dynamics with Landsat time-series and field inventory data: A comparison of empirical modeling approaches. Remote Sensing of Environment **114**(5): 1053–1068.

Rao, J.N.K. and Wu, C.F.J. 1988. Resampling Inference With Complex Survey Data. Journal of the American Statistical Association **83**(401): 231–241.

Rollins, M.G. 2009. LANDFIRE: a nationally consistent vegetation, wildland fire, and fuel assessment. International Journal of Wildland Fire **18**(3): 235–249.

Russel, R.E., Saab, V.A. and Dudley, J.G. 2007. Habitat-Suitability Models for Cavity-Nesting Birds in a Postfire Landscape. Journal of Wildlife Management **71**(8): 2600–2611.

Särndal, C.E., Swensson, B. and Wretman, J. 1992. Model assisted survey sampling. New York: Springer-Verlag. 694 p.

Schreuder, H.T., Ernst, R. and Ramirez-Maldonado, H. 2004. Statistical techniques for sampling and monitoring natural resources. Rocky Mountain Research Station.

Schwarz, G. 1978. Estimating the Dimension of a Model. The Annals of Statistics **6**(2): 461–464.

Serfling, R.J. 1980. Approximation theorems of mathematical statistics. Wiley. 402 p.

Shiver, B.D. and Borders, B.E. 1995. Sampling Techniques for Forest Resource Inventory. Wiley.

Solberg, S., Astrup, R., Gobakken, T., N\aesset, E. and Weydahl, D.J. 2010. Estimating spruce and pine biomass with interferometric X-band SAR. Remote Sensing of Environment **114**(10): 2353–2360.

Ståhl, G., Holm, S., Gregoire, T.G., Gobakken, T., Næsset, E. and Nelson, R. 2011. Model-based inference for biomass estimation in a LiDAR sample survey in Hedmark County, NorwayThis article is one of a selection of papers from Extending Forest Inventory and Monitoring over Space and Time. Can. J. For. Res. **41**(1): 96–107.

St-Onge, Hu, Y. and Vega, C. 2008. Mapping the height and above-ground biomass of a mixed forest using lidar and stereo Ikonos images. International Journal of Remote Sensing **29**(5): 1277–1294.

Strunk, J.L., Reutebuch, S.E., Andersen, H.-E., Gould, P.J. and McGaughey, R.J. 2012. Model-Assisted Forest Yield Estimation with Light Detection and Ranging. Western Journal of Applied Forestry **27**(2): 53–59.

Sullivan, A.A., McGaughey, R.J., Andersen, H.E. and Schiess, P. 2009. Object-oriented classification of forest structure from light detection and ranging data for stand mapping. Western Journal of Applied Forestry **24**(4): 198–204.

Temesgen, H., Monleon, V.J. and Hann, D.W. 2008. Analysis and comparison of nonlinear tree height prediction strategies for Douglas-fir forests. Can. J. Forest. Res. **38**(3): 553–565.

Tonolli, S., Dalponte, M., Neteler, M., Rodeghiero, M., Vescovo, L. and Gianelle, D. 2011. Fusion of airborne LiDAR and satellite multispectral data for the estimation of timber volume in the Southern Alps. Remote Sensing of Environment **115**(10): 2486–2498.

USFS. 2008. National Volume Estimator Library (NVEL).

Woods, M., Pitt, D., Penner, M., Lim, K., Nesbitt, D., Etheridge, D. and Treitz, P. 2011. Operational implementation of a LiDAR inventory in Boreal Ontario. The Forestry Chronicle **87**(4): 512–528.

Wulder, M.A., Han, T., White, J.C., Sweda, T. and Tsuzuki, H. 2007. Integrating profiling LIDAR with Landsat data for regional boreal forest canopy attribute estimation and change characterization. Remote Sensing of Environment **110**(1): 123–137.

Wykoff, W.R., Crookston, N.L. and Stage, A.R. 1982. User's guide to the stand prognosis model, USDA Forest Service, Intermountain Forest and Range Experiment Station, Ogden, Utah. Gen. Tech. Rep. INT-133 **112**.

The Forest Inventory and Analysis Database: Database Description and Users Manual Version 3.0 for Phase 2.